Universidade Federal do Pará
Centro de Geociências
Curso de Pós-Graduação em Geologia e Geoquímica

ANÁLISE INTEGRADA DOS DEPÓSITOS DE CAULIM NA REGIÃO DO RIO CAPIM: FÁCIES, ESTRATIGRAFIA, PETROGRAFIA E ISÓTOPOS ESTÁVEIS

TESE APRESENTADA POR

ANTÔNIO EMÍDIO DE ARAÚJO SANTOS JÚNIOR

Como requisito parcial à obtenção do Grau de Doutor em Ciências na Área de GEOLOGIA

Data de aprovação: 29/09/2006

Comitê de Tese

DILCE DE FÁTIMA ROSSETTI (orientadora)

ALCIDES NÓBREGA SIAL

VALDEREZ PINTO FERREIRA

BASILE KOTSCHOUBEY

WERNER TRUCKENBRODT

Belém
2006

DEDICATÓRIA

À Família Santos

AGRADECIMENTOS

Sumário

LISTA DE ILUSTRAÇÕES
FIGURAS

vii

TABELA

RESUMO

Os depósitos de caulim que ocorrem na porção média do Rio Capim, leste da Sub-Bacia de Cameta, inserem-se na Formação Ipixuna, de idade cretácea superior, a qual se destaca por apresentar uma das maiores concentrações mundiais de caulim de excelente qualidade para a indústria de celulose. Um grande volume de trabalhos acadêmicos com enfoque geoquímico foi conduzido nestes depósitos, porém sem levar em consideração os aspectos faciológicos e estratigráficos, que são relevantes para entender sua origem e ocorrência. Somente recentemente, trabalhos sedimentológicos e estratigráficos mais detalhados destes depósitos de caulim foram apresentados, o que gerou uma série de novas considerações a respeito dos paleoambientes de deposição. Este tipo de estudo despertou interesse para se conduzir uma investigação integrada considerando-se aspectos sedimentológicos, estratigráficos, petrográficos e isótopos estáveis de hidrogênio e oxigênio, a fim de discutir os processos geológicos que podem ter influenciado na origem e evolução dos depósitos de caulim *soft e semi-flint* da Formação Ipixuna.

A análise sedimentológica e estratigráfica apresentada neste estudo teve caráter complementar a investigações anteriores, tomando-se por base a presença de novas exposições ao longo das frentes de lavra que disponibilizaram novas informações importantes ao entendimento dos ambientes de deposição. Assim, a porção inferior da Formação Inpixuna caracteriza-se por uma unidade de caulim do tipo *soft*, o qual por apresentar-se com preservação das estruturas primárias, possibilitou melhor entendimento dos processos de sedimentação. Estes depósitos incluem principalmente arenitos e argilitos caulinizados formados em ambientes de canal de maré influenciado por sistema fluvial (associação de fácies A), canal de maré (associação de fácies B), planície de maré/mangue (associação de fácies C), e barra/planície de areia dominada por maré (associação de fácies D). Estes depósitos são atribuídos a sistema estuarino do tipo dominado por maré. A unidade superior, conhecida como semi-flint, é dominantemente maciça, porém um estudo em paralelo conduzido durante o desenvolvimento desta tese revelou a presença de lobos deltaicos e canais distributários.

O estudo petrográfico e de microscopia eletrônica de varredura nos depósitos estudados levou à melhor caracterização textural dos tipos de caulinita presentes nas unidades de kaolin *soft* e semi-*flint*. Apesar da composição original fortemente modificada destes depósitos, informações ópticas revelaram inúmeras feições reliquiares distintas. Os depósitos de caulim *soft* são

caracterizados por arenitos quartzosos caulinizados e pelitos laminados ou maciços, os quais são compostos por fragmentos líticos de rochas meta-vulcânicas e vulcânicas félsicas, bem como rochas metamórficas e graníticas. Estas litologias foram fortemente modificadas durante o processo de caulinização da Formação Ipixuna, processo que teria obliterado a composição primária dos grãos do arcabouço. Durante este processo, três tipos principais de caulinita foram geradas, definidas com base no tamanho e textura como Ka, Kb e Kc. A caulinita Ka ocorre dominantemente associada aos arenitos caulinizados, sendo caracterizada por cristais pseudohexagonais a hexagonais, com diâmetros de 10-30 μm, podendo ocorrer na forma de aglomerados formando "livretos" (*booklets)* ou sob forma vermicular contendo até 400 μm de comprimento. A caulinita Kb ocorre dominantemente nos pelitos, consistindo de cristais pseudohexagonais a hexagonais de 1-3 μm de diâmetro, ocorrendo na forma isolada, formando intercrescimentos dos tipos caótico, face-a-face, paralelo a pseudo-paralelo. A caulinita Kc ocorre como cristais pseudohexagonais a hexagonais com diâmetros regulares de 200 nm. Sua distribuição é dispersa ao longo da unidade de caulim *soft*, aumentando em abundância em níveis de paleossolo que ocorre no topo da unidade. Os depósitos de caulim *semi-flint* são constituídos principalmente de grãos retrabalhados dos depósitos de caulim *soft* e grãos provenientes de rocha-fontes metamórficas e graníticas. As caulinitas da unidade de semi-*flint* são dominantemente representadas por caolinita Kc, gerada principalmente durante intemperismo pretérito.

As integração de estudos faciológicos, estratigráficos, ópticos e isótopos estáveis de deutério (δD) e oxigênio ($\delta^{18}O$) dos depósitos de caulim do Rio Capim permitiu melhor entender a gênese e evolução dos tipos de caolinita Ka+Kb e Kc. Os depósitos de caulim *soft* apresentam valores de $\delta^{18}O$ variando de 6,04‰ a 19,18‰ nas caulinitas Ka e Kb, e de 15,38‰ a 24,86‰ nas caulinitas Kc. Os valores de δD variam de −63,06‰ a 79,46‰, e de −68,85‰ a −244,35‰, respectivamente. Os depósitos de caulim semi-*flint* são caracterizados por valores isotópicos de $\delta^{18}O$ e δD entre 15,08‰ e 21,77‰, e -71.31‰ e -87.37‰, respectivamente. Baseando-se nestes dados e na composição isotópica da água meteórica e de sub-superfície, foi possível concluir que as caulinitas não se formaram em equilíbrio com as condições intempéricas atuais, e sim representam a composição isotópica de seu tempo de formação, podendo refletir contaminações mineralógicas proveniente da substituição parcial e/ou total dos grãos originais do arcabouço. Os valores isotópicos das caulinita do tipo Kc da unidade de semi-*flint* são amplamente variáveis em

decorrência da variedade de fontes, incluindo caulinitas retrabalhadas dos depósitos subjacentes de caulim *soft,* bem como caulinitas formadas durante diferentes fases de intemperismo, além de fases tardias de caulinita geradas ao longo de fraturas.

ABSTRACT

The kaolin deposits that occur in the Rio Capim area, east of Cametá Sub-Basin, are inserted in the Ipixuna Formation. This unit distinguishs for presenting one of the largest worldwide kaolin concentrations of excellent quality to the cellulose industry. Beyond the economic character, a great volume of academic works focusing these kaolin deposits had led to pedological and geochemical approaches, but without taking into account their sedimentologic aspects, which are important to understand their genesis. Detailed sedimentologic and stratigraphic studies of the Rio Capim kaolin have been increasingly carried out in the last years, which led to the paleoenvironmental interpretations for the Ipixuna Formation, as well as to discuss better the mode of formation of the soft and semi-flint kaolin units that are typical of this unit. These works served to motivate the integration of sedimentologic and stratigraphic data with optical studies combined with hydrogen and oxygen isotope geochemistry in order to discuss the geologic processes involved in the origin and evolution of the soft and semi-flint kaolin units. The sedimentological analysis consisted in a more detailed facies description and stratigraphic analysis of newly open quarries that were not available during previous investigations. The additional exposures led to a better characterization of the lower kaolin unit, known as the "soft kaolin", which is well stratified, favoring facies analysis. Hence, the soft kaolin unit consists of kaolinitized sandstones and kaolinitized pelites that were formed in tidally influenced fluvial channels (Facies Association A), tidal channel (Facies Association B), tidal flat/mangrove (Facies Association C), and tidal sand bar/tidal sandy flat (Facies Association D). These depositional environments are attributed to a tide-dominated estuarine system.

Petrographic studies and scanning electronic microscopy (SEM) of the kaolin deposits in the study area had their composition was strongly modified after sedimentation. The soft kaolin consists of kaolinitized quartz sandstone and either laminated or massive pelites, which are composed by fragments of meta-volcanic lithic and volcanic felsic rocks, as well as metamorphic and granitics rocks. These lithologies were strongly modified during kaolinitization, as revealed by the intense replacement of the framework grains by kaolinite of three types, named herein as Ka, Kb and Kc kaolinites. Ka kaolinite occurs dominantly associated with kaolinitized sandstones, being characterized by pseudohexagonal crystals 10-30 μm in diameter, which are organized as booklets or vermicular forms that reach up to 400 μm in length. Kb kaolinite

dominantes in the pelites, and consists of pseudohexagonal crystals 1-3 μm in diameter, occurring as isolated, face-to-face and parallel to pseudo-parallel crystals. Kc kaolinite forms pseudohexagonal to hexagonal crystals of 200 nm in diameter. It occurs dispersed through the soft unit, increasing significantly in abundance in association with paleosols at the top of the unit. The semi-flint kaolin deposits are constituted mainly of reworked grains derived from the underlying soft kaolin unit that are mixed with grains derived from metamorphic and granitic sources. These deposits are dominantly composed of Kc kaolinite that was formed during weathering.

The deuterium (δD) and oxygen (δO) isotope analysis of the kaolin deposits from the study area helped to discuss better the evolution of the different types of kaolinites described above. Hence, the soft kaolin deposits display δO values varying between 6.04 ‰ and 19.18 ‰ in the Ka+Kb kaolinites, and between 15.38 ‰ and 24.86 ‰ in the Kc kaolinite. The δD values from this unit vary from − 63.06 ‰ to 79.46 ‰, and from −68.85‰ to -244.35‰ in the Ka+Kb and Kc kaolinites, respectively. The semi-flint kaolin deposits are characterized by δO and δD values ranging from 15.08‰ to 21.77‰, and from -71.31‰ to -87.37‰, respectively. Based on these data and on the isotopic composition of both meteoric and ground waters, it was possible to conclude that the kaolinites had not been formed in balance with modern weathering. These values represent the isotopic composition during the time of formation of the kaolinites, as well as mineralogical contamination of framework grains that are now replaced by kaolinites.

APRESENTAÇÃO

Esta tese de doutorado, intitulada "Análise integrada dos depósitos de caulim da região do Rio Capim: fácies, estratigrafia, petrografia e isótopos estáveis", está organizada em quatro capítulos. O primeiro capítulo refere-se ao contexto geológico, problemática do trabalho e aborda considerações científicas que vem sendo conduzidas nos depósitos de caulim da Formação Ipixuna durante as últimas décadas. Além disso, este capítulo enfoca os objetivos da tese e uma breve contextualização da metodologia empregada, a qual será em detalhe descrita em cada capítulo. Os demais capítulos referem-se a artigos científicos: Capítulo 2 – Depositional model of the Ipixuna Formation (Late Cretaceous-?Early Tertiary), Rio Capim Area, Northern Brazil; Capítulo 3 - Origin of the Rio Capim kaolin with basis on optical (petrographic and SEM) data; e capítulo 4 - Origin of the Rio Capim kaolinites (northern Brazil) revealed by $\delta^{18}O$ and δD isotope analysis. A análise sedimentológica consistiu nos estudos de campo incluindo-se descrição faciológica e estratigráfica afim de melhor definir as unidades estratigráficas inseridas no termo "Formação Ipixuna", bem como sua caracterização faciológica e paleoambiental. A continuidade dos estudos faciológicos/estratigráficos foi realizada devido à ocorrência de novas frentes de lavras com características faciológicas ainda não descritas. Este fato possibilitou a coleta de dados faciológicos e estratigráficos adicionais que contribuíram para em melhor entendimento da dinâmica evolutiva do sistema estuarino anteriormente proposto. A análise óptica de 60 seções delgadas e complementadas pela análise de microscopia eletrônica de varredura consistiu na análise petrográfica dos depósitos de Caulim, a fim de discutir a origem dos diferentes tipos de caulinta de acordo com as litologias e estratigrafia da Formação Ipixuna. As análises de isótopos estáveis $^1H/^2H$ e $^{16}O/^{18}O$ em caulinita foram conduzidas baseando-se na análise faciológica e estratigráfica, e petrográfica no intuito de discriminação de fases mineralógicas dos diferentes tipos de caulinita, entender a gênese e evolução dos depósitos de Caulim da porção média do Rio Capim e testar a aplicabilidade do método empregado.

1 INTRODUÇÃO

1.1 CONTEXTO GEOLÓGICO E RELEVÂNCIAS DO TRABALHO

A Sub-Bacia de Cametá esta limitada pelo Lineamento Tocantins (noroeste), Plataforma Bragantina (norte/nordeste) e Arco Capim (leste), e compreende uma área de aproximadamente 12.200 Km^2, sendo localizada no extremo sul do Sistema de Graben do Marajó. Seu preenchimento sedimentar é definido com base em dados de sub-superfície, sendo representado, principalmente, por depósitos cretáceos, terciários e quaternários, os quais foram formados durante a fase de abertura do Oceano Atlântico Equatorial, iniciada no Eocretáceo (Azevedo, 1991; Galvão, 1991) (Figura 1.1). A sucessão sedimentar cretácea inclui as formações Breves (Aptiano-Cenomaniano) e Limoeiro (Cretáceo Superior), formadas em ambientes variando de fluvial a marinho raso (Schaller, 1971; Villegas, 1994). Os estratos terciários são conhecidos como Formação Marajó (Paleoceno-Eoceno), e os quaternários como Formação Tucunaré (Quaternário), ambos atribuídos a ambientes marinho-raso a transicional (Schaller et al., 1971). Estas nomenclaturas estratigráficas não têm sido utilizadas para os depósitos que afloram na borda leste da Sub-Bacia de Cametá, os quais são representados, da base para o topo, pelas formações Itapecuru, Ipixuna e Barreiras, e depósitos Pós-Barreiras e Argila de Belterra. A Formação Itapecuru, aflorante ao longo das margens do Rio Capim, é faciologicamente bastante similar aos depósitos albianos da área de Açailândia (Anaisse Júnior, 1999) e Formação Alcântara do Grupo Itapecuru exposto na Bacia de São Luís-Grajaú (Rossetti, 1997). A Formação Ipixuna, de idade inferida cretácea superior-terciário inferior(?) (Jupiassú, 1970), é representada por estratos caulínicos, os quais foram previamente atribuídos a ambientes fluvio-lacustres (Góes, 1981) e, posteriormente, reinterpretados como registro de depósitos típicos de ambientes marinho-transicional (Santos Júnior, 2002). A Formação Barreiras, de idade miocênica média/superior (Arai et al., 1988), tem sido atribuída a ambientes transicionais do tipo estuarino (Arai et al., 1988; Rossetti et al., 1989; Rossetti et al., 1990; Rossetti, 2000, Rossetti, 2001; Santos Júnior, 2002). Os Sedimentos Pós-Barreiras, de idade suposta plio-pleistocênica (Rossetti, 2001), ocorrem discordantemente sobrepostos à Formação Barreiras, sendo atribuídos a processos gravitacionais e, em parte, eólicos (Rossetti et al., 1989). A Argila de Belterra
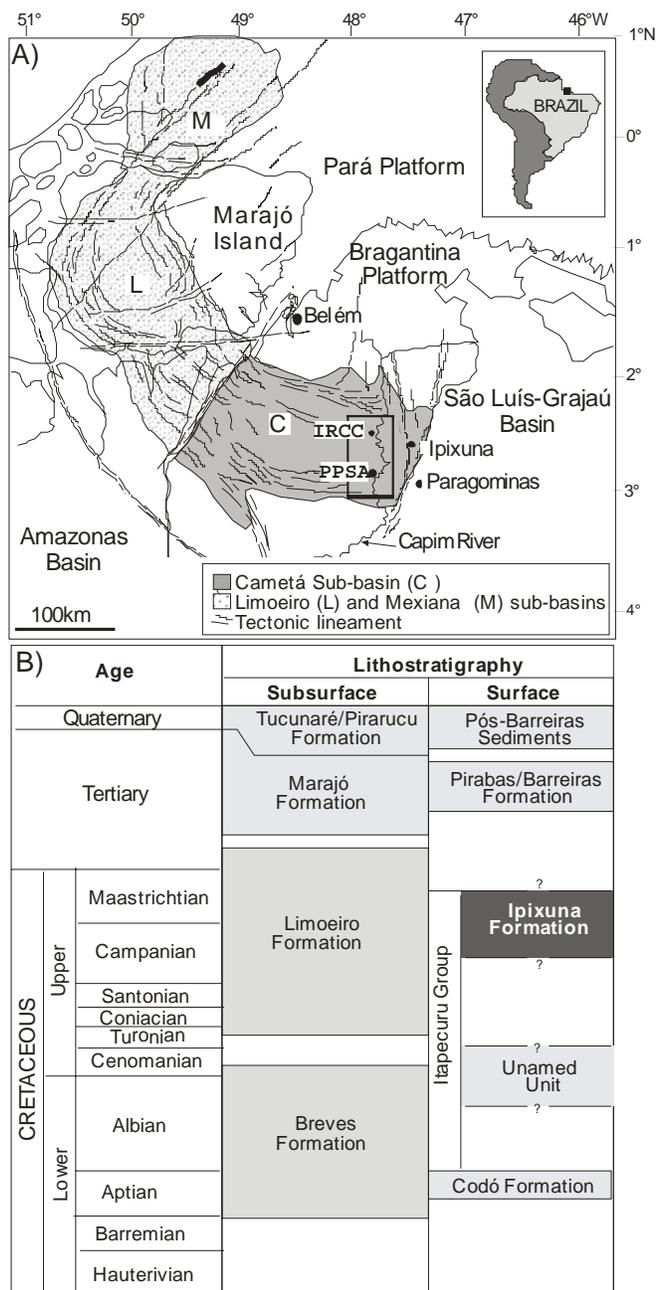
Figura 1.1: A) Mapa de localização da área de estudo, Sub-Bacia de Cametá, Sistema de Graben do Marajó, com indicação das minas de caulim estudadas, PPSA e RCC. SBC=Sub-Bacia de Cametá, SBL=Sub-Bacia de Limoeiro e SBM=Sub-Bacia de Mexiana. B) Carta Litoestratigráfica da Sub-Bacia de Cametá.

compreende uma cobertura sedimentar argilosa, maciça, tendo sua gênese relacionada à: a) formação *in situ*; b) transporte lateral e deposição de material saprolítico; e c)transporte vertical de material saprolítico por termitas (Truckenbrodt *et al.*, 1991; Kotschoubey *et al.*, 1996; 1999). A correlação estratigráfica entre as unidades descritas em superfície e sub-superfície sugere que os depósitos da Formação Ipixuna compreendem estratos da Formação Limoeiro. Esta interpretação baseia-se no posicionamento estratigráfico acima de depósitos albo-cenomanianos correlacionáveis à Formação Alcântara da Bacia de São Luís-Grajaú, o que leva a sugerir possível idade cretácea superior. Isto é ainda sugerido pela ocorrência de depósitos terciários de idade provável miocênica médio/superior sobrepostos à Formação Ipixuna.

A Formação Ipixuna na região do Rio Capim, leste da Sub-Bacia de Cametá, destaca-se por apresentar uma das maiores concentrações mundiais de depósitos de caulim de excelente qualidade à industria de celulose (Krebs & Arantes, 1973; Murray & Keller, 1993). Estes depósitos têm motivado diversos estudos de caráter científico, principalmente geoquímicos, enfocando os aspectos genéticos e evolutivos dos depósitos de caulim, porém sem ênfase na caracterização de seus aspectos sedimentológicos e estratigráficos. Somente recentemente foi feito um esforço no sentido de caracterização faciológica da Formação Ipixuna na Região do Rio Capim (Santos Jr., 2002), o qual possibilitou o estabelecimento preliminar de um modelo deposicional flúvio-estuarino para esta unidade, embora a evolução deste sistema através do tempo geológico ainda permaneceu por ser estabelecida. Os trabalhos geoquímicos propuseram origem in situ para os depósistos de caulim relacionados inicialmente ao desenvolvimento de perfil bauxítico e, posteriormente, ao intemperismo profundo ligado ao rebaixamento progressivo do lençol freático (Truckenbrodt et al., 1991; Kotschoubey et al., 1996; 1999). Porém, estudos preliminares nesta região vêm demonstrando haver uma relação direta entre as diversas fácies da Formação Ipixuna e os tipos de caulim. Além disto, o reconhecimento de superfícies de descontinuidades internas a Formação Ipixuna e coincidente com a delimitação dos depósitos de caulim conhecidos como soft e o semi-flint levou a suspeitar da importância do siginificado estratigráfico no entendimento genético e evolutivo dos tipos de depósitos de Caulim da região do Rio Capim (Santos Jr., 2002; Rossetti & Santos Jr. 2003). Esta observação levou a reforçar a idéia que a mudança no tipo de caulim possa estar vinculada a controle faciológico/estratigráfico. Estudos relacionados à caracterização morfológica e estrutural dos diferentes tipos de caulinita de acordo com os aspectos sedimentológicos e estratigráficos da Formação Ipixuna não tinham sido

sistematicamente conduzidos até o momento. O conhecimento detalhado das variações de fácies sedimentares de acordo com a caracterização das espécies de caulinita representa uma abordagem inédita sobre o desenvolvimento evolutivo das diferentes fases de caulinita da Formação.

O emprego de isótopos estáveis de oxigênio e hidrogênio como ferramenta para o reconhecimento de minerais intempéricos formados em tempos e, portanto, condições paleoambientais distintas podem revelar condições de equilíbrio isotópico com seu ambiente genético, já que uma vez formados, estes minerais retém sua assinatura isotópica, refletindo as condições climáticas do tempo de formação (Savin & Hsieh, 1997).

Por fim, os depósitos de caulim da área do Rio Capim são carentes de investigações científicas realizadas de forma integrada (p.e., faciologia, estratigrafia, petrografia e isótopos estáveis de O e H). Sendo assim, este trabalho se propôs à caracterização dos estratos caulínicos na Região do Rio Capim, procedendo-se a uma análise integrada de aspectos sedimentológicos, estratigráficos, ópticos (petrografia e microscopia eletrônica), mineralógicos e geoquímicos, a fim de possibilitar uma discussão sobre os fatores que influenciaram sua origem e evolução da Formação Ipixuna.

1.2 OBJETIVOS

Esta tese teve como objetivo caracterizar os estratos caulínicos da Formação Ipixuna na Região do Rio Capim procedendo-se a uma análise integrada dos aspectos sedimentológicos, estratigráficos, mineralógicos e de isótopos estáveis. Além disto, consistiu também no prosseguimento aos estudos faciológicos e estratigráficos da Formação Ipixuna, afim de melhor caracterizar o sistema estuarino proposto, bem como entender sua dinâmica evolutiva dentro do contexto de variações do nível do mar relativo. Os estudos ópticos foram conduzidos na finalidade de entender a gênese e evolução das diferentes fases de formação de caulinita, bem como caracterizar petrograficamente os depósitos de caulim de acordo com as características faciológicas/estratigráficas. A determinação da composição isotópica de oxigênio e hidrogênio dos depósitos de caulim da Região do Rio Capim foi empregada de acordo com as características faciológicas e estratigráficas, e petrográficas, a fim de gerar considerações paleoambientais de origem e evolução da Formação Ipixuna, bem como discutir a aplicabilidade do método.

1.3 MÉTODOS

Neste trabalho foram adotadas a seguinte metodologia: análise faciológica/estratigráfica, análise óptica e geoquímica de isótopos de O e H. O estudo faciológico/estratigráfico de detalhe consistiu no mapeamento complementar da arquitetura de fácies deposicionais, e confecção de perfis/seções verticais em novas frentes de lavra observando-se os parâmetros sedimentológicos (p.e., estrutura, textura, mineralogia, padrão de paleocorrentes, traços fósseis e geometria dos corpos sedimentares). Este método foi conduzido nos depósitos cretáceos da Formação Ipixuna na porção média do Rio Capim, devido as novas frentes de lavra regurlamente espostas nas minas da IRCC e PPSA, o que representou a coleta de dados paleoambientais adicionais e contribuiu para o melhor entendimento da dinâmica evolutiva deste sistema estuarino.

O estudo óptico consistiu na análise de 60 seções delgadas sob microscópio petrográfico e eletrônico de varredura, a fim de melhor caracterizar os principais constituintes mineralógicos e entender os processos sin- e pós-deposicionais que controlaram a geração dos diferentes tipos de caulinita. As amostras de caulim foram amostradas seguindo rígido controle faciológico e estratigráfico, de forma a registrar variações litológicas e de processos sedimentares, bem como melhor caracterizar o conteúdo mineralógico e observar os padrões morfológicos das caulinitas. Além disto, tomou-se cautela para se efetuar a coleta de amostras progressivamente abaixo e acima das superfícies de descontinuidade, de forma a possibilitar a análise de possíveis influências de processos associados ao desenvolvimento das mesmas na formação dos diferentes tipos de caulinita.

A análise isotópica de hidrogênio e oxigênio consistiu na separação granulométrica prévia das frações de caulinita Ka, Kb e Kc através de decantação, as quais foram previamente estipuladas pela microscopia óptica. As análises de isótopos estáveis foram realizadas seguindo metodologia dos laboratórios especializados da Universidade de Indiana (EUA). Os dados de isótopos estáveis de oxigênio e hidrogênio foram obtidos através da reação de amostras de caulinita com BrF_5 e por aquecimento a vácuo a 900ºC ou mais, após o início do *outgassing*, respectivamente. Adicionalmente foram feitas análises de isótopos da água meteórica e de subsurperfície para efeitos de comparação com os dados isotópicos da caulinita.

REFERÊNCIAS BIBLIOGRÁFICAS

ANAISSE JÚNIOR, J. 1999. *Fácies costeiras dos Depósitos Itapecuru (cretáceo), região de Açailândia, Bacia do Grajaú*. Belém, UFPa. Cento de Geociências. 86p. (Dissertação de Mestrado).

ARAI, M.; UESUGUI, N.; ROSSETTI, D.F.; GÓES, A.M. 1988. Considerações sobre a idade do Grupo Barreiras no nordeste do estado do Pará. In: CONGRESSO BRASILEIRO DE GEOLOGIA, 35, Belém, *Anais...* Belém, Sociedade Brasileira de Geologia. V.2, p. 738-752

AZEVEDO, R.P. 1991. *Tectonic Evolution of Brasilian Equatorial Continental Margin Basins*. Royal School of Mines Imperial College, London.412p. (Tese de Doutorado).

GALVÃO, M.V.G., 1991. *Evolução Termodinâmica da Bacia do Marajó, estado do Pará, Brasil*. Universidade de Ouro Preto. 193p. (Dissertação de Mestrado).

GÓES, A.M., 1981. *Estudo Sedimentológico dos Sedimentos Barreiras, Ipixuna e Itapecuru, no Nordeste do Estado no Pará e Noroeste do Maranhão*. Belém. Universidade Federal do Pará. 55 p. (Dissertação de Mestrado).

JUPIASSÚ, A.M.S. 1970. Madeira Fóssil – *Humiriaceae* de Irituia, Estado do Pará. *Boletim do Museu Paraense Emilio Goeldi*. Nova Série, 14: 1-12.

KOTSCHOUBEY, B.; DUARTE, A. L. S.; TRUCKENBRODT, W. 1999. Cobertura bauxítica e origem do caulim do Morro do Felipe, Baixo Rio Jari, Estado do Amapá. *Revista Brasileira de Geociências*. 29:331-338.

KOTSCHOUBEY, B.; TRUCKENBRODT, W.; HIERONYMUS, B. 1996. Depósitos de Caulim e Argila Semi-flint no nordeste do Pará. *Revista Brasileira de Geociências*. 26(2):71-80.

KREBS, A.S.J. & ARANTES, J.L.G., 1973. Pesquisa de caulim no Rio Capim, Estado do Pará. In: CONGRESSO BRASILEIRO DE GEOLOGIA, 27, Aracaju, *Anais...* Aracaju, SBG. V.1, p. 181-191.

MURRAY, H.H. & KELLER, W.D. 1993. Kaolins, Kaolins and Kaolins. In Kaolin Genesis and Utilization, eds. Murray, H., Bundy, W., Harvey, C., pp. 1-24, Clay Mineral Society Special Publication **1**.

ROSSETTI, D.F., 1997. Internal Archicteture of mixed tide and storm influenced deposits: an example from the Alcântara Formation, northern Brazil. *Sedimentary Geology*. 114:163-188.

ROSSETTI, D.F., 2000. Influence of low amplitude/ higth frequency relative sea level changes in a wave-dominated estuary (Miocene), São Luís basin, northern Brazil. *Sedimentary Geology*, 133: 295-324.

ROSSETTI, D.F., 2001. Sedimentary Evolution of Late Cenozoic Deposits in the Nortears of Pará State, Brasil: Evidence of sea level floctuações. *Journal of South Americam Earth Sciences*.

ROSSETTI, D.F. & SANTOS JR., A. E., 2003. Events of soft sediment deformation and mass failure in Upper Cretaceous estuarine deposits (Cametá Basin, northern Brazil) as evidence for seismic activity. *Sedimentary Geology*, 161:107-130.

ROSSETTI, D.F.; GÓES, A.M.; TRUCKENBRODT, W. 1990. A Influência Marinha nos sedimentos Barreiras. *Boletim do Museu Paraense Emílio Goeldi*. Belém. 2:17-29.

ROSSETTI,D.F.; TRUCKENBRODT, W.; GÓES, A.M. 1989. Estudo Paleoambiental e Estratigráfico dos Sedimentos Barreiras e Pós-Barreiras na Região Bragantina, Nordeste do Pará. *Boletim do Museu Paraense Emílio Goeldi*, Série Ciências da Terra, 1: 25-74.

SANTOS JR, A.E.A. 2002. *Reconstrução Peloambiental e Estratigráfica de Depósitos Cretáceos e Terciários expostos na borda sudeste da Sub-Bacia de Cametá, Norte do Brasil.* Belém. Universidade Fedaral do Pará. Centro de Geociências. P.131 (Dissertação de Mestrado).

SAVIN, S.M. & HSIEH, J.C.C. 1998. The hydrogen and oxygen isotope geochemistry of pedogenic clay minerals: principles and theoretical background. *Geoderma*. 82:227-253.

SCHALLER, H.; VASCONCELOS, D.N.; CASTRO, J.C., 1971. Estratigrafia Preliminar da Bacia Sedimentar da Foz do Rio Amazonas. In: CONGRESSO BRASILEIRO DE GEOLOGIA, 25., São Paulo. *Anais...* São Paulo; Sociedade Brasileira de Geologia. V.3, p.189-201.

TRUCKENBRODT, W.; KOTSCHOUBEY, B.; SCHELLMANN, W. 1991. Composition and origin of the clay cover on North Brazilian laterites. *Geologische Rundschau*, 80:591-610.

VILLEGAS, J.M.C. 1994. *Geologia Estrutural da Bacia do Marajó.* Belém, UFPA,Centro de Geociências. 119p. (Dissertação de Mestrado).

2. DEPOSITIONAL MODEL OF THE IPIXUNA FORMATION (LATE CRETACEOUS-?EARLY TERTIARY), RIO CAPIM AREA, NORTHERN BRAZIL

Antônio Emídio de Araújo SANTOS Jr

and Dilce de Fátima ROSSETTI

2.1 ABSTRACT

Exposures along open quarries located in the eastern Cametá Sub-Basin provide an opportunity to assess further discussion focusing on the depositional environments of the Upper Cretaceous-?Lower Tertiary Ipixuna Formation. The lower part of this unit emphasized herein, known as the "soft kaolin", consists mostly of kaolinitized sandstones and mudstones that exhibit well preserved sedimentary structures that are particularly favorable for facies analysis and paleoenvironmental reconstructions. The sandstones are chiefly cross-stratified, typically with low angle, locally reverse oriented foresets with reactivation surfaces and/or mud drapes. These characteristics, together with a trace fossil assemblage consisting of *Ophiomorpha, Thalassinoids, Planolites, Teichichnus, Taenidium* and *Skolithos,* conform to deposition in a coastal setting influenced by tidal processes. Although a previous study has documented tidal processes during deposition of the soft kaolin (Santos Jr. and Rossetti, 2003), this paper shows that the influence of tidal currents was much more important than initially proposed. Hence, the kaolinitized deposits are attributed to tidally influenced fluvial channel (Facies Association A), tidal channel (Facies Association B), tidal flat/mangrove (Facies Association C), and tidal sand bar/tidal sandy flat (Facies Association D), all together comprising a tide-dominated estuarine system.

Keywords: soft kaolin, Ipixuna Formation, Cametá Sub-Basin, tide-dominated estuary, sedimentary facies, paleoenvironment.

2.2 INTRODUCTION

Several mineralogical and geochemical studies (*e.g.*, Truckenbrodt *et al.*, 1991; Kotschoubey *et al*., 1996, 1999; Souza, 2000) have been undertaken on the Ipixuna Formation (Upper Cretaceous-?Lower Tertiary), which is exposed in the eastern Cametá Sub-Basin. These studies have been motivated by the fact that this unit contains one of the largest kaolin reserves in the world, the Rio Capim kaolin, which has received particular attention due to its high brightness. Despite the economic interest, sedimentologic studies aiming paleoenvironmental interpretations of the Rio Capim kaolin quarries are still inadequate to provide a detailed reconstruction of its mode of deposition.

Traditionally known as fluvial to lacustrine in origin (Góes, 1981), the Ipixuna Formation has been more recently related to a coastal depositional system (Santos Jr. and Rossetti, 2003). Sedimentary facies described in that study were attributed to tidal processes. Thereby, several tidally influenced depositional environments were recognized, which collectively led the authors to the interpretation of a wave-dominated estuary. This interpretation was based on the presence of tidal delta deposits along road cuts between the towns of Ipixuna and Paragominas, which were considered correlative to the soft kaolin unit exposed in the kaolin quarries (Santos Jr. and Rossetti, 2003). However, stratigraphic studies have revealed that this unit is more complex than initially thought, encompassing different stratigraphic units attributed to high-frequency depositional sequences (Rossetti, 2004; Rossetti and Santos Jr., 2006). Taking this into account, correlation of the tidal delta deposits with the soft kaolin unit of the Ipixuna Formation in the Rio Capim area is problematic. The continuous kaolin exploitation has resulted in a series of fresh exposures that allow more detailed facies and stratigraphic analyses. As a result, other facies assemblages can be characterized, providing additional elements for a more refined reconstruction of the depositional model.

The goal of this paper is to provide a more complete description of the facies and facies associations of the soft kaolin unit of the Ipixuna Formation. These are based on exposures recently available in two quarries, the IRCC and the PPSA in the Rio Capim area (Fig. 1), in order to furnish a better interpretation of both the sedimentary processes and the depositional environments. Based on these data, it is possible now to assay a wave-dominated estuarine model previously proposed for the soft kaolin.
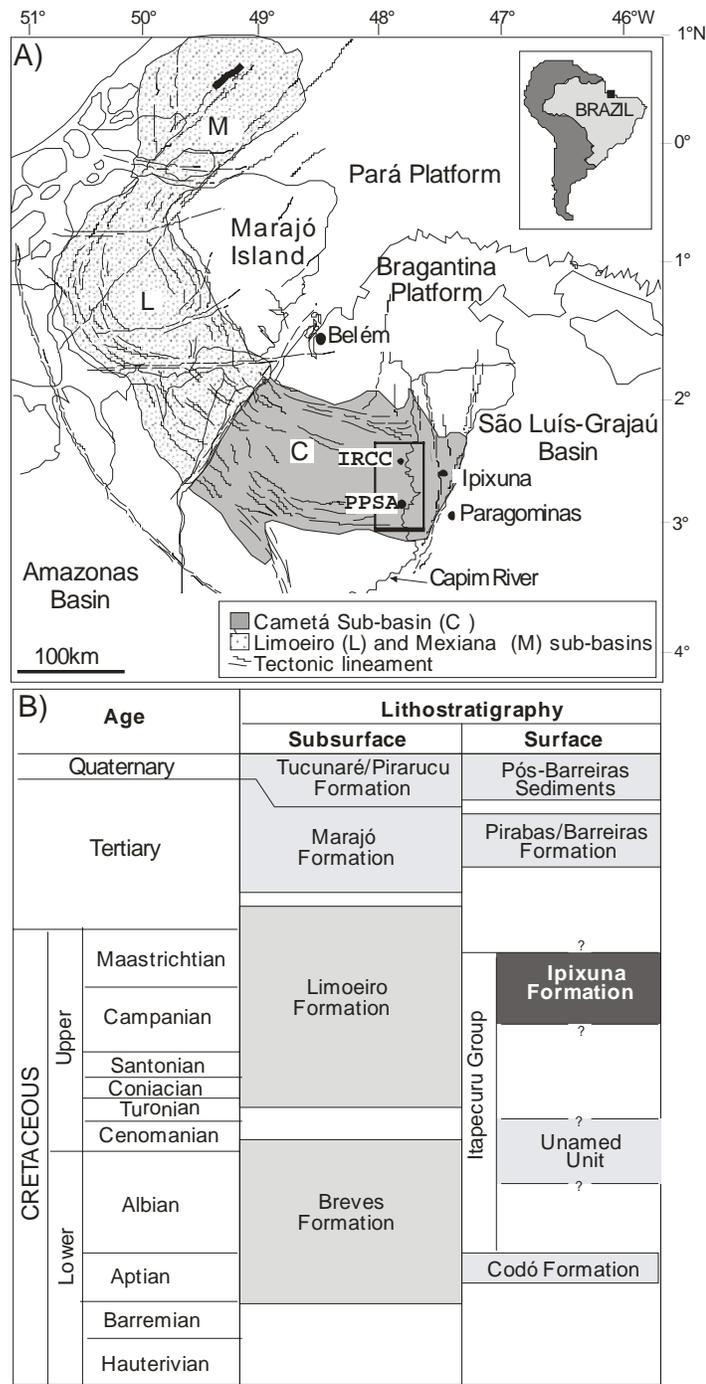
Figure 2.1: A) Location map of the study area in the Rio Capim area, Cametá Sub-Basin, with the studied kaolin quarries PPSA and RCC indicated. B) Stratigraphic chart representing the sedimentary successions in the Cametá Sub-Basin, both in the subsurface and surface exposures.

2.3 GEOLOGICAL FRAMEWORK

The Cametá Sub-Basin, together with the Limoeiro, Mexiana and Mocajuba sub-basins, constitute the Marajó Graben System, located at the mouth of the Amazon River, northern Brazil. These structures were formed by NW–SE and NNW–SSE normal faults, as well as NE–SW and ENE–WSW strike-slip faults during the opening of the Equatorial South Atlantic Ocean (Azevedo, 1991; Galvão, 1991; Villegas, 1994; Costa *et al.*, 2001).

The Cametá Sub-Basin is up to 10 km thick, and includes Cretaceous and Cenozoic deposits (Fig. 2), which are mostly known from subsurface data. The Cretaceous succession includes the Breves Formation (Aptian-Cenomanian) and the Limoeiro Formation (Late Cretaceous), considered to be fluvial and marine transitional in origin (Villegas, 1994). The Tertiary and Quaternary deposits include the Marajó Formation (Paleocene-Eocene) and the Tucunaré Formation (Pleistocene), both formed within marine to transitional environments.

Exposures of Cretaceous rocks in the Cametá Sub-Basin are only found in the eastern margin of the basin, where Albian/Cenomanian deposits are cut by a kaolinitized Upper Cretaceous unit referred to as the Ipixuna Formation. This unit is particularly well exposed in the Rio Capim Kaolin area, where it approaches thicknesses of 40 m and consists of kaolinitized mudstones and sandstones. Previously regarded as a single stratigraphic unit, the Ipixuna Formation has been recently subdivided into two intervals, bounded by a discontinuity surface that is marked by paleosol (Rossetti and Santos Jr., 2003; 2006; Rossetti, 2004). The lower part of the interval corresponds to the deposits referred to herein as the soft kaolin unit. The upper part corresponds to a hard kaolin unit, known as the semi-flint, due to the composition of flint-like fire clay that consist of endured kaolinite showing no plasticity when ground up. An intermediate unit characterized by soft-sediment deformed deposits bounded also by discontinuity surfaces occurs between the soft kaolin and semi-flint at some localities (Rossetti and Santos Jr., 2003). The facies analysis presented herein is focused solely in the soft kaolin unit, which bears the commercially exploited kaolin.
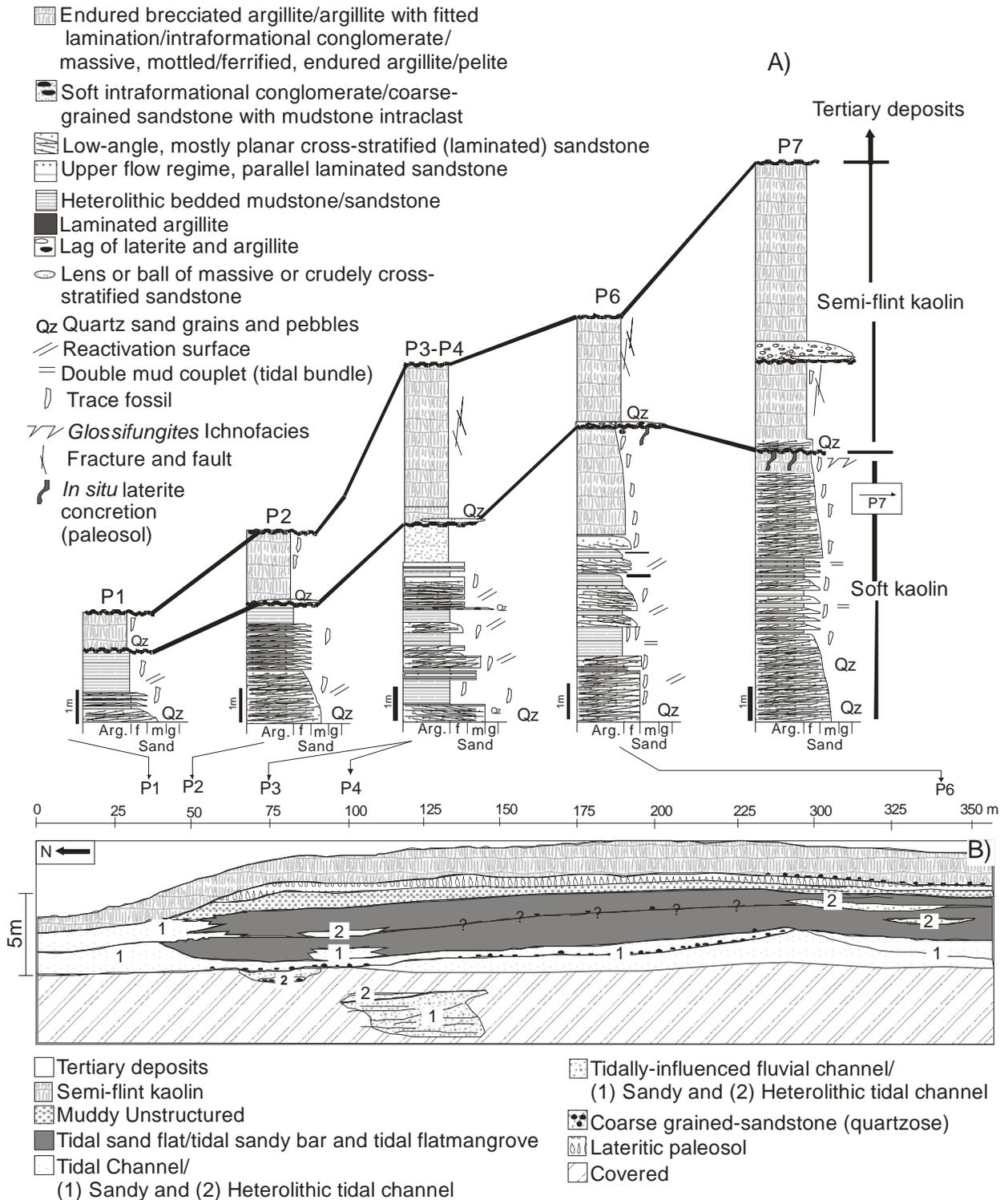
Figure 2.2: Measured lithostratigraphic profiles (A) and geologic cross-section (B) illustrating the sedimentologic characteristics and spatial distributions of facies and facies associations present in the soft kaolin unit of the Ipixuna Formation in the PPSA quarry. Profile P7 is not in shown this geological section, being located circa 200 m to the south.

2.4 FACIES ANALYSIS OF THE SOFT KAOLIN

The soft kaolin deposits of the Ipixuna Formation in the Rio Capim area correspond to a nearly 20 m thick, fining-upward unit, consisting of kaolinitized, locally lenticular or tabular sandstones, as well as mudstones, and conglomerates. Where the base of these deposits is exposed, an unconformity (cf. Rossetti, 2004) marked by a lag of mudstone clasts and iron-cemented, coarse-grained to pebbly sandstones separates them from the underlying Albian to Cenomanian rocks (Rossetti and Santos Jr., 2003). The top of the soft kaolin unit is also an unconformity, marked by a paleosol that local displays a thin (up to 20 cm thick) interval of lateritic concretions overlain by the semi-flint kaolin unit (Santos Jr. and Rossetti, 2003).

Despite the high degree of kaolinitization, which is primarily due to replacement of lithic grains and detritic clay minerals, the soft kaolin is characterized by well-developed primary stratification, providing the basis for reconstructing the depositional processes and paleoenvironmental settings. Based on geometry, sedimentary structures, grain sizes, and suite of trace fossils, four intergradational facies associations were recognized and attributed to (Figs. 2 and 3): 1. tidally-influenced fluvial channel (Facies Association A); 2. tidal channel (Facies Association B); 3. tidal flat/mangrove (Facies Association C); and 4. tidal sand bar/tidal sandy flat (Facies Association D). Facies Association A, dominant in the base of the studied quarries, grades upward into deposits that show stronger tidal influence producing a typical fining-upward successions. Facies associations B and C are better developed in the PPSA quarry, whereas Facies Association D is more abundant in the RCC quarry.

2.4.1 Facies Association A: Tidally influenced Fluvial Channel

Facies association A (Fig. 3A-E) is up to 5.5 m thick and occurs at the base of the soft kaolin deposits, where it consists primarily of sandstones composed of abundant quartz grains. Intraformational conglomerates and heterolithic mudstones/sandstones are also present. This facies association comprises fining- and thinning-upward packages that are up to 2.5 m thick and are bounded at the base by erosional discontinuity surfaces. Where exposures are laterally continuous, the basal surface of the fining/thinning-upward successions displays a broad concave upward shape, up to 300 m wide (Fig. 3A-D). Trace fossils are very rare in this facies association, including only undetermined vertical burrows.

Three facies are present in this association including, in order of decreasing abundance: tabular/trough cross-stratified or laminated sandstone (Facies St); intraformational conglomerate (Facies Ci); and heterolithic mudstone/sandstone (Facies Ht). The sandstones (Fig. 3E) are, in general, poorly sorted, consist of sub-rounded, coarse- to medium-grained sands, and display tabular and trough cross-stratification or cross-lamination (Facies St), the latter with set thicknesses averaging 0.3 m and less than 5 cm, respectively. The cross sets, which typically decrease in size upward, dip consistently at low angles (typically between 10-20°). Although they dip dominantly to the N/NE, oppositely dipping S/SW cross sets are common in this facies (Fig. 3D). Additionally, reactivation surfaces are abundant and define foreset packages averaging 10 cm thick, which are locally marked by mud drapes (Fig. 2).

Facies Ci is dominantly confined to the base of the fining-upward successions, and consists of poorly sorted conglomerates composed of clasts of laminated mudstones. These average 5 cm in diameter, and occur mixed with poorly sorted quartz granules. Sedimentary structures, where present, are incipient and dominated by crude trough cross stratification and normal grading.

Facies Ht consists of interbedded, fine to very fine-grained sandstones and laminated mudstones that form wavy and lenticular beddings. This facies is only locally found at the top of some fining/thinning upward successions, where it forms beds that are less than 0.4 m thick.
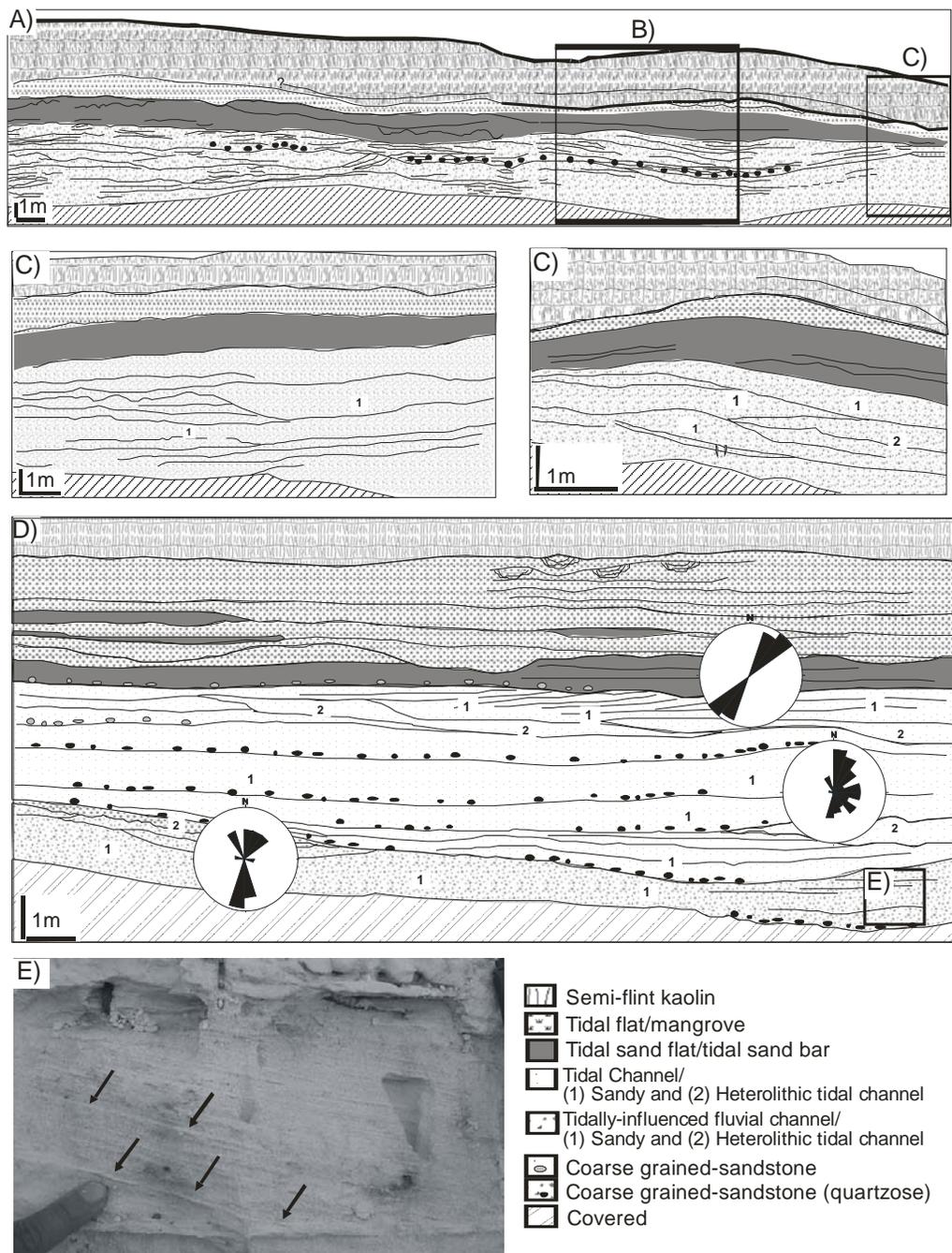
Figure 2.3: A-D) Representative geologic sections, illustrating the sedimentologic characteristics and spatial distributions of facies and facies associations of the soft kaolin unit of the Ipixuna Formation in the RCC quarry. Note that B and C are close-ups of Figure A, illustrating the tidally-influenced fluvial channel deposits (Facies Association A). Observe, also, that D contains rose diagrams with paleocurrent data obtained from cross-stratified sandstones of tidally influenced fluvial channel (Facies Association A) and tidal channel (Facies Association B), as well as parting lineation of upper flow regime tidal sand flat/sand bar (Facies Association D) deposits. E) Close-up photograph of tidal-influenced fluvial channel deposits (Facies Association A), showing foreset packages with mud drapes (arrows).

***Interpretation*:** Facies Association A is attributed to tidal-influenced fluvial channels. The presence of deposits with concave upward basal surfaces, though not exclusive to, is suggestive of flow confinement within channels. Where this feature is not present, the fining/thinning-upward facies successions are bounded by sharp, erosional basal surfaces, and attest to deposition during decreasing flow energy, as typical of channel fills. Facies Ci records episodes of highest energy, when channels were scoured into underlying muddy deposits. The muddy accumulations were eroded and re-deposited as lags at the channel bottom. Facies St was formed by migration of small to medium scale, 2D- and 3D-bedforms within channels, and Facies Ht records alternating sand and mud deposition formed as topset beds during channel abandonment.

Facies Association A is attributed to tidal-influenced fluvial channels formed in proximal estuarine areas, near the limits of the fluvial realm. Although weak, tidal currents might reach these inner estuarine areas and rework sediments brought from the fluvial channels. The recognition of this type of setting in the geological record might be problematic (e.g., Ashley and Renwick, 1983; Allen, 1991; Hori *et al.*, 2001; Leckie and Singh, 1991; Dalrymple *et al.*, 1992; Plink-Bjorklund, 2005), particularly where the distribution of the depositional environments throughout a proximal-distal transect cannot be observed, as in the case of the study area. However, the poor sorting, very coarse sand to gravel grain sizes, and scarcity or absence of bioturbation are features that led to claim a fluvial origin for this facies association, distinguishing it from other channel deposits formed under dominant tidal processes (see Facies Association B described below).

Facies Association A displays features that cannot be justified exclusively by unidirectional fluvial flows. The bipolar paleocurrent data, coupled with the common reactivation surfaces and mud drapes separating packages of foresets, are features suggestive of some degree of tidal reworking. The dominance of foresets dipping consistently at low angles is a further evidence of tidal influence, as migration of 2D- and 3D-bedforms in tidal settings typically results in cross sets that display low angle dipping foresets (Shanley *et al.*, 1992; Plink-Bjorklund, 2005).

Considering the foregoing interpretation, it is noteworthy that the position of Facies Association A, lying at the base of the soft kaolin unit, is a situation expected when a fluvial system is flooded during a transgression to form an estuarine valley (e.g., Dalrymple *et al.*, 1992; Zaitlin *et al.*, 1994).

2.4.2 Facies Association B: Tidal Channel

Facies Association B (Figs. 3D, 4 and 5) is up to 10 m thick and consists of : tabular and trough cross-stratified/laminated sandstone (Facies St) and horizontal laminated sandstone (Facies Sh), alternating sandstone and mudstone displaying heterolithic bedding (Facies Ht), and subordinate intraformational conglomerate (Facies Ci). These deposits, which are typically bounded at the base by broad concave upward surfaces with lengths of up to 200 m (Figs. 4A-C), are internally organized into fining- and thinning-upward successions averaging 3 m thick. More rarely, this facies association comprises entire intervals of heterolithic bedding (Fig 4B and C), which are cut internally by multiple erosive basal concave upward surfaces that are locally mantled by intraformational conglomerate.

Facies St consists of moderately sorted, coarse- to very fine-grained, tabular and trough cross-stratified sandstones having grains that are mostly subangular to subrounded. The cross sets, up to 0.3 m thick, consistently display low angle foresets. Paleocurrent measurements indicate main vectors to the NNE and SSW (Fig. 3D). A typical feature of Facies St is stacked packages of foresets averaging 5-10 cm thick that are defined by reactivation surfaces and/or mudstone drapes. Facies St locally grades laterally into fine- to very fine-grained, horizontal laminated sandstone (facies Sh). The sandstones are, in general, moderately sorted with subrounded grains and form packages that are 0.1-0.2 m thick, and commonly bounded by mud drapes.

Facies Ht comprises alternating layers of medium- to fine-grained sandstone and mudstone, forming wavy, lenticular and flaser bedding, that might dip at low angles (*i.e.*, $>10^{o}$). Individual lithological packages are up to 20 cm thick. Thicknesses of sandstone and mudstone beds are not constant upwards, rather varying progressively into alternating thicker and thinner bundles, the latter displaying a higher concentration of mud layers (Fig. 4D and E). The sandstone layers are moderately to well sorted. Thicker sandstone layers are internally characterized by plane parallel stratification, cross stratification, or are structureless. Locally, cross strata display oppositely dipping foresets. The mudstone and siltstone may display parallel lamination or appear massive.

Facies Ci occurs locally, typically mantling concave upward surfaces. It consists of sub-angular to sub-rounded mudstone and sandstone intraclasts up to 20 cm in diameter. Facies Ci is generally massive, or displays crude trough cross-stratification and normal grading.

A typical feature of Facies Association B is the abundance and variety of trace fossils, including *Thalassinoides, Planolites, Teichichnus, Taenidium* and *Skolithos* (Fig. 5).
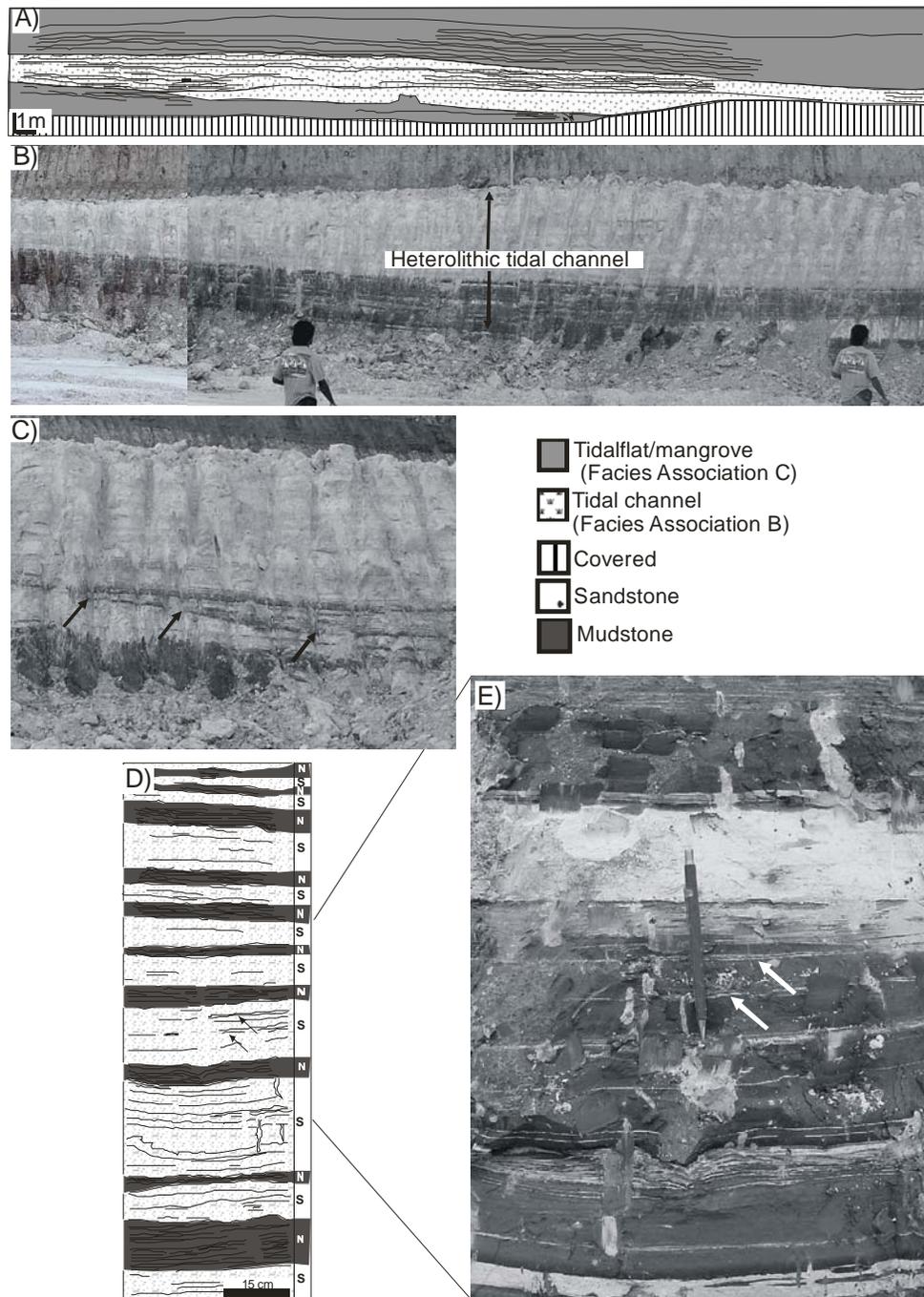
Figure 2.4: Tidal channel (Facies Association B) and tidal flat/mangrove (Facies Association C). A) Geologic section illustrating the spatial relationship between facies associations B and C. Note the gentle concave upward surface that defines the base of a tidal channel deposit. B) General view of a heterolithic tidal channel deposit (man = 1.65 m tall). Dark color = muddier deposits. C) Detail of the sharp, erosional base of a heterolithic tidal channel. D) Heterolithic deposits typical of facies associations B and C, illustrating a vertical succession attributed to tidal bundles. These consist of rhythmically alternating sandier (spring) and muddier (neap) cycles (S=spring; N=neap). Mud couplets attributed to ebb/flood fluctuation are locally present in some spring cycles (black arrows), and undetermined trace fossils are common (white arrows).
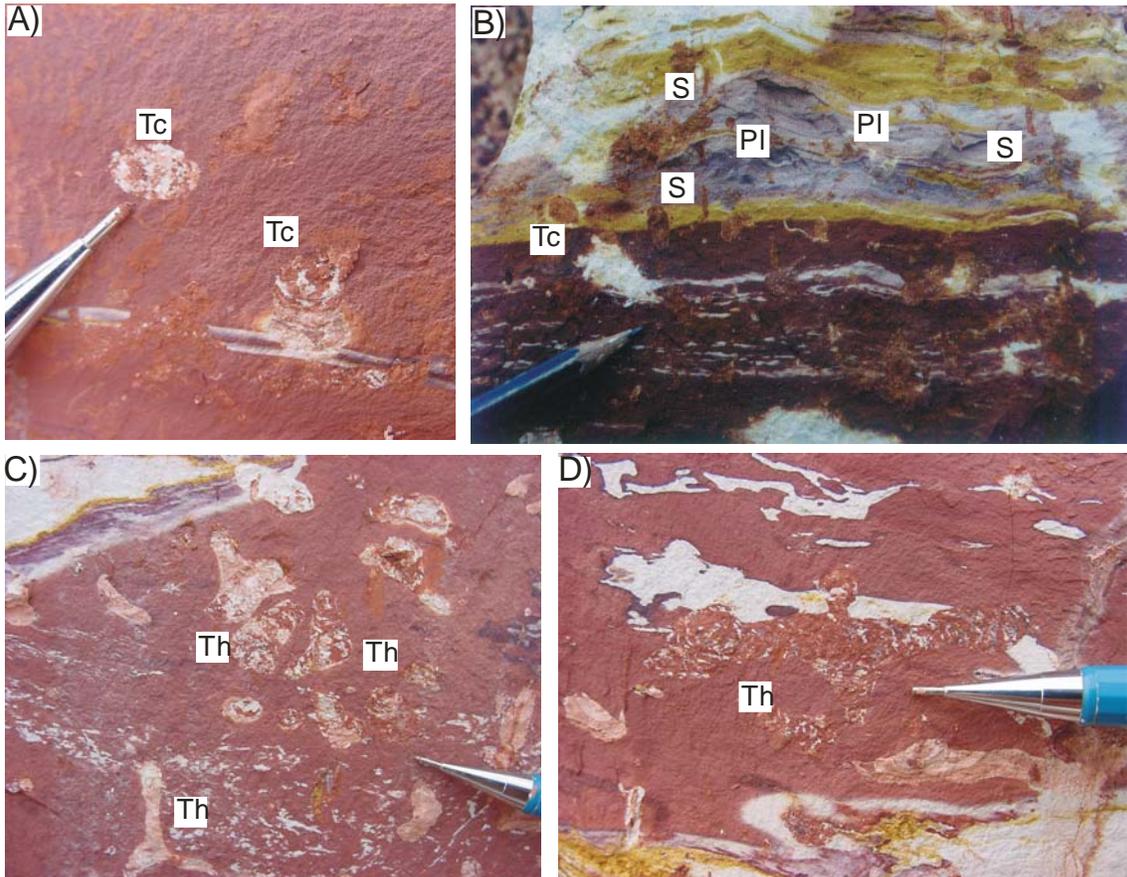
Figure 2.5: A-D) Details of trace fossils representative of tidal channel (Facies Association B) and tidal flat/mangrove deposits (Facies Association C): *Thalassinoides* (Th), *Planolites* (Pl), *Teichichnus* (Tc) and *Skolithos* (S).

Interpretation: Like facies association A, Facies Association B was also formed by confined flows within channels, as indicated by the basal concave upward erosional bounding surface. The internal organization, configuring thinning- and fining-upward successions formed by the upward gradation from intraformational conglomerates to sandstones and into heterolithic bedding of sandstone and mudstones, attests to deposition during waning flow, typical of channels prone to lateral accretion.

Internal features that favor channel deposition under the influence of tidal currents include: 1) an abundance of reactivation surfaces and mud drapes within cross sets; 2) oppositely dipping foresets; 3) low-angle dipping cross sets; and 4) alternating thicker and thinner packages of sandstones and mudstones within the heterolithic facies. Generation of all these structures requires fluctuating current energy, as occurs most typically in tidal settings In particular, the successions of alternating thicker and thinner bundles of the heterolithic facies are attributed to sediment aggradation under influence of tidal currents that vary in strength and duration on a daily and monthly basis. The alternations of sandier and muddier packages may be related to neap-spring tidal variations (Nio and Yang, 1991). The typical fining/thinning upward successions suggest that tidal channels filled up more or less continuously during rising sea level (Dalrymple *et al.*, 1992).

The proposed deposition by tidal processes in brackish water conditions is consistent with the ichnologic assemblage described in this facies association. The low-diversity association of *Ophiomorpha, Thalassinoides, Planolites, Teichichnus, Taenidium* and *Skolithos* is consistent with deposition in nearshore settings influenced by stressed environmental conditions (Benynon and Pemberton, 1992; MacEachern and Pemberton, 1994; Pemberton *et al.*, 2001; Uchman *et al.*, 2004).

Considering the proposed tidal channel interpretation for Facies Association B, the inclined heterolithic strata (Facies Ht) are related to lateral accretion on tidally influenced point bars, with sandstones and mudstones recording high and low tidal flow stages, respectively. This type of deposit is usually associated to the presence of channels with high sinuosity (Thomas *et al.*, 1987; Smith, 1988; Fenies and Faugères, 1998; Nouidar and Chellaï, 2001; Mack *et al.*, 2003; Gao, 2004; Plink-Bjorklund, 2005).

Sedimentary and biogenic features similar to the ones recorded here have been found in association with many tidal channel deposits described in the literature (*e.g.*, Clifton, 1983;

Smith, 1988; De Boer, 1989; Leckie and Singh, 1991; Nio and Yang, 1991; Plink-Bjorklund, 2005).

2.4.3 Facies Association C – Tidal Flat/?Mangrove

Facies Association C (Fig. 4A) is better developed in the PPSA quarry, is up to 5 m thick, and records the finest deposits of the soft kaolin unit. It consists essentially of tabular packages of distinctively yellow to red colored, highly bioturbated, heterolithic-bedded sandstones and mudstones. These deposits are laterally continuous for up to 1 km and are intergraded with facies associations B and D.

This association is internally characterized by an overall fining- and thinning-upward succession, and consists of only two facies: heterolithic mudstone/sandstone (Facies Ht) and mudstone (Facies M). Like Facies Association B, Facies Ht, represented mostly by *linsen*, is organized into several minor cycles of 0.3-0.4 cm. Then form packages of sandstones and mudstones that progressively change their thickness, varying from thicker to thinner upward (Fig. 3). Facies M consists of thicker packages of mudstones displaying only streaks of coarse-grained siltstones and very fine-grained sandstones.

Facies Association C is highly bioturbated, mainly recording traces that are comparable to those of the previous association. One except on is the absence of *Skolithos* and *Ophiomorpha.*

Interpretation: Facies Association C is interpreted as the record of tidal flat settings, which might have been associated with mangroves, though root marks were not recognized probably to the intense kalinitization. A tidal flat is consistent with the intergrading of this facies association with Facies Association B (Tidal Channel) and Facies Association D (Tidal Sand Flat/Sand Bar). Deposition in a flat-lying area is suggested by the tabular geometry and great lateral continuity of the association. The mudstones indicate deposition from suspensions in low energy environments, while the heterolithic deposits conform to a setting with alternating traction sediment transport and deposition from suspensions (Collinson, 1996). In addition to a genetic association with other tidal deposits, the upward change in thickness of sand/mud bundles of the heterolithic facies attests to tidal currents as the main depositional process.

The sole occurrence of heterolithic deposits and mudstones in Facies Association C suggests intertidal and supratidal deposition. The progradation of heterolithic deposits into mudstones produces a vertical fining-upward succession, consistent with tidal flat progadation (Klein, 1985). The thickness of the tidal flat succession in the study area indicates a macrotidal regime, with a minimum paleotidal range of 5 m.

The ichnologic assemblage is used as a further confirmation of the proposed depositional setting. Hence, like Facies Association B, the trace fossils are typical of estuarine environments. The absence of *Ophiomorpha* and *Skolithos* is due to decreases in energy, as these traces are more common in high-energy environments. *Ophiomorpha* and *Skolithos* are also typical of areas subjected to high sedimentation mobility (Zonneveld *et al.*, 2001; Malpas *et al.*, 2005; Savary *et al.*, 2004).

2.4.4 Facies Association D – Upper Flow Regime Tidal Sand Flat/Sand Bar

Facies Association D (Fig. 6A-G), up to 5 m, is very widespread in both of the studied quarries, where it grades laterally and vertically into facies associations B and C (Figs. 1 and 2). Like Facies Association C, these deposits are laterally continuous, forming tabular packages that are bounded at the base by either planar or only slightly undulating (though not erosive) surfaces. These deposits might also be lenticular, with lenses up to 0.4 m thick and 6 m long. Fining- and thickening-upward cycles are present.

This facies association differentiates from the previous association on the basis of predominance of horizontally stratified sandstones (Fig. 6A), with subordinate heterolithic deposits (Facies H). The sandstone consists of three facies: horizontal-laminated to low-angle dipping cross-stratified sandstones (Facies Shl), tabular- and trough cross-stratified sandstones (Facies St), and climbing current ripple cross-laminated sandstones (Facies Sc). These facies are characterized by well-sorted, well-rounded, fine- to very fine-grained sandstones, displaying high concentrations of heavy minerals on plane beddings (Fig. 6B). Sets in Facies Shl, which dominates in this association, ranges in thickness from 0.4-0.5 m, and indicates northward paleoflows. An interesting feature of Facies Sc is the abundance of parting lineations, which indicate a NE/SW azimuth for paleoflow (Fig. 6C). Other features associated with Facies Shl are pinch and swell structures and symmetrical (oscillation) ripple marks. In addition, undulating

laminations displaying internal truncations are common and form broad scours or swales with either symmetrical or asymetrical geometries (Fig. 6D). Facies Sc occurs only locally, being characterized by tabular or highly undulating lower set boundaries. Facies St and Sc are subordinate, and intergrade with facies Shl. Facies St alternates rhythmically with Facies Shl, resulting in individual packages 10-20 cm thick.

Heterolithic mudstone/sandstone (Facies Ht), alternating with trough cross-stratified sandstone (Facies St), occurs as lenses averaging 0.5 m thick and 8 m long. These are interbedded with the tabular sandstone described above. The sandstones show well-rounded, well sorted, fine- to medium-grained sand, and display cross lamination and small- to medium-scale cross stratification. Locally, cross sets with abundant reactivation surfaces and highly undulating set boundaries are present. Facies Ht and St are typically arranged into coarsening- and thickening-upward successions.

Trace fossils dispersed in this facies association consist of *Thalassinoides, Ophiomorpha, Skolithos, and Planolites* (Fig. 6E-G).
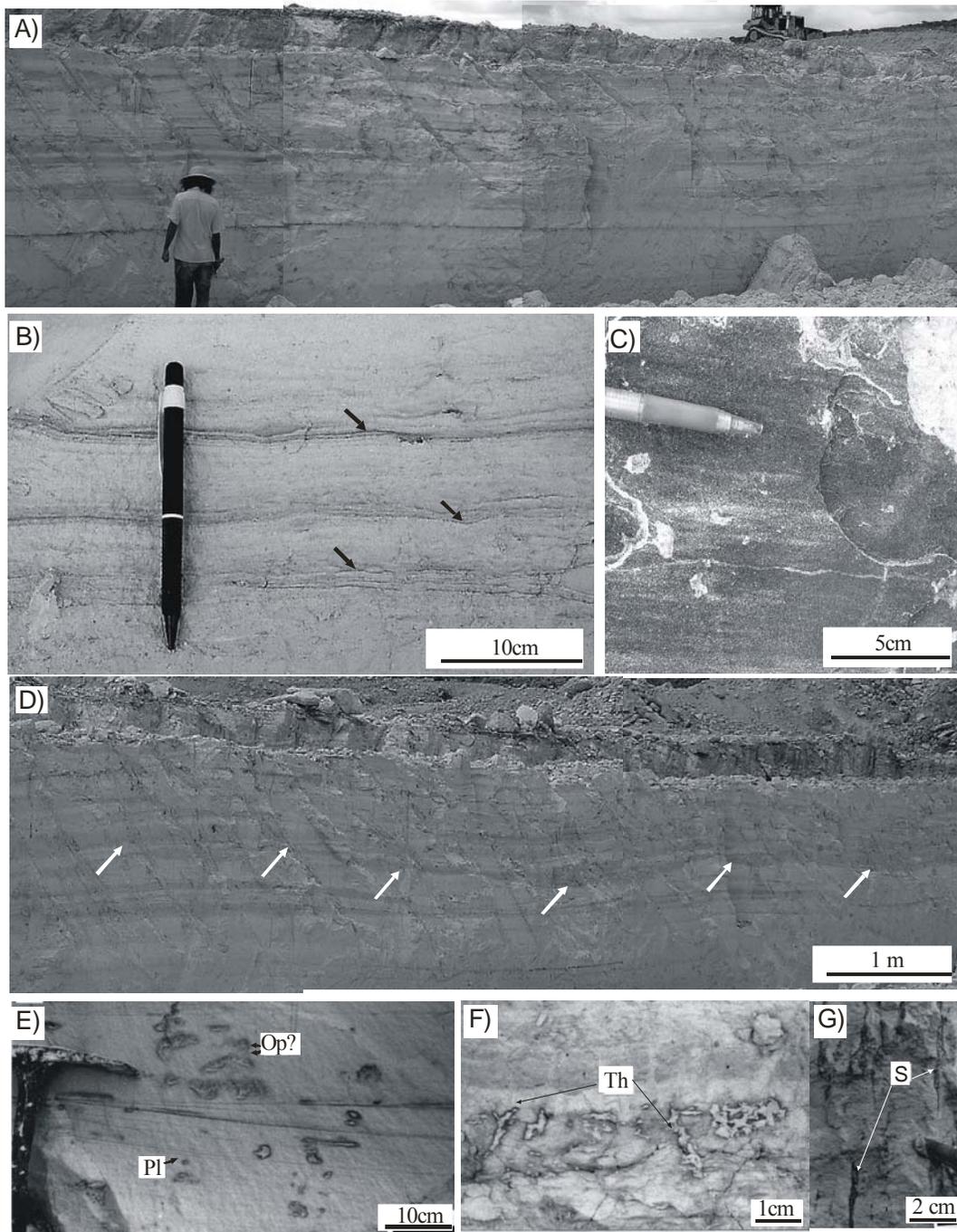
Figure 2.6: Upper flow regime tidal sand flat/sand bar (Facies Association D). A) General view of an outcrop illustrating tabular sandstones with horizontal to low-angle dipping cross stratification (Facies St) (man=1.65 m tall). B) Horizontal lamination with laminae highlighted by heavy minerals. C) Sandstone with parting lineation (pencil oriented parallel to paleoflow). D) Undulating lamination forming scour or swales locally filled by mudstone (white arrows). E-G) Trace fossils, representative of the upper flow regime tidal sand flat/sand bar. *Thalassinoides* (Th), *Planolites* (Pl) and *Skolithos* (S) and *Ophiomorpha* (Op).

***Interpretation*:** Facies Association D is interpreted as tidal sand bar/sand flat deposits, based on prevalence of tabular sandstones internally displaying horizontal to low-angle dipping stratification. These characteristics imply deposition along a shallow flat area. The abundance of parting lineation in Facies Shl indicates that sediment accumulation took place during prevailing upper-flow-regime conditions (Reineck and Singh, 1980; Yagishita *et al*., 2004). The rhythmic alternation of Facies Shl and Facies St indicates fluctuating conditions from upper to lower flow regime. Considering the overall proposed depostional setting, these facies might have been the product of tidal processes. The presence of swell and pinch, symmetrical ripple marks, and the large swales indicate frequent wave reworking (*e.g.*, de Raaf *et al.*, 1977). In particular, scours similar to the ones described here (Figure 6C) are common in nearshore areas that have undergone periods of higher energy flow, suggesting storm wave reworking (*e.g.*, Bourgeois, 1980; Cheel and Leckie, 1993; Hori *et al.*, 2001; Plink-Bjorklund, 2005). The abundance of heavy minerals is consistent with flux and reflux.

The above mentioned characteristics, added to the gradation of Facies Association D with the other facies associations described herein support deposition in an upper flow regime tidal sand flat depositional setting (see also Klein, 1985; MuCubbin, 1988; Plink-Bjorklund, 2005).

The lateral gradation of tidal sand flat deposits with sandstone lenses displaying fining- and thickening-upward cycles are suggestive of significant volume of sand accumulation along a series of tidal sand bars. Many ancient tidal sand bars are recorded by similar upward-coarsening lenticular sandstone bodies (Houthuys and Gullentops, 1988; Dalrymple, *et al.* 1992; Reading and Collinson, 1996; Willis, 2000; Heap *et al.*, 2004). Tidal bars are commonly recorded in association with upper flow regime tidal sand flat deposits in confined areas along coasts dominated by high tidal velocities (Dalrymple *et al.*, 1992; Plink-Bjorklund, 2005).

The ichnological assemblage, represented by disperse traces of mostly *Thalassinoides* is in agreement with the proposed setting, since these traces form typically in nearshore areas undergone to episodic or constant environmental changes (Wightman *et al.* 1987; MacEachern and Pemberton 1992; Pollard *et al.* 1993; Gowland 1996).

2.5 DISCUSSION OF THE DEPOSITIONAL SYSTEM

The new facies data presented herein confirms tidal currents as the main process responsible for deposition of the soft kaolin unit of the Ipixuna Formation. Evidence for tidal processes includes the abundance of cross sets with reactivation surfaces, commonly mantled by mud drapes, the local presence of tidal bundles, and reversed foresets. The ichnological assemblage represented by low diversity of traces, consisting of *Thalassinoides, Planolites, Teichichnus, Taenidium, Skolithos* and *Ophiomorpha,* attests a nearshore setting with stressing water conditions due to the mixture of marine and freshwater inflows. This, together with the variety of facies associations interpreted above, is consistent with a tide-dominated estuarine model (Fig. 7).
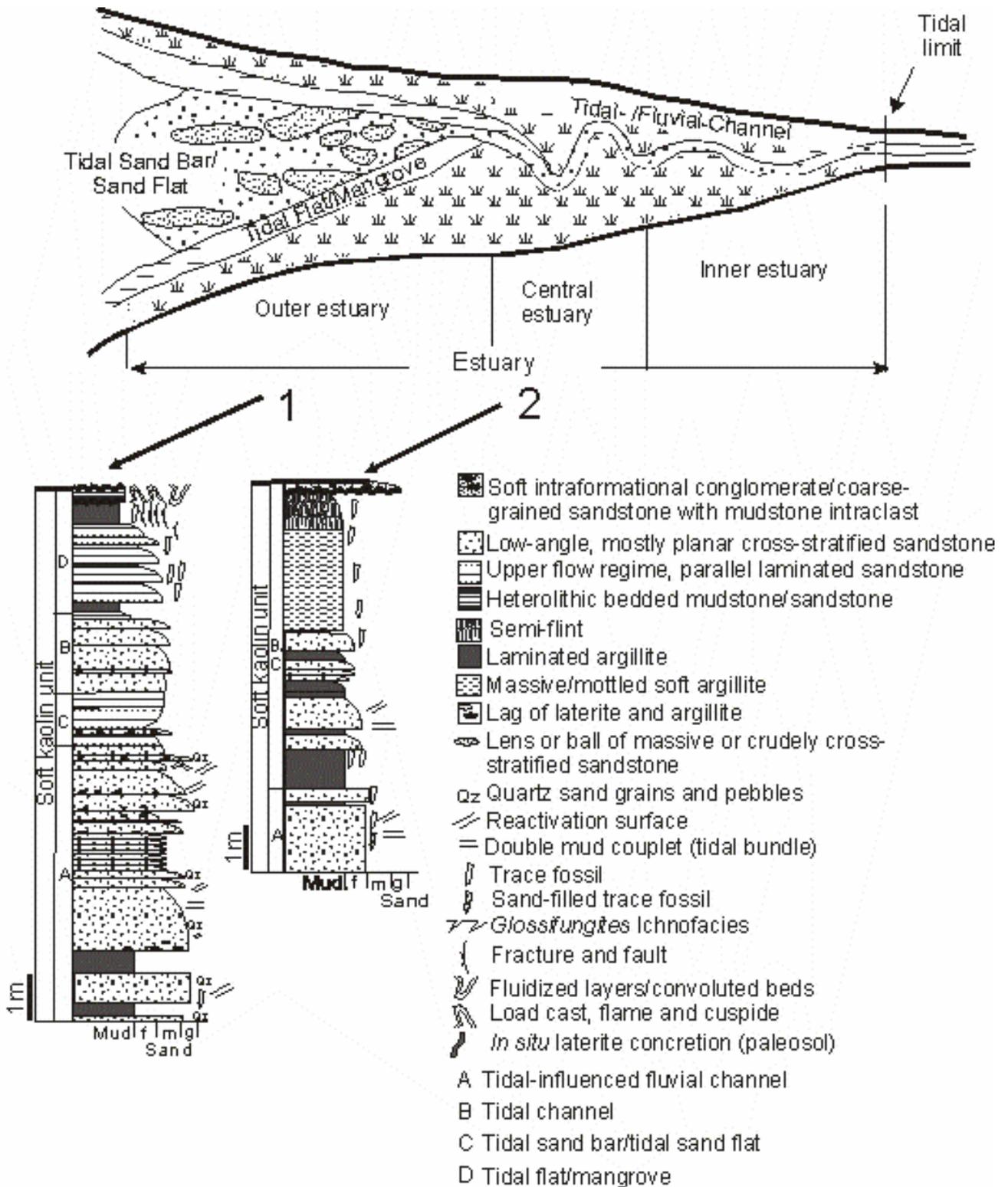
Figure 2.7: Schematic block diagram depicting the tidal dominated estuarine depositional model (after Dalrymple *et al.*, 1992) proposed for the soft kaolin in the Rio Capim area. (1=profile in the RCC quarry; 2=profile in the PPSA quarry).

A previous study of the Ipixuna Formation had tentatively suggested the action of tidal currents during its deposition. This paper, however, demonstrates that tidal processes were much more significant than initially thought, and controlled most of the sediment accumulation in all of the depositional environments identified in the soft kaolin unit. In addition, mapping of new exposures has led to a more complete characterization of the various facies associations and their spatial relationships.

A proposed correlation of the tidal deposits of the Ipixuna Formation from the studied quarries exposed along the Road BR-010, located 60 km apart, led to the proposal of a wave-dominated estuarine system for the soft kaolin unit (Santos Jr. and Rossetti, 2003). The data presented herein, however, support depositional settings that are more consistent with a tide-dominated estuarine model. A possibility exists, thus, that the tidal delta deposits present along the Road BR-010 are not correlatable with the soft kaolin unit. These tidal delta deposits might correspond to either an adjacent depositional system or a part of a barrier complex associated with the subsequent stage of the estuary evolution with increased influence of wave action.

The genetic association of tidal-influenced fluvial channel, tidal channel, tidal flat/mangrove, and tidal sand bar/tidal sandy flat deposits, is typical of tidal dominated estuarine system for the soft unit (*e.g.,* Woodroffe *et al.*, 1989; Leckie and Singh, 1991; Dalrymple *et al.*, 1992; Harris *et al.*, 1992; Chappell and Woodroffe, 1994; Mulrennan and woodroffe, 1998; Hori *et al.*, 2001; Heap *et al.*, 2004; Plink-Bjorklund, 2005). An abundance of tidal channel deposits that interfinger with sand bar and upper flow regime sand flat deposits are more commonly recorded in tide-dominated estuaries formed along mesotidal to macrotidal coast (Klein, 1985; Houthuys and Gullentops, 1988; Buatois and Mangano, 2003). Tidal bar and sand flat deposits had been previously recognized in the study area, but were thought to be volumetrically subordinate, have formed when upper flow regimes developed within channels (Santos Jr. and Rossetti, 2003). The newly available exposures reveal, however, that they constitute one of the main facies associations of the soft kaolin unit, second only to tidal deposits.

The distribution of the studied deposits, both vertically and laterally, provides information for interpreting the estuary evolution. The tidal-influenced, fluvial-channel deposits (Facies Association A), which are dominant near the base of the kaolin unit, attest to formation in inner estuarine areas. These deposits characterize the transition between fluvial and tidal sedimentation, thus displaying characteristics that are inherent from both fluvial and tidal processes (Dalrymple

et al., 1992; Hori *et al*., 2001; Cooper, 2002). Features diagnostic of tidal processes, such tidal bundles, are scarce or even absent from such settings due to the interference of fluvial influx (Leckie and Singh, 1991; Hori *et. al*., 2001; Cooper, 2002; Heap *et al.*, 2004). The velocity fluctuation of tidal currents results in highly unsteady flows, producing frequent reactivation surfaces with mud drapes, as observed in Facies Association A. The abundance of these surfaces separating foreset packages that are only few cm thick, facilitates the differentiation of tidal influence from other disturbances in fluvial system (*e.g.*, seasonal fluctuations; Ladipo, 1988; Thorez *et al.*, 1988).

The overall vertical gradation from tide-influenced fluvial channel (Facies Association A) to tidal channel (Facies Association B), tidal flat/mangrove (Facies Association C) and tidal sand bar/sand flat deposits (Facies Association D) records upward increasing tidal influence. As a result, features attributed to, or even diagnostic (*e.g.*, tidal bundles) of tidal currents become progressively more abundant upward, as do the trace fossils *Thalassinoides, Ophiomorpha, Planolithes, Teichichnus, Taenidium* and *Skolithos*, typical of coastal settings. The upward increase in tidal influence is also associated with a progressive increase in mud abundances, resulting in thinning- and fining- upward successions. Such facies arrangements are related to a rise in relative sea level during transgression.

Inclined heterolithic stratification (HIS) in association with tidal channel deposits is expected in meanders of straight-meandering-straight channel segments, typically formed in central estuarine areas of tidal-dominated estuaries (*e.g.*, Nichols and Biggs, 1985; Leckie and Singh, 1991; Dalrymple *et al.*, 1992; Reading and Collison, 1996; Plink-Bjorklund, 2005). The more frequent occurrence of tidal channel deposits in the PPSA quarry might suggest that, when transgression took place, this area was located closer to the central estuary.

On the other hand, the higher abundance of Facies Association D in the RCC quarry suggests a location nearer to the coast, as elongate sand bars associated with upper-flow-regime sand flats are typical of the seaward areas in tide-dominated estuaries (Dalrymple *et al*., 1992). The common occurrence of wave-generated structures (i.e, symmetrical ripple marks and truncating, low-angle dipping cross lamination) in facies association D conforms to an outer estuarine location (Dalrymple *et al.* 1992).

The soft kaolin deposits in the Rio Capim Kaolin area were formed during a period of rise relative sea level, with the RCC quarry recording an increased proximity to nearshore areas

relative to the PPSA quarry. The tide-dominated estuary formed along a broad WNW-ESE paleocoast, as proposed by the dominant NNE/SSW and NE/SW paleocurrent data obtained from the in-channel deposits.

2.6 CONCLUSION

The presence of sedimentary structures attributed to tidal processes coupled with trace fossil assemblages consisting of *Thalassinoides, Planolites, Teichichnus, Taenidium, Skolithos* and *Ophiomorpha,* suggest that the soft kaolin unit of the Ipixuna Formation in the Rio Capim Kaolin area was formed dominantly under the influence of tidal processes. In addition to facies associations consisting of tidal-influenced fluvial channel, tidal channel, tidal flat/mangrove, and tidal sand bar/tidal sand flat, these characteristics support a tide-dominated estuarine interpretation. The distribution of facies associations, represented by tide-influenced fluvial channel deposits that grade upward into other facies associations denoting increased tidal energy, indicates that deposition took place during a transgression. The increased occurrence of tidal channel, tidal flat/mangrove deposits in the PPSA quarry, and of tidal sand bar/tidal sandy flat in the RCC quarry reveals that the latter was located closer to the nearshore area. During the Late Cretaceous, the paleocoast was positioned circa 240 km landward of the present coast, as a result of relative sea-level rise. This depositional context must be taken into account when discussing the origin of the soft kaolin in the Rio Capim area.

REFERENCES

ALLEN, G.P., 1991. Sedimentary processes and facies in the Gironde estuary. A recent model for macrotidal estuarine systems. In: SMITH, D.G.; REISON, G.E.; ZAITLIN, B.A.; RAHMANI, R.A. (Eds.) *Clastic Tidal Sedimentology*. Canadian Society of Petroleum, p. 29 - 39. (Geologists Memoir, 16)

ASHLEY, G.M. & RENWICK, W.R., 1983. Channel morphology and processes at the riverine-estuarine transition, the Raritan River, New Jersey. In: COLLINSON, J.D. & LEWIN, J. (Eds.) *Modern and Ancient Fluvial Systems*. p. 207-218. (IAS Special Publication, 6)

AZEVEDO, R.P., 1991. *Tectonic Evolution of Brazilian Equatorial Continental Margin Basins*. Royal School of Mines Imperial College, London, 412 p. (PhD Thesis)

BENYNON, B.M. & PEMBERTON, S.G., 1992. Ichnological signature of a brackish water deposit. An example from the lower Cretaceous Grand Rapids formation, Cold Lake oil sand area, Aleberta. In: A CORE WORKSHOP - APPLICATIONS OF ICHNOLOGY TO PETROLEUM EXPLORATION. Society of Economic Paleontologist and Mineralogist. V.2, p.199-221.

BOURGEOIS, J., 1980. A transgressive shelf sequence exhibiting hummocky stratification: the Sebastian Sandstone (Upper Cretaceous), southwestern Oregon. *Journal of Sedimentary Petrology*, 50:681–702.

BUATOIS, L. A. & MÁNGANO, M. G., 2003. Sedimentary facies, depositional evolution of the Upper Cambrian–Lower Ordovician Santa Rosita formation in northwest Argentina. *Journal of South American Earth Sciences,* 16:343-363.

CHAPPELL, J. & WOODROFFE, C.D., 1994. Macrotidal estuaries. In: CARTER, R.W.G. & WOODROFFE, C.D. (Eds.) *Coastal Evolution: Late Quaternary Shoreline Morphodynamics*, Cambridge, Cambridge University Press, p. 187–218.

CHEEL, R.J. & LECKIE, D.A., 1993. Hummocky cross-stratification. *Sedimentology Review*, 1:103–122.

CLIFTON, H.E., 1983. Discrimination between subtidal and intertidal facies in Pleistocene deposits, Willapa bay, Washington. *Journal of Sedimentary Petrology,* 53: 353–369.

COLLINSON, J.D., 1996. Alluvial sediments. In: READING, H.G. (ed.) *Sedimentary Environments*: *Processes, Facies and Stratigraphy*. Oxford, Blackwell Science, p.37-82.

COOPER, J.A.G., 2002. The role of extreme floods in estuary-coastal behavior: contrasts between river- and tide-dominated microtidal estuaries. *Sedimentary Geology,* 150:123-137.

COSTA, J.B.S.; BEMERGUY R.L.; HASUI, Y.; BORGES, M.S. 2001. Tectonics and paleogeography along the Amazon River. *Journal of South American Earth Sciences,* 14:335-347.

DALRYMPLE, R.W.; ZAITLIN, B.A.; BOYD, R. 1992, Estuarine facies models: conceptual basis and stratigraphic implications. *Journal of Sedimentary Petrology,* 62:1130-1146.

DE BOER, P.L.; OOST, A.P.; VISSER, M.J. 1989. The diurnal inequality of the tide as a parameter for recognizing tidal influences. *Journal Sedimetology Petrology*, 59:912-921.

DE RAFF, J.F.M.; BOERSMA, J.R.; VAN GELDER, A. 1977. Wave generated structures and sequences from a shallow marine succession/Lower Carboniferous, Country Cork, Ireland. *Sedimentology,* 24:451-483.

FENIES, H. & FAUGÈRES J.C., 1998. Facies and geometry of tidal channel-fill deposits (Arcachon Lagoon, SW France). *Marine Geology,* 150:131-148.

GALVÃO, M.V.G., 1991. *Evolução Termodinâmica da Bacia do Marajó, Estado do Pará, Brasil*. Ouro Preto. Universidade de Ouro Preto, 193 p. (Dissertação de Mestrado).

GAO, C., 2004. Sedimentary facies changes and climatic-tectonic controls in a foreland basin, the Urumqi River, Tian Shan, Northwest China. *Sedimentary Geology,* 169: 29-46.

GÓES, A.M., 1981. *Estudo Sedimentológico dos Sedimentos Barreiras, Ipixuna e Itapecuru, no Nordeste do Estado no Pará e Noroeste do Maranhão*. Belém, Universidade Federal do Pará, Cetro de Geociências, 55 p. (Dissertação de Mestrado).

GOWLAND, S., 1996. Facies characteristics and depositional models of highly bioturbated shallow marine siliciclastic strata; an example from the Fulmar Formation (Late Jurassic), UK Central Graben In: HURST, A. (Ed.) *Geology of the Humber Group: Central Graben and Moray Firth, UKCS*, 114, p. 185–214. (Special Publication of the Geological Society of London).

HARRIS, P.T.; PATTIARATCHI, C.B.; COLE, A.R.; KEENE, J.B. 1992. Evolution of subtidal sandbanks in Moreton Bay, eastern Australia. *Marine Geology,* 103:225–247.

HEAP, A. D.; BRYCE, S.; RYAN, D.A. 2004. Facies evolution of Holocene estuaries and deltas: a large-sample statistical study from Australia. *Sedimentary Geology*, 168:1-17.

HORI, K.; SAITO, Y.; ZHAO, Q.; CHENG, X.; WANG, P.; SATO, Y.; LI, C. 2001. Sedimentary facies of the tide-dominated paleo-Changjiang (Yangtze) estuary during the last transgression. *Marine Geology*, 177:331-351.

HOUTHUYS, R. & GULLENTOPS, F., 1988. Tidal Transverse bars building up a longitudinal sand body (Middle Eocene, Belgium). In: BOER, P.L.; GELDER A.V.; NIO A.D (Eds.) *Tide-influenced Sedimentary Environments and Facies*. Sedimentology and Petroleum Geology. Reidel, Dordrecht , p. 153-166.

KLEIN, G.V., 1985. Intertidal flats and intertidal sand bodies. In: Davis Jr., R.A. (Ed.) *Coastal Sedimentary Environments*, Spring-Verlag, Massachusetts, p. 187-219.

KOTSCHOUBEY, B.; DUARTE, A. L. S.; TRUCKENBRODT, W. 1999. Cobertura bauxítica e origem do caulim do Morro do Felipe, Baixo Rio Jari, Estado do Amapá. *Revista Brasileira de Geociências*, 29:331-338.

KOTSCHOUBEY, B.; TRUCKENBRODT, W.; HIERONYMUS, B., 1996. Depósitos de caulim e argila semi-*flint* no nordeste do Pará. *Revista Brasileira de Geociências*, 26:71-80.

LADIPO, K.O., 1988. Example of tidal current periodicities from an Upper Cretaceous sandstone sucession (Anambra Basin, S.E. Nigeria). In: BOER, P.L.; VAN GELDER, A.; NIO, S.D. (Eds.) *Tide-Influenced Sedimentary Environments and Facies*, Reidel, Dordrecht, p. 333-358.

LECKIE, D.A. & SINGH, C., 1991. Estuarine deposits of the Albian Paddy Member (Peace River Formation) and lowermost Shaftesbury Formation, Alberta, Canada. *Journal of Sedimentary Petrology*, 61:825-849.

MACEACHERN, J.A. & PEMBERTON, S.G., 1992. Ichnological aspects of Cretaceous shoreface successions and shoreface variability in the Western Interior Seaway of North America. In: PEMBERTON, S.G. (Ed.) *Applications of Ichnology to Petroleum Exploration.* Core Workshop, p. 57–84. (SEPM 17).

MACEACHERN, J.A. & PEMBERTON, S.G., 1994. Ichnological aspects of incised-valley systems from the Viking Formation of the Western Canada sedimentary basin, Alberta, Canada In: DALRYMPLE, R.W.; BOYD R.; ZAITLIN B.A. (Eds.) *Incised-Valley Systems: Origin and Sedimentary Sequences.* Society for Sedimentary Geology. p. 129–157. (Special Publication 51)

MACK, G. H.; LEEDER M.; PEREZ-ARLUCEA, M.; BAILEY, B. D. J. 2003. Early Permian silt-bed fluvial sedimentation in the Orogrande Basin of the Ancestral Rocky Mountains, New Mexico, USA. *Sedimentary Geology,* 160:159-178.

MALPAS, J.A.; GAWTHORPE, R.L.; POLLARD, J.E.; SHARP, I.R., 2005. Ichnofabric analysis of the shallow marine Nukhul Formation (Miocene), Suez Rift, Egypt: implications for depositional processes and sequence stratigraphic evolution. *Palaeogeography, Palaeoclimatology, Palaeoecology,* 215:239-264.

MCCUBBIN, D.G., 1988. Barrier-Island and Strand Plain Facies. In: SCHOLL, P.A. & SPEARING D. (Eds.) *Sandstone Depositional Environments*. American Association of Petroleum Geologists, Tulsa. p.247-279.

MULRENNAN, M.E. & WOODROFFE, C.D., 1998. Holocene development of the Mary River plains, Northern Territory, Australia. *Holocene,* 8:565–579.

NICHOLS, M.M. & BIGGS, R.B., 1985. *Estuaries*. In: DAVIS, R.A. (Ed.) *Coastal Sedimentary Environments,* Spring-Verlag, p. 77-186.

NIO, S.D. & YANG, C.S., 1991. Diagnostic attributes of clastical tidal deposists: a review. In: SMITH, D.G. REISON, G.E. ZAITLIN B.A.; RAHMANI, R.A. (Eds.) *Clastical Tidal Sedimentology,* Canadian Society of Petroleum Geologists, Memoir 16, p. 3-28.

NOUIDAR, M. & CHELLAÏ, E. H., 2001. Facies and sequence stratigraphy of an estuarine incised-valley fill: Lower Aptian Bouzergoun Formation, Agadir Basin, Morocco. *Cretaceous Research,* 22:93-104.

PEMBERTON, S.G.; SPILA, M.; PULHAM, A.J.; SAUNDERS, T.; MACEACHERN, J.A.; ROBBINS, D.; SINCLAIR, I.K., 2001. Ichnology and sedimentology of shallow to marginal marine systems: Ben Nevis and Avalon Reservoirs, Jeanne D'Arc Basin, *Geological Association of Canada, Short Course Notes* 15, 343 pp.

PLINK-BJORKLUND, P., 2005. Stacked fluvial and tide-dominated estuarine deposits in high-frequency (fourth-order) sequences of the Eocene central Basin, Spitsbergen. *Sedimentology*, 52:391-428.

POLLARD, J.E.; GOLDRING, R.; BUCK, S.G. 1993. Ichnofabrics containing *Ophiomorpha*: significance in shallow-water facies interpretation, *Journal of the Geological Society,* 150:149–164.

READING, H.G. & COLLINSON, J.D., 1996. Clastic Coasts. In: READING, H.G. (Ed.) *Sedimentary Environments*: *Processes, Facies and Stratigraphy*. Oxford, Blackwell Science, p.154-231.

REINECK, H.E. & SINGH, I.B., 1980. *Depositional Sedimentary Environments*. Springer, Berlin, 551 pp.

ROSSETTI, D.F., 2004. Paleosurfaces from northeastern Amazonia as a key for reconstructing paleolandscapes and understanding weathering products**.** *Sedimentary Geology,* 169:151-174.

ROSSETTI, D.F. & SANTOS JR., A. E., 2003. Events of soft sediment deformation and mass failure in Upper Cretaceous estuarine deposits (Cametá Basin, northern Brazil) as evidence for seismic activity. *Sedimentary Geology*, 161:107-130.

ROSSETTI, D.F. & SANTOS JR., A.E.A., 2006. Analysing the origin of the Upper Cretaceous-?Lower Tertiary Rio Capim semi flint (Pará State, Brazil): under a sedimentologic perspective. *Sedimentary Geology*, 186:133-144.

SANTOS JR., A.E.A. & ROSSETTI, D.F., 2003. Paleoambiente e estratigrafia da Formação Ipixuna, Area do Rio Capim, Leste da Bacia de Cameta. *Revista Brasileira de Geociências,* 33:313-324.

SAVARY, B.; OLIVERO, D.; GAILLARD, C. 2004. Calciturbidite dynamics and endobenthic colonisation: example from a late Barremian (Early Cretaceous) succession in southeastern France**. *Palaeogeography, Palaeoclimatology, Palaeoecology*, 211:221-239.

SHANLEY, K.W.; MCCABE, P.J.; HETTINGER, R.D. 1992. Tidal influence in Cretaceous fluvial strata from Utah. USA: a key to sequence stratigraphic interpretation. *Sedimentology*, 39:905-930.

SMITH, D.G., 1988. Modern point bar deposits analogues to the Athabasca oil sands, Alberta, Canada In: DE BOER, P.L.; VAN GELDER, A.; NIO, S.D. (Eds.) *Tide-Influenced Sedimentary Environments and Facies*, Reidel, Dordrecht , p. 417-432.

SOUSA, D.J.L., 2000. *Caracterização Geológica, Mineralógica, Química e Física do caulim da RCC, Rio Capim Caulim (PA)*. Belém. Universidade Federal do Pará, Centro de Geociências, 116 pp. (Dissertação de Mestrado)

THOMAS, R.G.; SMITH, D.G.; WOOD, J.M.; VISSER, J.; CALVERLEY-RANGE, E.A.; KOSTER, E.H. 1987. Inclined heterolithic stratification-terminology, description, interpretation, and significance. *Sedimentary Geology,* 53:123–179.

THOREZ, J.; GEOMAERE, E.; DREESEN, R. 1988. Tide- and Wave-influenced depositional environments in the Psamites Du Controz (Upper Famennian in Belgium). In: BOER, P.L.; VAN GELDER, A.; NIO, S.D. (Eds.) *Tide-Influenced Sedimentary Environments and Facies*, Reidel, Dordrecht, p. 389-415.

TRUCKENBRODT, W.; KOTSCHOUBEY, B.; SCHELLMANN, W. 1991. Composition and origin of the clay cover on North Brazilian laterites. *Geologische Rundschau*, 80:591-610.

UCHMAN, A.; DRYGANT, D.; PASZKOWSKI, M.; PORĘBSKI, S. J.; TURNAU, E. 2004. Early Devonian trace fossils in marine to non-marine redbeds in Podolia, Ukraine: palaeoenvironmental implications. *Palaeogeography, Palaeoclimatology, Palaeoecology,* 214:67-83.

VILLEGAS, J.M.C., 1994. *Geologia Estrutural da Bacia do Marajó*. Belém. Universidade Federal do Pará, Centro de Geociências. 119 p. (Dissertação de Mestrado)

WIGHTMAN, D.M.; PEMBERTON, S.G.; SINGH, C. 1987. Depositional modeling of the Upper Mannville (Lower Cretaceous), East Central Alberta: implications for the recognition of brackish water deposits. In: TILLMAN, R.W. & WEBER, K.J. (Eds.) *Reservoir Sedimentology*, Society of Economic Paleontologists and Mineralogists, p. 189-220. (Special Publication 40)

WILLIS, A. 2000. Tectonic control of nested sequence architecture in the Sego Sandstone, Neslen Formation and Upper Castlegate Sandstone (Upper Cretaceous), Sevier Foreland Basin, Utah, USA**. *Sedimentary Geology,* 136:277-317.

WOODROFFE, C.D.; CHAPPELL, J.; THOM, B.G.; WALLENSKY, E., 1989. Depositional model of a macrotidal estuary and floodplain, South Alligator River, northern Australia. *Sedimentology,* 36:737–756.

YAGISHITA, K.; ASHI, J.; NINOMIYA S.; TAIRA, A. 2004. Two types of plane beds under upper-flow-regime in flume experiments: evidence from grain fabric. *Sedimentary Geology*, 163:229-236.

ZAITLIN, B.A.; DALRYMPLE, R.W.; BOYD, R.; LECKIE, D., 1994. The stratigraphic organization of incised valley systems: implications to hydrocarbon exploration and production- with examples from the Western Canada Sedimentary Basin. Canadian Society of Petroleum Geologists, Alberta, 260 pp.

ZONNEVELD, J.P.; GINGRAS, M. K.; PEMBERTON, S. G.; 2001. Trace fossil assemblages in a Middle Triassic mixed siliciclastic-carbonate marginal marine depositional system, British Columbia. *Palaeogeography, Palaeoclimatology, Palaeoecology,* 166:249-276.

ACKNOWLEDGEMENTS

3. ORIGIN OF THE RIO CAPIM KAOLIN WITH BASIS ON OPTICAL (PETROGRAPHIC AND SEM) DATA

Antônio Emídio de Araújo SANTOS Jr.
and Dilce de Fátima ROSSETTI

3.1 ABSTRACT

The Ipixuna Formation (Late Cretaceous-?Early Tertiary) exposed in the Rio Capim area, northern Brazil, was subdivided recently into three stratigraphic horizons, informally known as the lower soft kaolin unit, the intermediate kaolin unit, and the upper, endured, semi-flint kaolin unit. These units had their primary texture and composition strongly modified after deposition. Petrographic and scanning electronic microscopic (SEM) investigation revealed many remaining features that allow distinguishing the soft and the semi-flint kaolin deposits into two depositional sequences. The soft kaolin unit consists of well structured, sub-angular to sub-rounded, and locally angular, kaolinitized quartzose sandstones and kaolinitized sandstones that are interbedded with either laminated or massive pelites. These lithologies, composed by grains and lithic fragments related to felsic volcanic and meta-volcanic sources, as well as metamorphic and granitic rocks, had their texture and composition strongly modified, mostly likely during diagenesis, resulting deposits with an actual wacky nature. Kaolinitization produced three types of kaolinites, categorized according to size and texture, as Ka, Kb and Kc kaolinites. Ka kaolinite, typical of the sandstones, consists of hexagonal to pseudohexagonal crystals 10-30 μm in diameter, and occurs as agglomerates of booklets or vermicular crystals that reach up to 400 μm in length. Kb kaolinite, which dominates in the mudstones, consists chiefly of hexagonal and pseudohexagonal crystals averaging 1-3 μm in diameter that occur isolated, or as intergrowths of chaotic, face-to face or, less commonly, parallel to pseudo-parallel crystals. Kc kaolinite, which is abundant only in association with paleosols, displays hexagonal to pseudohexagonal crystals with regular sizes around 200 nm in diameter. The semi-flint is attributed to a distinctive depositional unit formed by sediments from variable sources, but with a significant contribution from the underlying soft kaolin. This is suggested by a high volume of sandstones displaying grains that are sub-rounded to rounded and consisting of homogeneous, dark brown masses of

kaolinite that are strongly highlighted by films of iron oxides. As opposed to the soft kaolin unit, the semi-flint is dominated by endured Kc kaolinite, which mostly likely results from combination of weathering during transportation and pedogenesis acting in several phases of sediment subaerial exposure.

Keywords: Petrology, Rio Capim kaolin, Cametá Sub-basin, kaolinite, origin, source area.

3.2 INTRODUCTION

The Ipixuna Formation that occurs in the Cametá Sub-basin, northern Brazil, is a geological unit of great economic interest for bearing one of the largest kaolin deposits in the world, the Rio Capim Kaolin. This unit has been investigated by several workers, who have mostly emphasized its sedimentologic, stratigraphic and geochemical aspects (Góes 1981; Sousa 2000; Santos Jr. 2002; Rossetti and Santos Jr. 2003; Santos Jr. and Rossetti 2003). One important issue still open for debate concerning to these deposits is to decipher the origin of the kaolinite in order to better develop exploitation methods. Previous studies have suggested that the Rio Capim Kaolin is a product of deep weathering related to progressive drop of ground water affecting a single stratigraphic unit (Truckenbrodt et al. 1991; Kotschoubey et al. 1996; 1999; Costa and Moraes 1998; Sousa 2000). Despite these contributions, the origin of these kaolin deposits deserves to be further addressed considering newly available sedimentological and stratigraphic data (Santos Jr. 2002; Rossetti and Santos Jr. 2003; Santos Jr. and Rossetti 2003). According to these authors, the kaolin deposits do not conform to a single stratigraphic unit. An unconformity separates the Ipixuna Formation into a lower soft kaolin unit and an upper hard kaolin unit, the latter consisting of flint-like fire clay with no plasticity when grounds up, known as semi-flint. Therefore, the soft and the semi-flint kaolin units have been attributed to distinctive depositional sequences. Additionally, a thin package of highly deformed deposits attributed to syn-sedimentary seismic activity is locally found between these two sequences, which are bounded by discontinuity surfaces that laterally merge into the sequence boundary (Rossetti and Santos Jr. 2003).

Taking this geological framework into account, a detailed characterization of various types of kaolinite according to the stratigraphic horizons recognized within the Ipixuna Formation is required to provide new information that can serve to the purpose of further discussing the origin of the Rio Capim Kaolin. Two types of kaolinite have been characterized in this area. These consist of a finer-grained kaolinite with high structural disorder, and a coarser-grained kaolinite with lower structural disorder, this occurring mostly as booklets (Kotschoubey et al. 1999). According to these authors, these types of kaolinite reflect lithological differences. Hence, the finer-grained kaolinites formed from replacement of clay mineral in muddy deposits, while the coarser-grained kaolinites resulted from replacement of feldspar grains in sandy deposits.

This paper provides detailed petrographic and scanning electronic microscopic (SEM) descriptions of the kaolin units of the Rio Capim area (Fig. 1A) aiming to better understand the origin of the different types of kaolinites, as well as discuss their temporal relationships.

3.3 GEOLOGICAL FRAMEWORK

The Cametá Sub-basin is inserted in the eastern margin of the Marajó Graben System, which formed in association with the opening of the Atlantic Ocean during the Late Jurassic to Early Cretaceous (Azevedo 1991; Galvão 1991; Villegas 1994; Costa et al. 2001). This sub-basin is filled by Cretaceous and Cenozoic deposits (Fig. 1B) that are up to 10 km thick. Cretaceous deposits are represented by the Breves (Aptian-Cenomanian) and the Limoeiro (Late Cretaceous) formations, while the Cenozoic deposits include the Marajó (Paleocene-Eocene) and Tucunaré (Pleistocene) formations. The majority of these deposits, formed in depositional settings ranging from fluvial to shallow marine (Villegas 1994), occurs in sub-surface. However, exceptional exposures are found along kaolin quarries in the Rio Capim area, where Upper Cretaceous-? Lower Tertiary deposits (Jupiassú 1970) crop out, being known by the lithostratigraphic term of Ipixuna Formation. This formation is up to 40 m thick, and consists of a lower soft kaolin unit, an intermediate kaolin unit, and an upper semi-flint kaolin unit (Fig. 2A), which are bounded by discontinuity surfaces, some marked by paleosols (Fig. 2A and B). The intermediate kaolin unit occurs only locally, and reaches up to 3 m thick. These deposits pinch out laterally, resulting in

direct superposition of the soft and the semi-flint kaolin units (Santos Jr. and Rossetti 2003; Rossetti 2004).

Despite the kaolinitized muddy nature, many workers have shown that the kaolin units in the Rio Capim area consist of lithologies varying from mudstones to conglomerates (Truckenbrodt et al. 1991; Kotschoubey et al. 1996; Santos Jr. and Rossetti 2003, 2006; Rossetti and Santos Jr. 2003, 2006; Rossetti 2004). The soft kaolin unit is well stratified, mostly encompassing sandy and muddy sedimentary facies attributed to tidal-influenced fluvial channel, tidal channel, tidal sand bar, sand flat and tidal flat/mangrove associated to a tidal estuarine system (Santos Jr. and Rossetti 2003, 2006). The intermediate kaolin unit, composed of heterolithic deposits, as well as mudstones and sandstones, forms a horizon bounded by discontinuity surfaces containing a variety of soft sediment deformation (e.g., convolute fold, cuspide, ball-and-pillow fracture, fault) structures related to seismic activity (Rossetti and Santos Jr. 2003). The semi-flint kaolin unit, traditionally known as massive in nature, has been more recently regarded as the record of distributary channels and mouth bars associated to either a deltaic or wave-dominated estuarine setting (Rossetti and Santos Jr. 2006). According to these authors, thin layers of quartzose sandstones present in these deposits are related to transgressive lags.
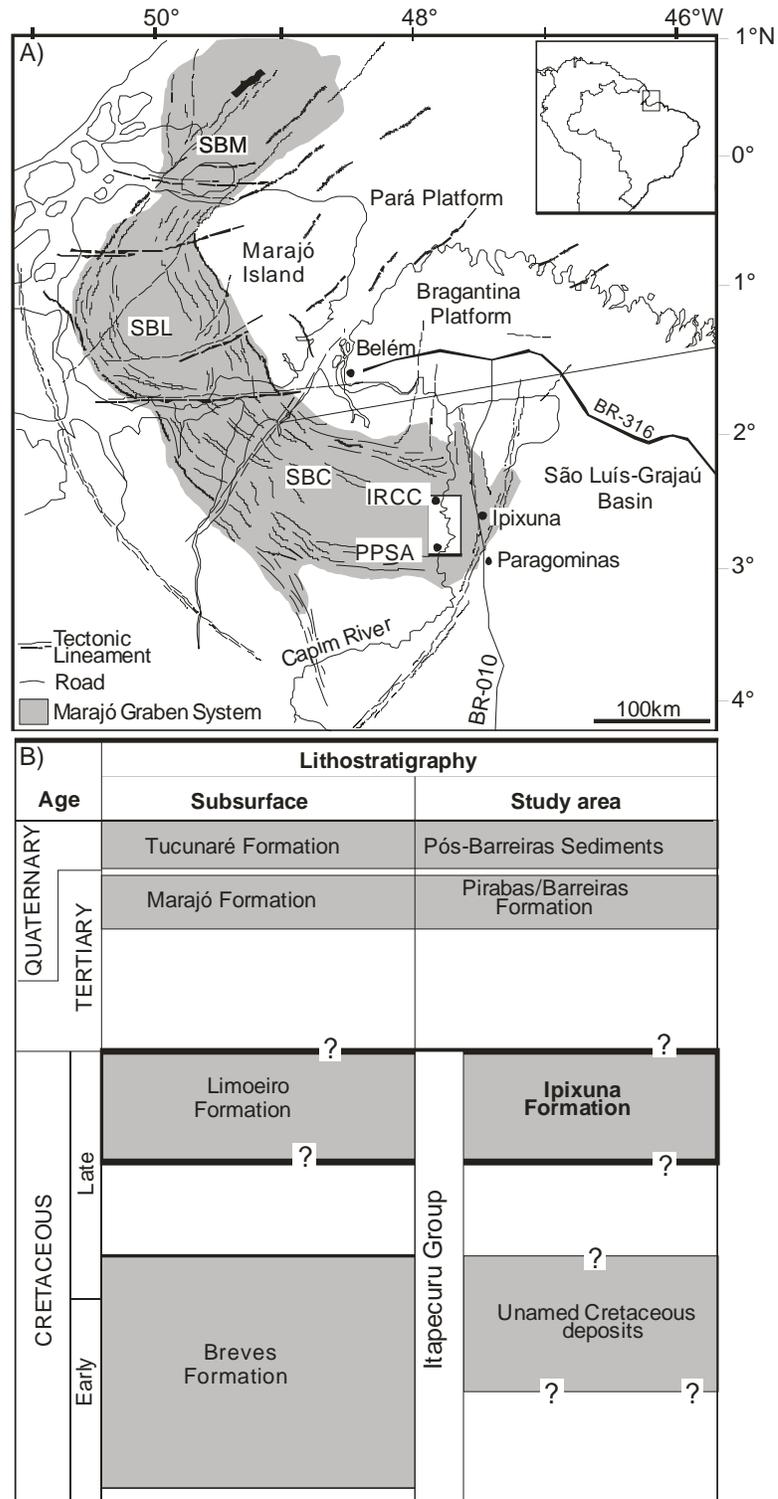
Figure 3.1 A) Location of the study area in the eastern Cametá Sub-Basin, Marajó Graben System, with indication of the two studied quarries, the IRCC and PPSA. SBC=Cametá Sub-Basin, SBL=Limoeiro Sub-Basin and SBM=Mexiana Sub-Basin. B) Lithostratigraphic chart of the Cametá Sub-Basin.
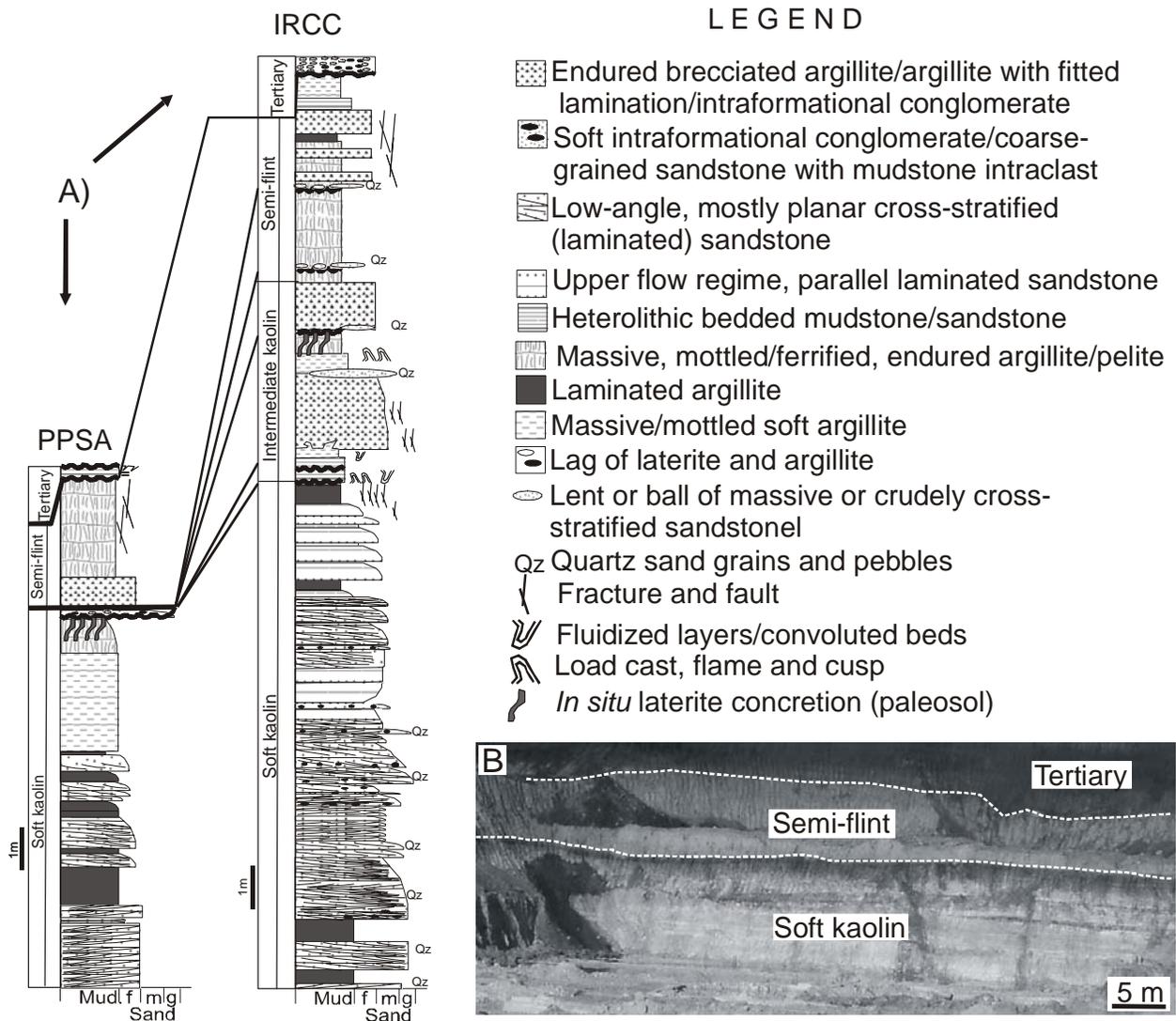
Figure 3.2. A) Lithostratigraphic profiles representative of the Ipixuna Formatin in the studied quarries. B) General view of the Ipixuna Formation in the PPSA quarry, illustrating the soft kaolin and the semi flint kaolin units separated by a sharp discontinuity surface, attributed to an unconformity. Note also the unconformity at the top of the semi flint kaolin, which is overlain by Tertiary deposits.

3.4 METHODS

This work was based on the petrographic and SEM analysis of 63 samples of kaolinitized sandstone, siltstone and mudstone collected from the Ipixuna Formation exposed along two kaolin quarries in the eastern Cametá Sub-basin (Fig. 1A). Sampling aimed to properly record the three stratigraphic kaolin units, as well as their internal sedimentary facies.

All samples were impregnated with epoxy cements before starting thin section preparation, given their soft, and sometimes, friable nature. After this procedure, the samples were cut and polished using a Logitech System. For the SEM analysis, both small fragments and powered samples were mounted on stubs using silver tape, in order to analyze texture and morphology of individual kaolinite crystals. After gold coating, the samples were analysed under a LEO 1450 VP electronic microscope from the Goeldi Museum, applying secondary electrons and backscattering. The study of SEM images was combined with EDS analysis in order to help identifying the various mineral species.

3.5 DESCRIPTION OF THE KAOLIN UNITS

Petrographic and SEM analyses revealed particular optical characteristics when the soft and the semi-flint kaolin units of the Ipixuna Formation were compared, with abrupt changes occurring at their boundaries. On the other hand, the intermediate unit could not be distinguished from the semi-flint kaolin and for this reason they will be described together herein. The following characterization of texture and mineralogy of the kaolin units takes into account only lithologies varying from sandstones to mudstones, and excludes conglomerates, also abundant in the upper two kaolin units. Given the high degree of kaolinitization, the lithologic classification provided below is far from representing a primary sediment composition. The most likely original sediment types are suggested in the discussions.

3.5.1 Soft kaolin

The soft kaolin unit is composed mainly by interbedded sandstone and pelite. The first, representing the main lithology, includes kaolinitized quartzose sandstones and kaolinitized

sandstones. Kaolinitized quartzose sandstones (Fig. 3A-H) dominate in the lower portion of the soft kaolin unit. They vary from fine- to coarse-grained and are, in general, moderately to well sorted, with grains that are sub-angular to sub-rounded, and locally angular. Their framework composition (Fig. 3A) consists of quartz (about 40-60%), and secondarily muscovite, feldspar and lithics (<5%). The remaining of the sandstones is composed by a kaolinitized "matrix", as well as large, rounded kaolinitized clasts up to 2 cm in length. The quartz grains are dominantly monocrystalline, and have their boundaries displaying different degrees of replacement by kaolinite. Only relics of grains are found floating within the kaolinite masses where replacement was more significant. In addition to the monocrystalline quartz, there is a significant volume of limpid, either bipyramidal or cuneiform quartz grains with straight extinction, as well as numerous vacuoles and embayments filled by either kaolinite or kaolinitized mud (Fig. 3B,C). Muscovite grains (Fig. 3D) are often bent and show anomalous birefringence due to partial replacement by large kaolinite crystals. Feldspars (Fig. 3E,F) are altered and replaced by kaolinite. Where grains are better preserved, albite twinning was observed. The lithics (Fig. 3G) consist mostly of mudstones and, secondarily, a mixture of muscovite, feldspar and quartz. These grains, in general larger than the average framework grains, display either bipyramidal or cuneiform quartz crystals. These are orientated according to a main direction that matches to the maximum elongation axis of muscovite crystals, suggesting an incipient foliation. The interstitial space of the sandstones consists of a kaolinitized 'matrix" often containing enlarged areas, as well as ghosts of grains that were entirely kaolinitized (Fig. 3H). Where this "matrix" is less common, the framework grains display punctual contacts.

Upward in the sections, the sandstones become progressively less quartzose, given place to the kaolinitized sandstones. These sandstones are dominantly fine-grained, though medium and even coarse grain sizes are locally present. The contact between grains are punctual and, less commonly, concave-convex. The grains, moderately sorted and sub-angular to angular, consist mainly of either partly or entirely kaolinited grains (Fig. 4A, D). Quartz, feldspar, muscovite and lithic grains are locally present. Bipyramidal (Fig. 4E) or cuneiform quartz grains are limpid or, most commonly, occur as "ghosts" with only relicts of the original composition. The latter consists of numerous particles of a transparent mineral with low birefringence similar to quartz. The remaining parts of these grains are highly replaced by kaolinite. Partly or entirely kaolinitized grains display a bipyramidal shape similar to quartz grains (Fig. 4F). The first shows

many relics of the original mineral composition, which are alike those observed in the ghosts of quartz grains. A large volume of the kaolinitized grains, even those with bipyramidal shapes, displays numerous black inclusions (Fig. 4G) that are not present in the kaolinitized "matrix". Lithic grains might display composition similar to the quarztoze sandstones described above or, more often, are composed by a dark kaolinitized massive material mixed with either limpid or partly kaolinitized bipyramidal quartz, feldspar and muscovite crystals (Fig. 4H).

The pelites (Fig. 5A,B), which increase in volume upward in the sections, consist of kaolinitized siltstones and mudstones that might be laminated forming heterolithic deposits. Large, well-rounded areas up to 0.5 mm in diameter with same composition than the surrounding deposits are locally present. Siltstones from the lower portion of the sections might display a high volume of quartz grains that are mostly angular. They also display prismatic, bipyramidal kaolinitized grains (Fig. 5B). Pelites with brown kaolinites are particularly widespread in the uppermost portion of the soft kaolin, where many fractures filled either by iron or clear kaolinites (Fig. 5C). These fractured pelites grade into reworked deposits displaying rounded clasts of similar composition than the surrounding pelites (Fig. 5D).

The above-described lithologies display three types of kaolinites, categorized according to size and texture as Ka, Kb and Kc kaolinites. Ka kaolinite (Fig. 6A-C) consists of hexagonal to pseudohexagonal crystals 10-30 μm in diameter that occur as agglomerates of booklets (Fig. 6A) or vermicular (Fig. 6B) shapes that reach up to 400 m in length. Either single or composite booklets are present, the latter being formed by a set of laterally coalescing single booklets. Euhedral, elongated prismatic kaolinite crystals 1-3 μm in length growth out from the booklet sheets (Fig. 6C). Many Ka kaolinites display anomalous birefringence and grade into muscovite grains. Kb kaolinite (Fig. 6D-G) consists of hexagonal and pseudohexagonal crystals averaging 1-3 m in diameter (Fig. 6D) that occur isolated, as intergrowths of chaotic, face-to face (Fig. 6E) or, less commonly, parallel to pseudo-parallel (Fig. 6F) crystals similar to the ones described by Pickering and Hurst (1989). This type of kaolinite occurs also arranged as booklets that are 5-10 μm in length. Lozenge kaolinite crystals intergrow with this type of kaolinite, and crudely developed single rectangular booklets are common (Fig. 6G). Kb kaolinite is either distributed homogeneously in the thin sections, or form masses containing agglomerates of Ka kaolinites dispersed within them. In addition, part of this kaolinite occurs in association with bipyramidal crystal ghosts, as well as kaolinitized grains of the framework. Kc kaolinite (Fig. 6H) also

displays hexagonal to pseudohexagonal forms, but the crystals have regular sizes around 200 nm in diameter.

Amongst all the kaolinite types described above, the sandstones bear the largest volume of Ka kaolinites, with Kb kaolinites being subordinate, and Kc kaolinites absent or, less commonly, rare. Ka kaolinites often form aggregates of sand grain sizes. Part of this kaolinite is also dispersed in the kaolinitized "matrix" in association with Kb kaolinites. On the other hand, Kc kaolinites occur consistently dispersed over the other two types of kaolinites. The pelites are dominated by Kb kaolinites, with Ka kaolinites being either rare or absent. Kc kaolinites are more frequent in this lithology than in the sandstones. Its volume increases progressively upward, reaching a maximum in the fractured pelites with brown kaolinites that occur near the contact with the discontinuity surface at the top of the soft kaolin.
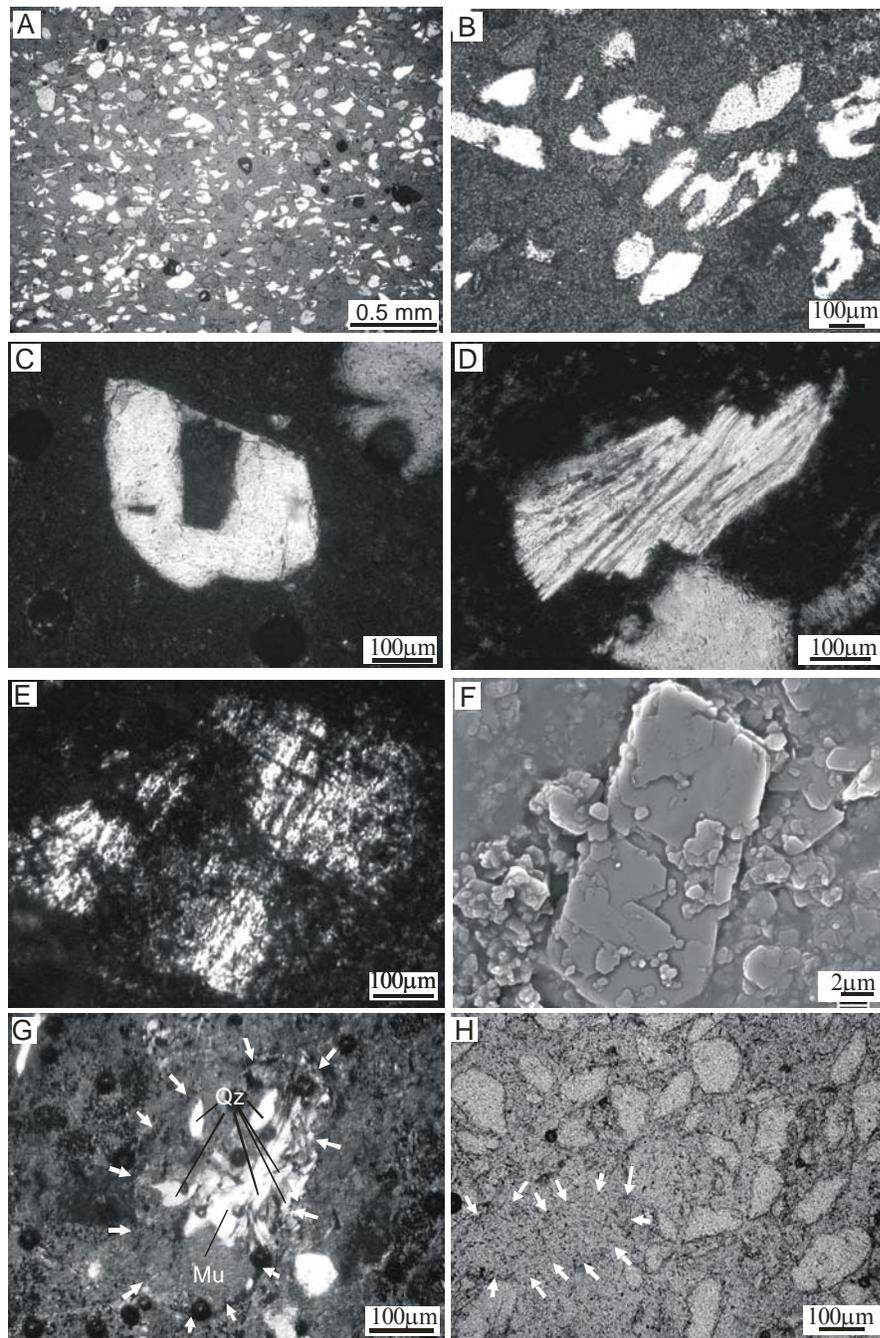
Figure 3.3 Kaolinitized quartzose sandstone, representative of the lower portion of the soft kaolin unit, illustrating: A) a broad view of the framework dominated by monocrystalline quartz grains; B,C) quartz grains with bipyramidal or cuneiform shapes, as well as vacuoles and embayments filled by kaolinite; D) muscovite grain partly replaced by kaolinite; E,F) feldspar grain partly replaced by kaolinite (note the albite twinning and prismatic shape); G) a lithic fragment (arrows) composed by muscovite, cuneiform quartz and a kaolinite, the latter resulting from replacement of other mineralogical constituents of the grain (note the that the quartz crystals-Qz are broadly aligned parallel to the maximum elongation axis of the muscovite-Mu); H) ghosts of totally kaolinitized grains (arrows) with texture similar to the matrix. (A-E and G=crossed polars; F= SEM, secondary electrons; H=parallel polars).
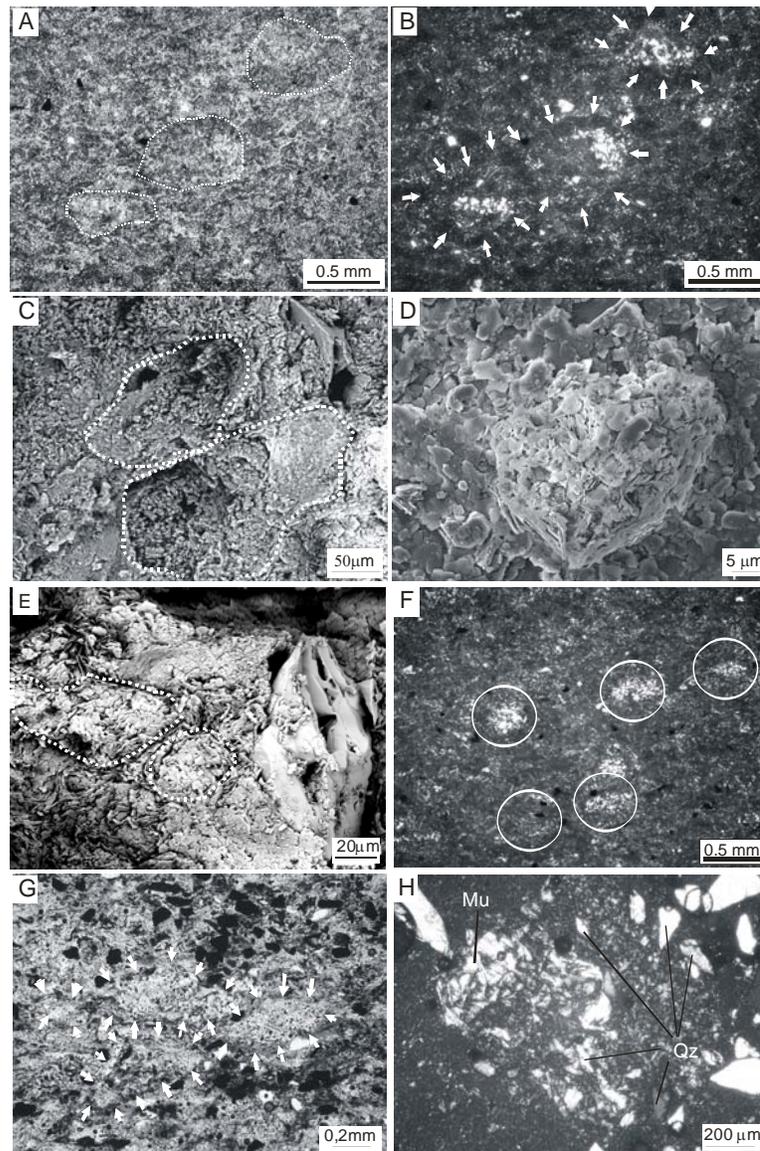
Figure 3.4 Kaolinitized sandstone, representative of the middle and upper portion of the soft kaolin unit. A-B) A view of an intensely kaolinitized framework with parallel (A) and crossed polars (B), where the contours of well rounded grains are still preserved (hatched lines and arrows in A and B, respectively). Note many relics of a mineral (cristobalite?; light color) not replaced by kaolinite. C) SEM view (back scatter) of the framework, highlighting two, well rounded, kaolinitized sand grains (hatched lines). D) A detail of a a grain completely replaced by Kb kaolinites crystals (SEM, back scatter). E) Bipyramidal quartz within a kaolinitized framework with two ghosts of sand grains (SEM, back scatter). F) Bipyramidal-shaped cristobalite (?; circles) floating within a kaolinitized "matrix", which might represent either individual euhedral grains or crystals from lithic grains that were left behind during kaolinitization (crossed polars). G) Kaolinitized bipyramidal grains (arrows), with numerous black inclusions, probably a product of replacement of the grains by kaolinite (crossed polars). H) A detail of a large, kaolinitized lithic grain with relics of pyramidal quartz and muscovite crystals (crossed polars).
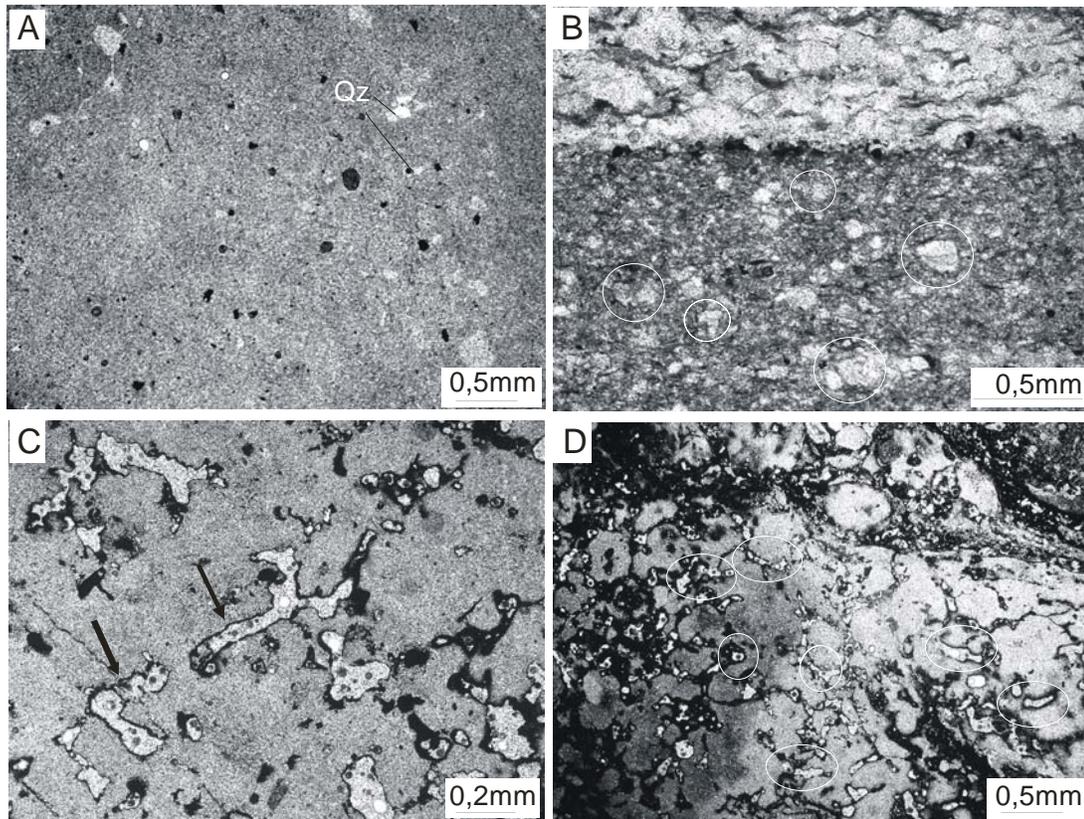
Figure 3.5 Deposits from the top of the soft kaolin unit. A) A general view of massive, kaolinitized mudstone with a few, disperse grains of quartz. B) Heterolithic deposits formed by alternating laminae of light brown to greenish brown siltstone (dark color) and very-fine grained sandstone (light color). Note the relicts of prismatic and/or bipyramidal quartz grains (circles) within the siltstone. C) Kaolinitized mudstone from a paleosol horizon at the top of the soft kaolin unit. Note the several areas cemented by clear kaolinite, related to fractures and/or roots (arrows). D) A reworked deposit from the top of the paleosol horizon, forming sandstone cemented by clear kaolinite (arrows) and iron oxides (black color).
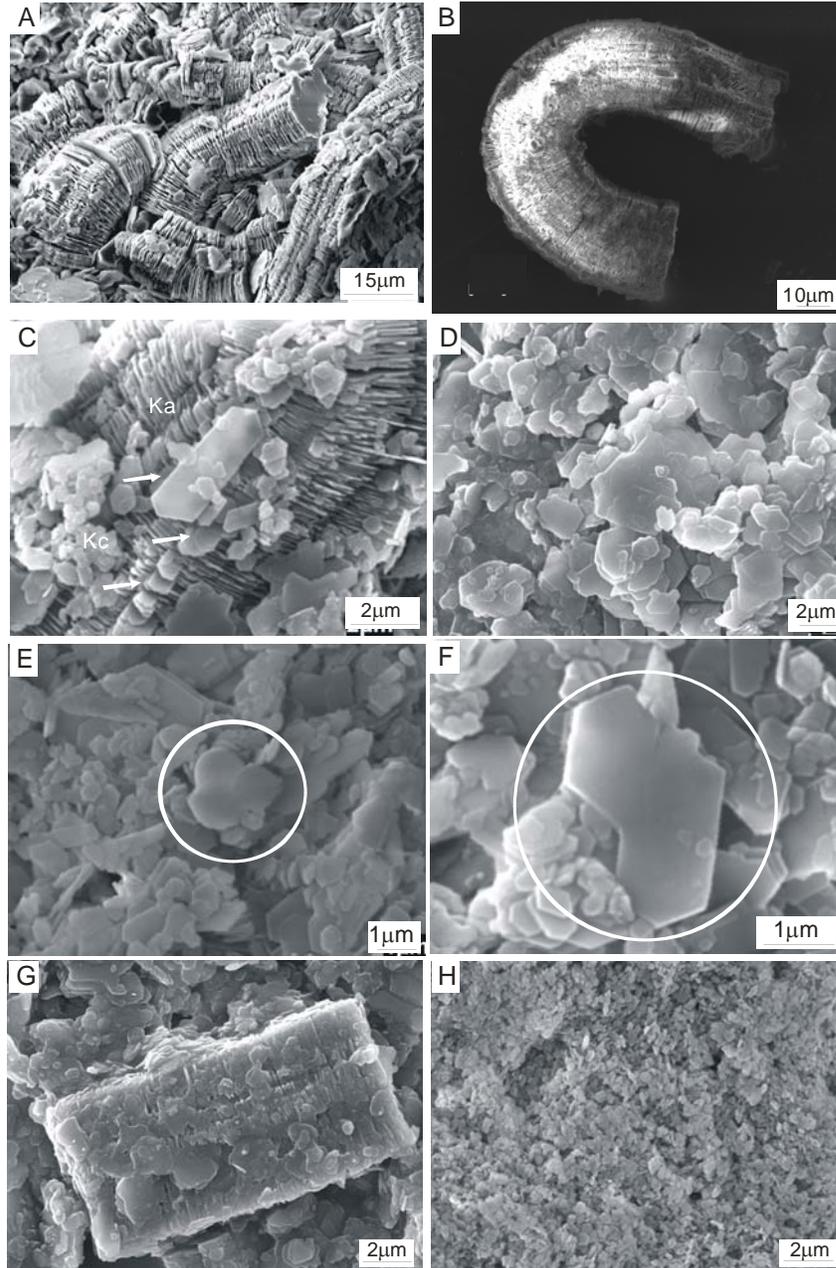
Figure 3.6 Kaolinite from the soft kaolin unit. A) Agglomerate of Ka kaolinites, consisting of booklets of hexagonal to pseudohexagonal crystals up to 30 μm in diameter. B) U-shaped, vermicular Ka kaolinite. C) A booklet of Ka kaolinite with superimposed prismatic rectangular crystals that grow out from the kaolinite sheets. Note the local agglomerate of Kc kaolinite in the lower left side of the picture. D) Kb kaolinite composed by hexagonal and pseudohexagonal crystals averaging 1-3 μm in diameter. E) Kb kaolinite, consisting of crystals with face-to face arrangement (circle). F) Kb kaolinite, consisting of crystals with parallel to pseudo-parallel arrangement (circle). G) A crudely developed booklet of kaolinite, attributed to result from replacement of a feldspar grain. H) Kc kaolinite, consisting of hexagonal to pseudohexagonal crystals with regular size around 200 nm in diameter, typical of the paleosol horizon from the top of the soft kaolin unit.

3.5.2 Intermediate and semi-flint kaolin units

In addition to conglomerates, these units are dominated by sandstones, mudstones and heterolithic deposits. As previously-mentioned, the latter, restricted to the intermediate unit, forms either slightly undulating or highly folded deposits. Kaolinitized, well rounded, moderately sorted, fine-grained to silty sandstones alternate with massive mudstones, defining laminations. The intermediate unit is, in general, soft. It becomes harder only in its upper portion where paleosols are present, but even so, it is softer than the semi-flint kaolin. Its base displays Kb, and more rarely Ka, kaolinites, both pervasively draped by Kc kaolinites (Fig. 7A). The volume of the latter increases substantially upward (Fig. 7B).

The intermediate kaolin is sharply overlain by massive, endured mudstones and sandstones of the semi-flint kaolin unit. The mudstones (Fig. 7C) are homogeneous and consist of yellowish-brown Kc kaolinite and, secondarily, Kb kaolinites, with the first increasing in volume upward. The mudstones from the top of the semi-flint unit might be entirely composed by Kc kaolinites. They also show numerous irregular fractures and fenestrae of variable sizes (Fig. 7C) that are filled by clear kaolinites.

Two types of sandstones occur in the intermediate and semi-flint units: quartz-sandstone and kaolinitized sandstone. Quartz-sandstones, which occur only in association with layers attributed to transgressive lags (Rossetti and Santos Jr. 2006), are very friable, contrasting with the overall surrounding endured, kaolinitized deposits. These sandstones are moderately to well sorted, well rounded, and vary from fine to medium grain sizes. Kaolinitized sandstones are mostly moderately- to poorly-sorted, with very fine to medium grains sizes that are, in general, sub-rounded to rounded (Fig. 7D). The grains, which display punctual and, very rarely, concave-convex contacts, consist of a homogeneous mass of dark brown kaolinite composed dominantly by Kc kaolinites (Fig. 7E), with only relicts of Kb kaolinites. Their boundaries are strongly highlighted by coatings of iron oxide, present even between grains. The interstitial space was completely filled by cement of clear kaolinite. Samples displaying this characteristic revealed to contain well-developed booklets of kaolinites (i.e., Ka kolinite), as well as iron oxides and halloysite. The iron oxides form spheres or regular size (Fig. 7F), while the halloysite forms an interlaced network of either tabular (Fig. 7G) or elongated, hairy (Fig. 7H) crystals. Nevertheless, the SEM microscopic analysis also revealed that a great part of the interstitial space consists of

Kc kaolinites. Eventually, the framework grains might be fractured and filled by the clear kaolinite.
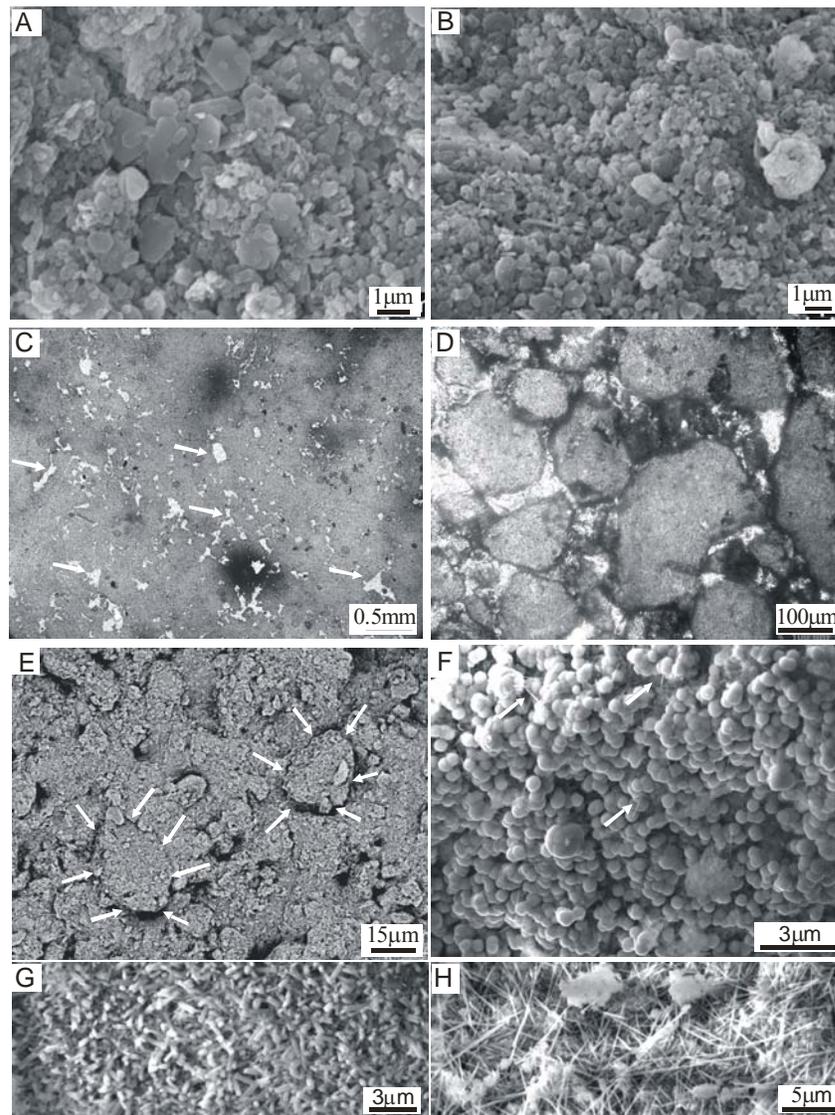
Figure 3.7 Endured mudstones and sandstones representative of the intermediate and semi-flint kaolin units. A,B) Texture of kaolinites from the lower portion of the intermediate kaolin unit, where Kb kaolinites occur in association with Kc kaolinites, with the volume of the latter increasing significantly upward (B) in association with a paleosol horizon.(SEM, secondary electrons). C) Kaolinitized mudstone of the semi flint unit, characterized by a massive texture and displaying fractures and fenestrae filled by clear kaolinite (arrows) (parallel polars). D) Kaolinitized sandstone of the semi flint unit, consisting of sub-rounded to rounded, very fine to medium grains sizes composed by dark brown Kc kaolinites coated by iron oxides. Note the clear kaolinite cementing the interstitial space (bright color) (parallel polars). E) Sandstone from the semi-flint unit, characterized by a strongly kaolinitized fabric, but where sand grains can be distinguished (arrows) from the "matrix" of similar composition (SEM, back scatter). F) A detail of the interstitial space of a sandstone from the semi-flint unit, cemented by spherules of iron oxides. Note a few hairy crystals of halloysite (arrows) (SEM, secondary electrons). G, H) Details of tabular (G) and hairy (H) halloysite crystals that occur cementing the kaolinitized sandstones of the semi-flint unit (SEM, secondary electrons).

3.6 DISCUSSION

Taking into account the high degree of kaolinitization of the studied deposits, reconstructing their primary nature, as well as determining the several phases of kaolinite formation, are issues hard to be approached. Previous studies have proposed granitic and metamorphic sources throughout the kaolin deposits of the Ipixuna Formation (Nascimento and Góes 2005). Truckenbrodt et al. (1991) and Kotschoubey et al. (1996, 1999) have proposed that the kaolinite derives from replacement of feldspar grains and muddy matrix in arkosic deposits during progressive deep weathering.

In general, determining sandstone provenance is one of the most problematic issues in sedimentary geology. This is because one must consider the influence of various factors (e.g., type of rock, relief, climate, tectonics, flow dynamics, depositional environment) acting in the source area, as well as during sediment transportation, deposition and evolution after burial (Folk 1974; Basu 1975; Young 1975) in order to discuss sediment sources. In addition to all these factors, the present location of the studied deposits in a tropical area further contributed to modify their primary characteristics due to weathering. Despite this high complexity, the detailed optical (i.e., petrographic and SEM) information presented herein, when analysed within a faciological and stratigraphic framework, contributes to further discuss the origin of the kaolinites in the Rio Capim area.

3.6.1 Composition and genesis of the soft kaolin unit

The great thickness and the well stratified nature of the soft kaolin unit of the Ipixuna Formation have been used to propose an origin related to *in situ* alteration of feldspar grains from arkosic deposits, as well as clay minerals from mudstones due to deep weathering (Kotschoubey *et al*. 1996; 1999). Determining whether deep weathering or diagenesis was responsible for kaolinitization is an issue opened for debate. Optical observations concerning to the three categories of kaolinites described herein confirm an origin related to kaolinitization of various types of material. The enhancement of Kc kaolinite towards the top unconformity is taken as a good evidence of a genesis related to weathering and, possibly, soil formation. The presence of many fractures filled by clear kaolinite is possibly related to the action of roots.

On the other hand, the majority of the Kc kaolinite seems to have been formed by replacement of Ka and Kb kaolinites, as suggested by: 1. its occurrence consistently over Ka and Kb kaolinites; and 2. the inverse proportion in the volume of Kc kaolinites with respect to the other kaolinites.

The increased abundance of Ka and Kb kaolinites in mudstones and sandstones, respectively, is a good indication that the first resulted from replacement of sand grains, while the second is chiefly related to replacement of detrital clay minerals. These mineral transformations predate the formation of Kc kaolinites, suggesting that Ka and Kb kaolinites had an origin unrelated to weathering associated to the top unconformity, being most likely formed by contact with intrastratal fluids during a previous burial.

The quartzose sandstones display regular quartz grains derived either from granitic or metamorphic rocks, or even both. The upward gradation from quartzose to kaolinitized sandstones attests to a change in sand composition. The almost complete disappearance of regular quartz grains upward in the soft kaolin unit is taken as further evidence to support diversified sediment source. The presence of monazite and topaz points to igneous contribution (Nascimento and Góes 2005). However, if only a granitic source would be considered, the volume of quartz grains should have remained constant even if the grain size decreased (Tortosa et al. 1991). Despite the overall increase in the abundance of finer-grained sandstones upward in the soft kaolin unit, the fact that many intervals with kaolinitized sandstones are of same grain size as the quartzose sandstones led to suspect of a possible change in sediment source. The presence of heavy minerals such as kyanite and staurolite confirms a metamorphic contribution for these

sediments (Nascimento and Góes 2005). The domain of monocrystalline, instead of polycrystalline, quartz grains are more typical of high degree of metamorphism (Yong 1975). On the other hand, the abundance of bipyramidal quartz grains with straight extinction, embayments and vacuoles attests the presence of sediments derived from felsic volcanic rocks (e.g., Folk 1974; Scholle 1979). Lithic fragments containing bipyramidal quartz crystals parallel to muscovites suggest either an incipient foliation or primary bedding, leading to invoke a contribution from either fine-grained volcaniclastics or volcanic rocks with a certain degree of metamorphism.

The prevalence of bipyramidal quartz, either as grains or crystals within lithic grains, conforms to a great influence of felsic volcanic fragments. The kaolinitized grains displaying bipyramidal or cuneiform shapes similar to quartz, but which have been replaced either entirely or partly by kaolinite, might record grains belonging to the silica group, but of a different species more suitable for replacement. Ghosts of grains with bipyramidal shape led to suspect on the presence of cristobalite. As quartz, cristobalite is a mineral formed by sheets of tetrahedra pointing alternately up and down, resulting in a bipyramidal shape. In addition, this mineral is usually found in association with volcanic rocks (e.g., Nesse 1991), thus being consistent with the proposed interpretation. Unfortunately, because only relicts of this mineral are preserved, its optical characterization was not enough to draw any further conclusions. The numerous black inclusions associated to these grains are taken as residues left behind during dissolution, followed by replacement by kaolinite, an interpretation consistent with the fact that this type of material is absent in the kaolinitized matrix.

If the foregoing interpretation is correct, then a great portion of the kaolinitized sandstones is formed by lithic grains of volcanic sources. In fact, it is possible that much of the bipyramidal quartz and cristobalite (?) of the sandstone framework are, in fact, crystals from lithic grains that were left behind during kaolinitization. This is suggested with basis on the presence of many areas of the kaolinitized "matrix" with ghosts of grains with floating crystals within. Thus, part of the "matrix" is in fact a pseudomatrix formed by replacement of the framework grains by kaolinite. Kaolinitization of the framework grains was pervasive, affecting not only lithic grains, but also feldspar, muscovite and, less intensely, granitic and metamorphic quartz.

Kaolinitization of framework grains produced large kaolinite crystals as agglomerates of booklets, which form part of the Ka kaolinite. The crudely developed, large, rectangular booklets probably record kaolinitized feldspar grains. This is suggested because this shape is similar to many feldspar grains that are still preserved in the framework. Large kaolinite booklets resulted also from replacement of muscovite, which is indicated by the fact that many large booklets with anomalous birefringence grade into muscovites. The presence of large kaolinite crystals associated with both feldspar and muscovite grains are probably due to the larger volume of Al, as well as Si and O, available from alteration of these minerals. Lozenge kaolinite crystals intergrown with Ka booklets suggest a phase of kaolinite precipitation postdating the formation of booklets.

Despite the fact that most of the Kb kaolinite resulted from kaolinitization of clay minerals from mudstones, as previously stated, this work shows that part of it was also derived from alteration of framework grains. This is revealed by the occurrence of this type of kaolinite in association with ghosts of quartz and cristobalite (?) grains and crystals from lithic fragments. In summary, although the largest volume of Kb kaolinite resulted from replacement of mudstone layers, a considerable amount of this kaolinite resulted from replacement of framework grains. In this case, dissolution of SiO_2 provided elements that combined with Al from circulating fluids in order to form Kc kaolinites.

3.6.2 Composition and genesis of the semi flint kaolin unit

Hard, semi-flint kaolin deposits resembling the ones from the Rio Capim area have been described in association with many other kaolin deposits worldwide. The origin of these endured kaolin overlying soft kaolin deposits has been a matter of great debate (e.g., Bates 1964; Hurst and Bosio 1975; Murray and Partridge 1982; Truckenbrodt et al. 1991; Murray and Keller 1993; Yuan and Murray 1993; Chen et al. 1997; Kotschoubey et al. 1999; Montes et al. 2002). These authors have often related the hard kaolin deposits to kaolinites with high degree of structural disorder. The action of inorganic acids and microbes in soils and weathering crusts is known to cause the destruction of clays, with the consequent decrease of structural disorder (Hurst and Pickering Jr. 1997; Hradil and Hostomsky 2002). Other workers have attributed the origin of the

semi-flint kaolin to clay flocculation in the presence of alkaline seawater (Kesller 1956; Schofield and Sampson 1954; Pickering and Hurst 1989; Dombrowski 1993).

The genesis of the semi-flint kaolin in the Rio Capim area has been interpreted to be closely related to the underlying soft kaolin, with the hard kaolin recording the uppermost portion of progressive downward weathering (e.g., Sousa 2000). The origin of the semi flint kaolin has been also related to *in situ* precipitation of amorphous kaolinite by descending solutions under influence of organic acids, combined with the action of bacterias (Kotschoubey et al. 1996). In the following, optical data are integrated with sedimentological and stratigraphic information recently available in the literature in order to propose that the semi-flint and the soft kaolin units had different depositional and evolutionary histories. In addition, it is stated that the Kc kaolinite, rather than representing *in situ* precipitation, resulted from multiple origins.

It is proposed herein that a significant volume of the Kc kaolinite in the semi flint kaolin unit was produced by pedogenesis. Likewise the soft kaolin unit, this is suggested by an overall increase in the volume of Kc kaolinite relative to Ka and Kb kaolinites upward in the semi flint kaolin. As our unpublished work focusing on oxygen and hydrogen isotopes demonstrates that the Kc kaolinite has values that contrast with modern soil waters, it is proposed that this type of kaolinite was most likely formed under influence of the paleosol developed in association with the unconformity at the top of the Ipixuna Formation (Rossetti 2004).

Despite the pedogenetic influence, it is possible that the Kc kaolinite from the semi flint kaolin unit had a more diversified origin. An important information to recall from previous work is the presence of an unconformity between the soft and the semi flint kaolin units, implying in distinctive depositional sequences, as previously mentioned (Santos Jr. 2002; Rossetti and Santos Jr. 2003; Santos Jr. and Rossetti 2003). An ongoing study focusing on heavy minerals comparing these units attests to mineralogical assemblages having different textural characteristics. Hence, there is an abrupt increase in grain roundness when crossing the basal unconformity, which led to suspect that part of the semi-flint kaolin might have been formed by reworking of the underlying soft kaolin.

A large volume of kaolinitized, mud-supported breccias and conglomerates has been reported in these deposits, which is consistent with intense sediment reworking (e.g., Kotschoubey et al. 1996; Santos and Rossetti 2003; Rossetti and Santos Jr. 2006). In addition, according to the latter authors, an important part of the semi-flint kaolin encompasses deposits

representative of mouth bar deposits, requesting a primary sandy composition. This study revealed that even the muddier hard kaolin is, at least in great part, composed by sand grain sizes, and not muds as originally thought. The well to moderate grain roundness, as well as the iron-oxide coatings predating mechanical compaction, as suggested by their presence even where grains are in contact, conform to deposition of this kaolin as sands. It is suspected that the sands might have been produced by reworking of the underlying soft kaolin unit. Together with the heavy mineral assemblage, this is suggested because, as opposed to the underlying kaolinitized sandstones from the soft kaolin unit, these sandstones are formed by grains consisting exclusively of completely homogeneous masses of dark brown Kc kaolinites.

As the uppermost part of the soft kaolin was exposed to weathering during development of a sequence boundary between the soft and the semi flint kaolin units (Rossetti, 2004), the formation of Kc kaolinites, represented by interlocking of crystals <200 nm in diameter, was favored. Reworking of this material in a new depositional setting (in this instance, deltaic mouth bars) might have resulted in sandstones composed by rounded grains of kaolin already displaying a certain degree of hardness promoted by the prevalence of Kc kaolinites.

The presence of distinctive clear Kc kaolinite filling up the interstitial spaces of the sandstones, as well as the fractures, indicates that the semi flint kaolin was further endured due to cementation. The fact that the SEM analysis revealed halloysite and Ka kaolinites in samples displaying clear kaolinite led to argue that this cement is actually represented by a mixture of these minerals. In particular, it has been claimed that the presence of halloysite might contribute to increase significantly the hardness of kaolin deposits due to the intricate crystals intergrowth (e.g., Grant 1963; Bates 1964; Osborne et al. 1994). In this instance, the volume of halloysite is probably low, but they occur only in the semi-flint kaolin. The occurrence of this mineral as cement in kaolin deposits is usually related to pedogenesis (e.g., Keller 1977, 1982). Halloysite precipitating together with Ka and Kc kaolinites in the interstitial porosity probably have contributed to endure the semi-flint kaolin unit.

In addition of a derivation from the underlying soft kaolin unit, the sediments that gave rise to the semi-flint had a contribution directly from metamorphic rocks. This is suggested also by an ongoing study that reveals the presence of euhedral staurolite and kyanite, as well as the occurrence of hornblende, with no evidence of dissolution, characteristics not present in the underlying soft kaolin unit. Furthermore, a sedimentary source is proposed for the quartz

sandstones, which were related to intense reworking associated with marine flooding surfaces (Rossetti & Santos Jr. 2006).

3.7 FINAL REMARKS

The present optical study allows is consistent with the attribution of the soft and the semi-flint kaolin units to distinctive depositional sequences. In addition to the unconformity mapped between these sequences, the recognition of different sediment sources is consistent with such an interpretation. Furthermore, the kaolinite from these deposits had distinctive origins, as great part of the soft kaolin represents kaolinitization of framework grains of sandstones and replacement of other clay minerals from mudstones. Kaolinitization was intense enough to modify most of the primary composition. However, detailed optical studies revealed many relicts of the original texture, suggesting that the kaolinitized sandstones were formed by lithic grains of felsic volcanic, as well as volcaniclastics or meta-volcanic rocks. Diagenesis of these sandstones promoted significant compositional changes, with strong kaolinitization of the framework grains. Lithic grains, as well as grains having a probable cristobalite composition, were more suitable for replacement than quartz grains. The kaolinitization process contributed to produce a deposit with a large volume of pseudomatrix, which gave them the actual wacky composition. The abundance of relicts and ghosts of grains, as well as enlarged areas between grains that appear to float in the matrix, however, led to the conclusion that these are artificial wackes produced during kaolinitization.

The upward almost disappearance of regular quartz grains in the soft kaolin unit is explained by a change in both sedimentary conditions and sediment sources. This situation might have been favored by the estuarine nature of the depositional setting (Rossetti and Santos Jr. 2003; Santos Jr. and Rossetti 2003). Hence, the quartzose sandstones from the base of the sections might record higher energy flows associated to the initial transgression of the estuarine system. During this process, unstable grains have higher potential to be lost due to the strong reworking by tidal currents and waves, which favors deposition of sands rich in quartz grains at the estuary axis. As the estuary is filled with sediment, there is a greater interaction of marine and fluvial flows, with the latter dominating in inner estuarine areas. The deposits located in the

middle and upper portions of the studied sections formed in a variety of tidal depositional settings typical of inner and middle estuarine areas. The sediment in these settings derived mainly from fluvial inflows, resulting in sandstones with composition of the framework grains that varied with relation to the quartzose sandstones. Diagenesis of these deposits led to an intense kaolinitization, but with preservation of primary structures. Burial promoted the replacement of sandstones and mudstones by Ka and Kb kaolinites. Kc kaolinites formed later on by replacement of Ka and Kb kaolinites in association with pedogenesis related to the development of the unconformity that bounds the top of the soft kaolin unit.

The semi flint kaolin, on the other hand, resulted from sediments reworked from the underlying soft kaolin deposits, which were mixed with an additional nearby metamorphic source. This would have brought Kc kaolinites from the upper, slightly endured portion of the soft kaolin. The reworked sediment would have been reduced to sand grain sizes, adopting a dirt appearance during transportation, and becoming coated by iron oxide. Weathering acting during transportation contributed to further endure the kaolin grains. Following deposition, additional Kc kaolinite was formed throughout the semi flint kaolin due to pedogenetic processes associated to the unconformity that marks the top of the Ipixuna Formation. Further Kc kaolinite was introduced by cementation of sandstones and filling of fractures.

Despite the sharp boundaries and the softer nature, the intermediate unit displays sedimentological features with more affinity to the semi-flint kaolin than to the soft kaolin unit. The intermediate and the semi-flint kaolin units also have comparable heavy mineral characteristics, as well as prevalence of Kc kaolinites. The data presented herein, however, was not enough to decide if the intermediate kaolin is the remaining of a distinctive depositional unit or part of the semi-flint kaolin unit, as previously pointed out (Rossetti, 2004).

REFERENCES

AZEVEDO, R.P. 1991. Tectonic Evolution of Brazilian Equatorial Continental Margin Basins. Royal School of Mines Imperial College, London, 412 p. (PhD thesis)

BASU, A. 1975. Petrology of Holocene fluvial sand derived from plutonic source rocks: implication to provenance Interpretation. Bloomington, Indiana University, 138 p. (M.Sc. Dissertation).

BATES, B.F. 1964. Geology and Mineralogy of the Sedimentary kaolins of the Southeastern United States. In: BAILEY, W.F. (ed.). *A review: Clay and Clay Minerals*. New York. Macmillan, p. 177-194. Procedures of the Twelfth Nacional Conference 1963

CHEN, P.Y.; LIN, M.L.; ZHENG, Z. 1997. On the origin of the name kaolin and the kaolin deposits of the Kauling and Dazhou areas, Kiangsi, China. *Applied Clay Science* **12,** 1-25.

COSTA, J.B.S.; BEMERGUY R.L.; HASUI, Y.; BORGES, M.S. 2001. Tectonics and paleogeography along the Amazon River. *Journal of South American Earth Sciences* **14,** 335-347.

COSTA M.L. & MORAES E.L. 1998. Mineralogy, geochemistry and genesis of kaolins from the Amazon region. *Mineralium Deposita* **33,** 3-297.

DOMBROWSKI, T. 1993. Theories of origin for the Georgia Kaolins. In:. MURRAY, H., BINDY, W., HARVEY, C., (Ed.) *Kaolin genesis and Utilization*, p. 75-98. (Clay Mineral Society Special Publication **1)**.

FOLK, R.L. 1974. Mineral composition of sedimentary rocks. In:_____. *Petrology of Sedimentary rocks.* Austin, Texas, Hemphill Publishing Company. p. 65-145.

GALVÃO, M.V.G. 1991. *Evolução Termodinâmica da Bacia do Marajó, Estado do Pará, Brasil*. Ouro Preto. Universidade de Ouro Preto. 193 p. (Dissertação de Mestrado)

GÓES, A.M. 1981. *Estudo Sedimentológico dos Sedimentos Barreiras, Ipixuna e Itapecuru, no Nordeste do Estado no Pará e Noroeste do Maranhão*. Belém, Universidade Federal do Pará, Centro de Geociências. 55 p. (Dissertação de Mestrado).

GRANT, W.H. 1963. Weathering of Stone Moutain granite. New York, Pergamon Press, p. 65-74. Clay and Clay Minerals, 11th Conference.

HRADIL, D., & HOSTOMSKÝ, J. 2002. Effect of composition and physical properties of natural kaolinitic clays on their strong acid weathering rates. *Catena* **49,** 171-181.

HURST V.J., & BOSIO N.J. 1975. Rio Capim Kaolin deposits, Brazil. *Economic Geology* **70,** 990-992.

HURST, V.J. & PICKERING JR., S.M. 1997. Origin and classification of coastal plain kaolins, southeastern USA, and the role of groundwater and microbial action. *Clays and Clay Minerals* **45,** 272-285.

JUPIASSÚ, A.M.S. 1970. Madeira Fóssil – Humiriaceae de Irituia, Estado do Pará. *Boletim do Museu Paraense Emilio Goeldi* **14,** 1-12.

KELLER, W.D. 1977. Scan electron micrographs of kaolin colleted from diverse environments of origin-IV. Georgia kaolin and kaolinizing source rocks. *Clay and Clay Minerals* **25,** 311-345.

KELLER, W.D. 1982. A most diverse rock in genesis, texture, physical properties, and uses. *Geological Society of America Bulletin* **93,** 27-36.

KESLER, T.L. 1956. Environment and origin of the Cretaceous kaolin deposits of Georgia and South Carolina. *Economic Geology* **51,** 541-554.

KOTSCHOUBEY, B.; DUARTE, A.L.S.; TRUCKENBRODT, W. 1999. Cobertura bauxítica e origem do caulim do Morro do Felipe, Baixo Rio Jari, Estado do Amapá. *Revista Brasileira de Geociências* **29,** 331-338.

KOTSCHOUBEY, B.; TRUCKENBRODT, W.; HIERONYMUS, B. 1996. Depósitos de caulim e argila semi-flint no nordeste do Pará. *Revista Brasileira de Geociências* **26,** 71-80.

MONTES, C.R.; MELFI, A.J.; CARVALHO, A.; VIEIRA-COELHO, A.C.; FORMOSO, M.L.L. 2002. Gênesis, mineralogy and geochemistry of kaolin deposits of the Jarí River, Amapá State, Brazil. *Clays and Clay Minerals* **50,** 494-503.

MURRAY, H.H. & KELLER, W.D. 1993. Kaolins, Kaolins and Kaolins. In: MURRAY, H.; BUNDY, W.; HARVEY, C (Ed.). *Kaolin Genesis and Utilization.* p. 1-24, (Clay Mineral Society Special Publication **1**).

MURRAY, H.H. & PARTRIDGE, P. 1982. Genesis of rio Jarin kaolin. In: H. VAN OLPHEN, F. VENIALE (E.), *Developments in Sedimentology*, Amsterdam, Elsevier, p. 279-291.

NASCIMENTO, M.S. & GÓES, A.M. 2005. Distribuição estratigráfica e proveniência de minerais das formações Ipixuna e Barreiras, região do Rio Capim, Sub-Bacia de Cametá, Estado do Pará. *Revista Brasileira de Geociências* **35,** 49-58.

NESSE, W.D. 1991. *Introduction to optical mineralogy*. Second edition. Oxford, Oxford University Press, 335 p.

OSBORNE, M.; HASZELDINE, R.S.; FALLICK, A.E. 1994. Variation in Kaolinite morphology with growth temperature in isotopiclly mixed pore-fluids, Brent Group, UK North Sea. *Clay Minerals* **29,** 591-608.

PICKERING, S.M. & HURST, V.J. 1989. Commercial Kaolins in Georgia. Occurrence, Mineralogy, Origin, Use. *Geological Society Guidebooks* **9,** 29-75.

ROSSETTI, D.F. 2004. Paleosurfaces from northeastern Amazonia as a key for reconstructing paleolandscapes and understanding weathering products**.** *Sedimentary Geology* **169,** 151-174.

ROSSETTI, D.F. & SANTOS JR., A.E. 2003. Events of soft sediment deformation and mass failure in Upper Cretaceous estuarine deposits (Cametá Basin, northern Brazil) as evidence for seismic activity. *Sedimentary Geology* **161,** 107-130.

ROSSETTI, D.F. & SANTOS JR., A.E.A. 2006. Analysing the origin of the Upper Cretaceous-?Lower Tertiary Rio Capim semi flint (Pará State, Brazil): under a sedimentologic perspective. *Sedimentary Geology* **186,** 133-144.

SANTOS JR., A.E.A. 2002. *Reconstrução Paleoambiental e Estratigráfica de Depósitos Cretáceos e Terciários Expostos na Borda Sudeste da Sub-Bacia de Cametá, Norte do Brasil.* Belém. Universidade Federal do Pará, Cetro de Geociências. 131 p. (Dissertação de Mestrado).

SANTOS JR., A.E.A. & ROSSETTI, D.F. 2003. Paleoambiente e estratigrafia da Formação Ipixuna, Área do Rio Capim, Leste da bacia de Cametá. *Revista Brasileira de Geociências* **33,** 313-324.

SANTOS JR., A.E.A. & ROSSETTI, D.F. 2006. Depositional model of the Ipixuna Formation (Late Cretaceous-?Early Tertiary), Rio Capim Area, northern Brazil. *Latin American Journal of Sedimentology and Basin Analysis* (in press).

SCHOFIELD, R.K. & SAMPSON, H.R. 1954. Flocculation of kaolinite due to the attraction of oppositely charged faces. *Faraday Society Discussion* **18,** 135-145.

SCHOLLE, P.A. 1979. A color illustrate guide to constituents, textures, cements and porosity of sandstones and associated rocks. *American Association of Petroleum Geologist*, Tulsa, 201 p.

SOUSA, D.J.L. 2000. *Caracterização Geológica, Mineralógica, Química e Física do Caulim da RCC - Rio Capim Caulim (PA).* Belém, Universidade Federal do Pará, Cetro de Geociencias, 116 p. (Dissertação de Mestrado).

TORTOSA, A.; PALOMARES, M.; ARRIBAS, J. 1991. Quartz grain types in Holocene deposits from the Spanish Central System: some problems in provenance analyis. In: MORTON, A.C., TODD, S.P.; HAUGHTON, P.D.W. (ed.) *Development in Sedimentary Provenance Studies*, p. 47-54. (Geological Society Special Publication, 57).

TRUCKENBRODT, W.; KOTSCHOUBEY, B.; SCHELLMANN, W. 1991. Composition and origin of the clay cover on North Brazilian laterites. *Geologische Rundschau*. **80,** 591-610.

VILLEGAS, J.M.C. 1994. *Geologia Estrutural da Bacia do Marajó*. Belém, Universidade Federal do Pará, Centro de Geociências, 119 p. (Dissertação de Metrado).

YOUNG, S.W. 1975. *Petrography of holocene fluvial derived from regional metamorphic source rocks.* Bloomington, Indiana University, 93 p. (M.Sc. Dissertation).

YUAN, J. & MURRAY, H.H. 1993. *Mineralogical and physical properties of the Maoming Kaolin from Guandong Province, South China*. P. 249-260. (Clay Mineral Society Special Publication **1)**

ACKNOWLEDGMENTS

4. ORIGIN OF THE RIO CAPIM KAOLINITES (NORTHERN BRAZIL) REVEALED BY δ^{18}O AND δD ISOTOPE ANALYSIS

Antônio Emídio de Araújo SANTOS Jr,
Dilce de Fátima ROSSETTI
and Haydn H. MURRAY

4.1 ABSTRACT

Deuterium (δD) and oxygen (δ^{18}O) isotope data from the Rio Capim kaolin, northern Brazil, were combined with optical studies in order to better understand the genesis and evolution of the kaolinites. The results show that δ^{18}O isotope values from a lower soft kaolin unit range from 6.04‰ to 19.18‰ for Ka (size ranging from 1 to 3 μm) and Kb (size ranging from 10 to 30 μm) kaolinites, and from 15.38‰ to 24.86‰ for Kc (size <200 nm) kaolinites. The δD values range from −63.06‰ to 79.46‰ for the Ka+Kb kaolinites, and from −68.85‰ to −244.35‰ for the Kc kaolinites. An upper semi flint kaolin unit, dominated by Kc kaolinites, displays δ^{18}O and δD isotope values ranging from 15.08‰ to 21.77‰, and -71.31‰ to -87.37‰, respectively. Based on these data, and on the δ^{18}O and δD values obtained for the surface meteoric water and groundwater, it can be concluded that the kaolinites are not in equilibrium with the modern weathering environment, but they reflect isotopic compositions of the formation time, probably due to the interaction with groundwaters. However, mineralogical contaminations derived from replacements of framework grains also had great influence in the isotopic composition of these kaolinites. In addition, the isotope values of the Kc kaolinites from the semi-flint kaolin unit is variable, which is due to the presence of Kc kaolinites of different origins, including kaolinites derived from the underlying soft kaolin unit, kaolinites formed during different phases of paleoweathering, as well as later phases of coarse-grained kaolinites formed along fractures. Due to these complexities, binary diagrams contrasting δ^{18}O and δD isotope values, worldwide applied for distinguishing supergenic from hypogenic kaolinites, as well as those formed under weathering conditions, can not be applied to interpret the origin of the kaolinites in the Rio Capim Kaolin.

Keywords δ^{18}O and δD, optical studies, Rio Capim kaolin, kaolinite, origin, genesis.

4.2 INTRODUCTION

Hydrogen and oxygen isotopes have been increasingly applied to approach the environmental conditions prevailing during formation of clay minerals (Savin and Epstein, 1970a,b; Lawrence and Taylor, 1971,1972; Savin and Lee, 1988; Zhou and Dobos, 1994; Mizota and Longstaffe, 1996; Savin and Hsieh, 1997; Stern et al., 1997; Gilg, 2000; Vitali et al., 2002; Gilg et al., 2003; Tabor and Montanez, 2005). In pedogenic minerals from weathered deposits, these isotopes are in equilibrium with meteoric waters (Savin and Epstein, 1970a; Lawrence and Taylor, 1971,1972; Mizota and Longstaffe, 1996; Savin and Hsieh, 1997; Girard et al., 2000), while their interaction with pore-waters and circulating hydrothermal waters takes place in burial and hydrothermal environments, respectively (Sheppard et al., 1969; Marumo et al., 1980; Sun and Eadington, 1987; Cruz and Reyes, 1998; Boulvais et al., 2000). δD and $\delta^{18}O$ from kaolinites in weathering profiles allow establishing a straight linear equation, traditionally known as the kaolinite line, as well as estimating the isotope fractionation factor (α) (Savin and Epstein, 1970a). Likewise, a supergene/hypogene line (S/H) has been used to separate clay minerals formed under earth surface and high burial temperatures, respectively (Sherppard et al., 1969). In addition to kaolinite (Savin and Epstein, 1970a, Liu and Epstein, 1984; Savin and Lee, 1988; Zhou and Dobos, 1994; Gilg and Sheppard, 1996; Cruz and Reyes, 1998; Boulvais et al., 2000; Gilg, 2000; Girard et al., 2000; Gilg et al., 2003), montmorillonite, glauconite, illite and many other minerals have been applied in these investigations (Savin and Epstein, 1970a; James and Baker, 1976; Savin and Lee, 1988). Furthermore, the isotope composition of surface and near-surface modern waters (Bowen and Wilkinson, 2002; Fricke and O'Neil, 1999; Bowen and Revenaugh, 2003) relative to SMOW (Standard Mean Ocean Water) has been used to define the Meteoric Water Line (Freidman, 1953; Craig, 1961; Epstein et al., 1965). All these concepts have been applied to discuss the environmental conditions during the deposition and post-deposition time of clayey deposits, particularly regarding to paleotemperature (Savin and Lee, 1988; Yapp, 1986; Gilg and Sheppard, 1996).

Although experiments with stable isotopes support a relationship between δD and $\delta^{18}O$ obtained from clay minerals and paleotemperature, this approach is not so straightforward, as other factors must be taking into account, including latitude, altitude, and distance from the coastline (Savin, 1977; Savin and Hsieh, 1998). Due to these complexities, further studies

emphasizing δD and δ^{18}O isotopes must be undertaken to provide a full comprehension of the behavior of these values along ancient clayey deposits, particularly considering a larger volume of analogs that can be used as a basis for comparisons.

The Ipixuna Formation exposed in the Rio Capim area, northern Brazil, is well known for its kaolin reserves, one of the largest in the world. Due to the economic interest, this unit has been increasingly under investigation, with many publications presented in the last years concerning to aspects including the depositional environment, provenance, petrography and geochemistry (Góes, 1981; Truckenbrodt et al., 1991; Kotschoubey et al., 1996; 1999; Costa and Moraes, 1998; Rossetti and Santos Jr., 2003, 2006; Rossetti, 2004; Sousa, 2000; Santos Jr., 2002; Santos Jr. and Rossetti, 2003, 2006; Nascimento and Goes, 2005). As a result of these studies, the Ipixuna Formation has been subdivided into two stratigraphic units, consisting of a lower soft kaolin unit, and an upper semi flint kaolin unit, bounded by discontinuity surfaces associated with lateritic paleosols. Despite the presence of these weathering surfaces, optical studies have indicated different types of kaolinite in the Ipixuna Formation, with a large volume appearing to be unrelated to surface processes. The occurrence of these weathering surfaces, combined with the fact that kaolinite is the major constituent in the Ipixuna Formation, favors the application of δD and δ^{18}O isotope in order to distinguish the various kaolinite generations present in these deposits. In addition to help better understand the genesis and evolution of the kaolinites from the Rio Capim area, this study attempts to contribute testing the applicability of these methods for reconstructing the environmental conditions involved in the kaolinite formation.

4.3 GEOLOGY

The Ipixuna Formation encompasses Upper Cretaceous-?Lower Tertiary kaolinitized sandstones and mudstones that are well exposed in the eastern Cametá Sub-Basin, where the Rio Capim Kaolin focused herein is located. The genesis of this basin, situated in the Marajó Graben System, is linked to the strike-slip deformation that took place along the Equatorial Brazilian Margin during the opening of the South Atlantic Ocean (Azevedo, 1991; Galvão, 1991; Villegas, 1994; Costa et al., 2001). The Cametá Sub-Basin displays mostly fluvial to shallow marine deposits recorded by a sedimentary pile up to 10 km thick comprising the Breves (Aptian-

Cenomanian), Limoeiro (Late Cretaceous), Marajó (Paleocene-Eocene) and Tucunaré (Pleistocene) formations (Fig. 1).

The Ipixuna Formation exposed in the Rio Capim area reaches up to 40 m thick. The lower soft kaolin unit records an overall fining- and thinning-upward succession up to 20 m thick, characterized from bottom to top by tidally influenced fluvial channel, tidal channel, tidal flat/mangrove, and tidal sand bar/tidal sandy flat, attributed to an estuarine system (Santos Jr., 2002; Santos Jr. and Rossetti, 2006). Tidally influenced fluvial and tidal channels are defined by sharply based, locally concave up, fining- and thinning-upward successions formed by tabular to trough cross-stratified or laminated sandstones, as well as intraformational conglomerates and heterolithic mudstones/sandstones. Tidal channel deposits are distinguished from tidally influenced fluvial channels based on the abundance of both reactivation surfaces and mud drapes along cross sets, and trace fossils including *Thalassinoides, Planolites, Teichichnus, Taenidium* and *Skolithos.* Tidal flat/mangrove records the finest deposits of the soft kaolin unit, consisting of tabular packages of highly bioturbated (mostly *Skolithos* and *Ophiomorpha*), heterolithic-bedded sandstones and mudstones. Tidal sand bars and tidal sandy flats, which contain *Thalassinoides, Ophiomorpha, Skolithos, and Planolites,* form laterally continuous, either lenticular or tabular packages bounded at the base by either planar or only slightly undulating (though not erosive) surfaces, which internally display horizontally stratified sandstones with abundant parting lineation that are interbeded with heterolithic deposits. As a result of these facies characterization, the traditional attribution to a fluvial-lacustrine depositional setting to the soft kaolin unit (Góes, 1981) has been reconsidered in favor of an estuarine system (Rossetti and Santos Jr., 2003, 2006; Rossetti, 2004; Santos Jr., 2002; Santos Jr. and Rossetti, 2003, 2006).

The upper semi-flint kaolin unit is either massive or incipiently structured, comprising sandstone, mudstone, intraformational conglomerate and heterolithic deposits attributed, at least in part, to distributary channel and mouth bar depositional environments associated to either a deltaic or wave-dominated estuarine setting (Rossetti and Santos Jr. 2006). The distributary channels are characterized by concave up kaolinitized sandstones and mudstones displaying a basal lag of quartz sandstones. These deposits intergrade with strata displaying a series of inclined lines, defining lobed bodies that are locally highlighted by distinctively soft, massive mud layers.
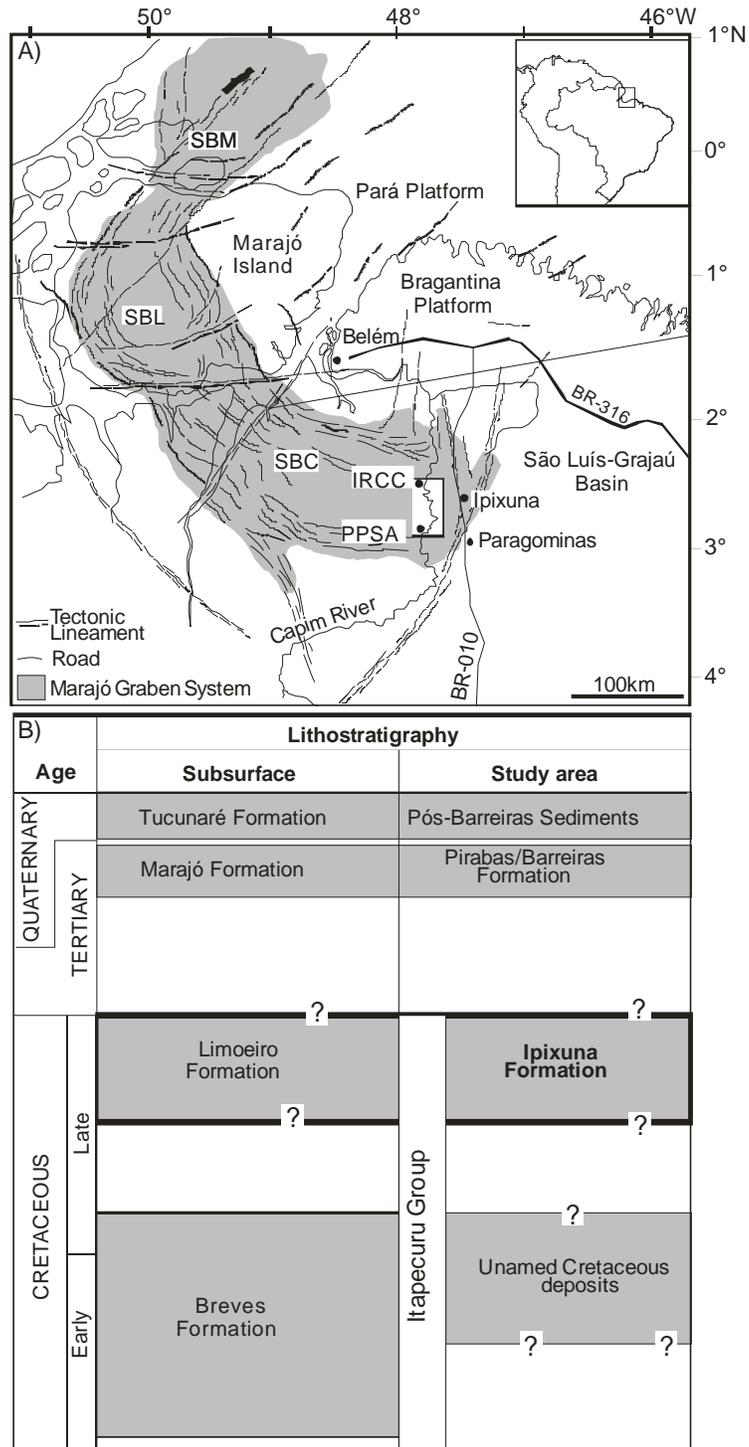
Figure 4.1 A) Location of the study area in the eastern Cametá Sub-Basin, Marajó Graben System, with indication of the two studied quarries, the IRCC and PPSA (SBC=Cametá Sub-Basin, SBL=Limoeiro Sub-Basin, SBM=Mexiana Sub-Basin). B) Lithostratigraphic chart of the Cametá Sub-Basin.

Our ongoing studies reveal that the soft kaolin unit described above displays three types of kaolinite, categorized according to size and texture, as Ka, Kb and Kc kaolinites. Ka kaolinite, typical of the sandstones, consists of hexagonal to pseudohexagonal crystals 10-30 μm in diameter, and occurs as agglomerates of booklets or vermicular crystals that reach up to 400 μm in length. Kb kaolinite, which dominates in the mudstones, consists chiefly of hexagonal and pseudohexagonal crystals averaging 1-3 μm in diameter. Both kaolinites might entirely or partly replace grains of the framework, including quartz, feldspar, muscovite, as well as igneous (mostly volcanic) and metamorphic lithics. Kc kaolinite displays hexagonal to pseudohexagonal crystals with regular sizes around 200 nm in diameter (Fig. 2).

The soft kaolin consists mostly of Ka and Kb kaolinites, with the first dominating in the sandstones and the latter in the mudstones. In addition, Kc kaolinite occurs subordinately, always mantling the other kaolinite types, which suggests its formation, at least in part, from the coarser-grained kaolinites. Kc kaolinite increases significantly in abundance upward in the soft kaolin unit, where it is associated with a paleosol horizon linked to the unconformity that separates the soft and the semi-flint kaolin units. As opposed to the soft kaolin unit, the semi-flint is dominated by endured Kc kaolinite, though the other types of kaolinite might also occur at the base of the unit, as well as associated with fractures abundant in its top.
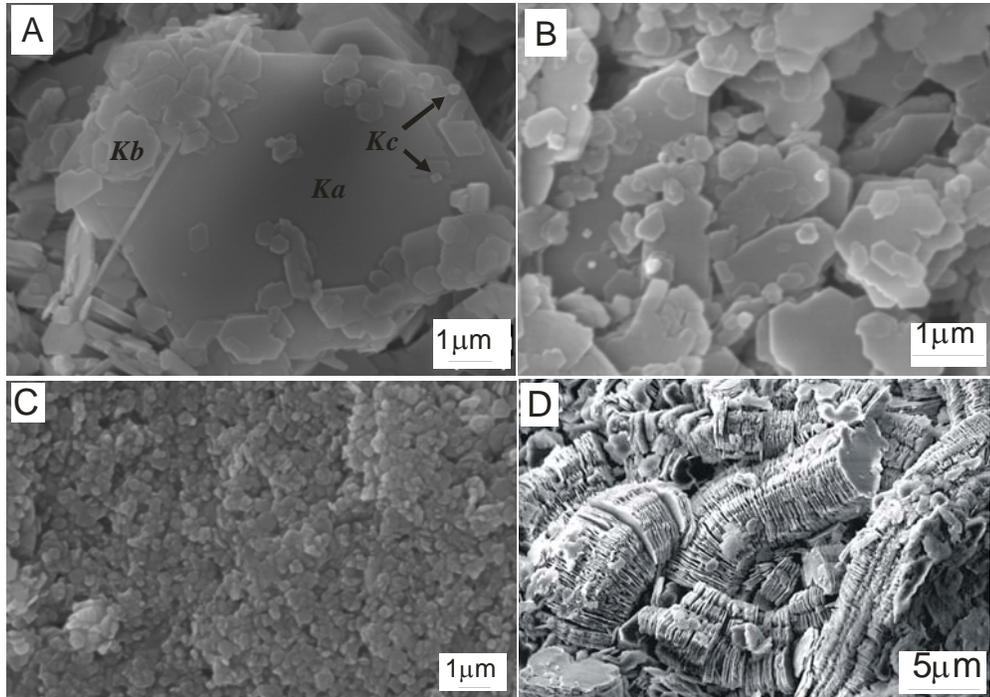
Figure 4.2 Types of kaolinites from the Rio Capim area. A-B) Ka and Kb kaolinites, typical of sandstones (A) and mudstones (B) of the soft kaolim unit, respectively. C) Kc kaolinite, typical of the semi-flint kaolin unit. D) Kaolinite booklets.

4.4 METHODS

The $\delta^{18}O$ and δD values were measured in 113 samples using the procedures described by Clayton and Mayeda (1963) and Coleman et al. (1982), respectively. The samples were obtained from representative profiles along two quarries (i.e., IRCC and PPSA) of the Rio Capim area, located circa 60 km apart, and aimed to record different lithofacies, including kaolinitized sandstones, pelites and conglomerates from the two kaolin units described above.

Preliminarily, three parcels were obtained from selected samples in order to record the three types of kaolinites (i.e., Ka, Kb, and Kc) observed by optical studies. Each kaolin sample was first dispersed in a solution containing distilled water and sodium hexametaphosphate. The samples were then carefully disaggregated ultrasonically for 10 seconds and, subsequently, sieved to separate the fractions >64 μm, from which kaolinite booklets (Ka kaolinite) were hand picked under a binocular. The grain sizes <64 μm were separated through settling according to Stokes' Law to obtain the fractions <200 nm, 1 to 3 μm, and 10 to 30 μm, recording the Kc, Kb and Ka kaolinites. The latter was added to the booklets hand picked from the <64 μm. Each fraction was purified using distilled water at least three times and concentrated by centrifugation. They were then heated at $100^{\circ}C$ in a vacuum chamber oven for 24 hours in order to remove adsorbed water between octahedric and tetrahedrical sheets.

For $\delta^{18}O$ isotope extraction, 5 mg of each parcel were put in a copper tube and heated at 100°C under high vacuum for 1 hour. Following this procedure, bromine pentafluoride (BrF5) was introduced to release the oxygen that was reacted with a graphite disk in an intensive light to produce CO_2. The CO_2 was trapped in a glass tube using liquid N_2. To obtain the $\delta^{18}O$ data, the samples were analyzed on a Finingan-MAT DELTA mass spectrometer. For δD isotope analysis, 1 mg of kaolinite from each parcel was inserted in a vacuum system containing He and extracted on-line directly from Thermo-Finnigan TCEA (thermal conversion elemental analyzer), operated at 1,440°C. Kaolinite (KGA), and serpentine plus kaolinite (KGA) standards were routinely measured together with the kaolinite samples to verify the accuracy of the $\delta^{18}O$ and δD data. $\delta^{18}O$ and δD values are reported in parts permil (‰) relative to Standard Mean Ocean Water (SMOW). All $\delta^{18}O$ and δD data were analyzed from Geological Laboratory of the Indiana University, EUA.

The preliminary tests revealed that the Ka e Kb kaolinites displayed similar $\delta^{18}O$ and δD isotope values (Tab. 1), and for this reason the fractions >1μm were systematically analyzed as one single parcel to include the Ka and Kb kaolinites.

$\delta^{18}O$ and δD data were also obtained from rainfall and groundwater samples collected during the raining season on May 2005. Four samples were collected, two from meteoric water at the surface and two from groundwater at depths of 60 m (IRCC quarry) and 150 m (PPSA quarry). The isotope values were measured using a Thermo Finnigan Delta Plus XP isotope ratio mass spectrometer. For the hydrogen extraction, a HDevice inlet was applied to reduce 0.7 uL of water on hot chromium at 850°C for 60 seconds. For the oxygen extraction, a Gas Bench was used at 34°C for 12 hours aiming CO_2-H_2O equilibration. For both isotopes, the samples were compared to two internal laboratory standards (Boulder Water and Miami Water) with distinct isotopic compositions in order to calibrate the machine slope. The two internal laboratory standards were calibrated using international standards (VSMOW).

4.4.1 $\delta^{18}O$ and δD isotope data

The $\delta^{18}O$ and δD values obtained for the soft and semi-flint kaolin units, as well as for the local surface meteoric and groundwater, are illustrated in Table 1 and plotted in Figures 4.3 to 4.5.

In general, $\delta^{18}O$ and δD values obtained for the soft kaolin samples from both quarries display similar patterns of variation. Hence, the Ka+Kb kaolinites have $\delta^{18}O$ values ranging from 6.04‰ to 18.83‰, with an average of 14.83‰, and from 12.79‰ to 19.18‰, with an average of 16.47‰, in the PPSA and IRCC quarries, respectively. For the Kc kaolinites, these values range from 15.38‰ to 24.86‰, with an average of 19.67‰, and 16.42‰ to 23.32‰, with an average of 19.29‰ for the PPSA and IRCC quarries, respectively. The δD values for the Ka+Kb kaolinites of the PPSA quarry range from −63.99‰ to -73.87‰, with an average of −68.35‰, disregarding sample E14. These kaolinites in the IRCC quarry revealed values ranging from −63.06‰ to −79.46‰, with an average of −70.10‰, disregarding sample E-126, which shows an anomalous value of −42.56‰. For the Kc kaolinite, the δD values vary from −74.42‰ to −221.64‰, with an average of −100.02‰, and from −68.85‰ to −244.35‰, with an average of −114.21‰ for the PPSA and IRCC, respectively. Despite these overall variable results, it is

noteworthy that the Kc kaolinite from samples located at the paleosol horizon in the PPSA quarry (see E18-E21) displays δD isotope values that are very uniform, between −76.13‰ and −79.42‰. It is noteworthy that the $\delta^{18}O$ curve of the Kc kaolinite in the soft kaolin unit shows the same pattern of variation when compared to the values obtained in stratigraphic equivalent Ka+Kb kaolinites.

The Kc kaolinite from the semi-flint kaolin unit displays $\delta^{18}O$ and δD isotope values that are comparably less variable than in the soft kaolin unit. Hence, $\delta^{18}O$ values range from 18.21‰ to 19.88‰, with an average of 18.56‰, and from 15.08‰ to 21.77‰, with an average of 17.47‰ in the PPSA and IRCC quarries, respectively. The δD varies from -75.38‰ to -87.37‰, with an average of -80.86‰, and -71.31‰ to -90.10‰, with an average of -78.29‰ in the PPSA and IRCC quarries, respectively.

The present-day meteoric water indicates $\delta^{18}O$ and δD values of −1.3‰ and −0.3‰, and −4.1‰ and −1.1‰ in the PPSA and IRCC quarries, respectively. These values for the groundwater collected in the Ipixuna Formation at a depth of 60, indicate −4.9‰ for the oxygen and −22.5‰ for the hydrogen (Fig. 5).

	PPSA Quarry			
			δD_{kao}	
	Samples		kc	ka+kb	kc
A	E1	6.04+	18.64	-68.13	-79.06
	E2	11.79	18.38	-65.35	-74.42-
	E3	18.83+	19.28	-70.27	-83.01
	E4	16.02	22.90	-68.53	-193.44
	E5	17.64	18.11	-64.57	-119.19
	E6	11.39	15.63	-68.14	-113.01
	E7	11.17	19.83	-68.85	-115.76
	E8	16.61	18.77	-67.67	-95.71
	E9	16.90	18.84	-66.05	-107.48
	E10	11.79	16.45	-67.16	-111.10
	E11	13.87	17.28	-68.49	-91.47
	E12	17.82	22.06	-65.88	-132.68
	E13	18.35	22.07	-69.86	-141.39
	E14	16.88	22.38	-80.68#	-189.10
	E15	14.57	24.86+	-67.85	-140.08
	E16	17.29	19.96	-63.99-	-221.64+
	E17	15.87	22.46	-69.85	-127.03
	E18	12.25	15.38-	-72.76	-79.42
	E19	15.12	17.09	-71.42	-76.13
	E21	16.44	23.11	-73.87+	-76.13
	Average	14.83	19.67	-68.35	-100.02
B	E22		18.03		-81.05
	E88		19.88+		-75.72
	E24		18.24		-84.78
	E26		18.43		-87.37+
	E28		18.21-		-75.38-
	Average		18.56		-80.86

	IRCC Quarry			
		$\delta^{18}O_{kao}$		δD_{kao}	
	Samples	ka+kb	kc	ka+kb	kc
A	E124	12.91	17.17	-67.38	-68.85-
	E95	14.16	19.09	-63.06-	-90.39
	E96	14.89	19.91	-65.22	-101.79
	E97	18.19	18.32	-72.53	-107.32
	E98	16.17	19.43	-66.38	-79.56
	E99	13.14	17.09	-72.79	-162.41
	E100	14.77	20.20	-69.84	-77.59
	E101	15.54	17.08	-69.13	-147.61
	E102	17.79	23.32+	-72.67	-201.60
	E103	12.79-	21.54	-69.94	-176.93
	E104	18.38	22.71	-67.80	-199.96
	E105	18.01	19.21	-71.64	-74.03
	E106	17.11	19.07	-71.57	-79.03
	E107	17.70	18.92	-67.48	-126.21
	E108	18.57	19.57	-66.39	-115.78
	E109	17.73	18.18	-67.32	-244.35+
	E110	14.87	16.97	-67.47	-111.10
	E111	16.91	18.01	-67.40	-105.45
	E112	16.55	18.49	-68.77	-70.24
	E113	16.16	17.86	-70.35	-116.03
	FI206	19.18+	19.98	-69.64	-71.48
	E114	16.90	22.40	-65.87	-104.82
	E115	17.17	20.71	-73.04	-95.71
	E125	15.31	16.42-	-77.92	-92.27
	E126	18.90	21.04	-42.56#	-95.55
	E116	17.05	19.70	-79.46+	-76.54
	E117	16.46	18.06	-76.49	-85.58
	E127	17.97	19.69	-75.02	-111.83
	Average	16.47	19.29	-70.10	-114.21
B	E118		17.99		-75.44
	FI217		21.77+		-81.57
	FI218		18.56		-71.35
	E119		15.90		-80.76
	FI219		18.43		-71.31-
	E120C		16.18		-82.98
	E121		15.08-		-73.69
	E122		17.31		-77.39
	FI210		15.98		-90.10+
	Average		17.47		-78.29

Table 1 δD and $\delta^{18}O$ isotope values of the kaolinites from the study area (A=soft kaolin unit; B=semi-flint kaolin unit; Ka=Ka kaolinite; Kb=Kb kaolinite; Kc=Kc kaolinite.
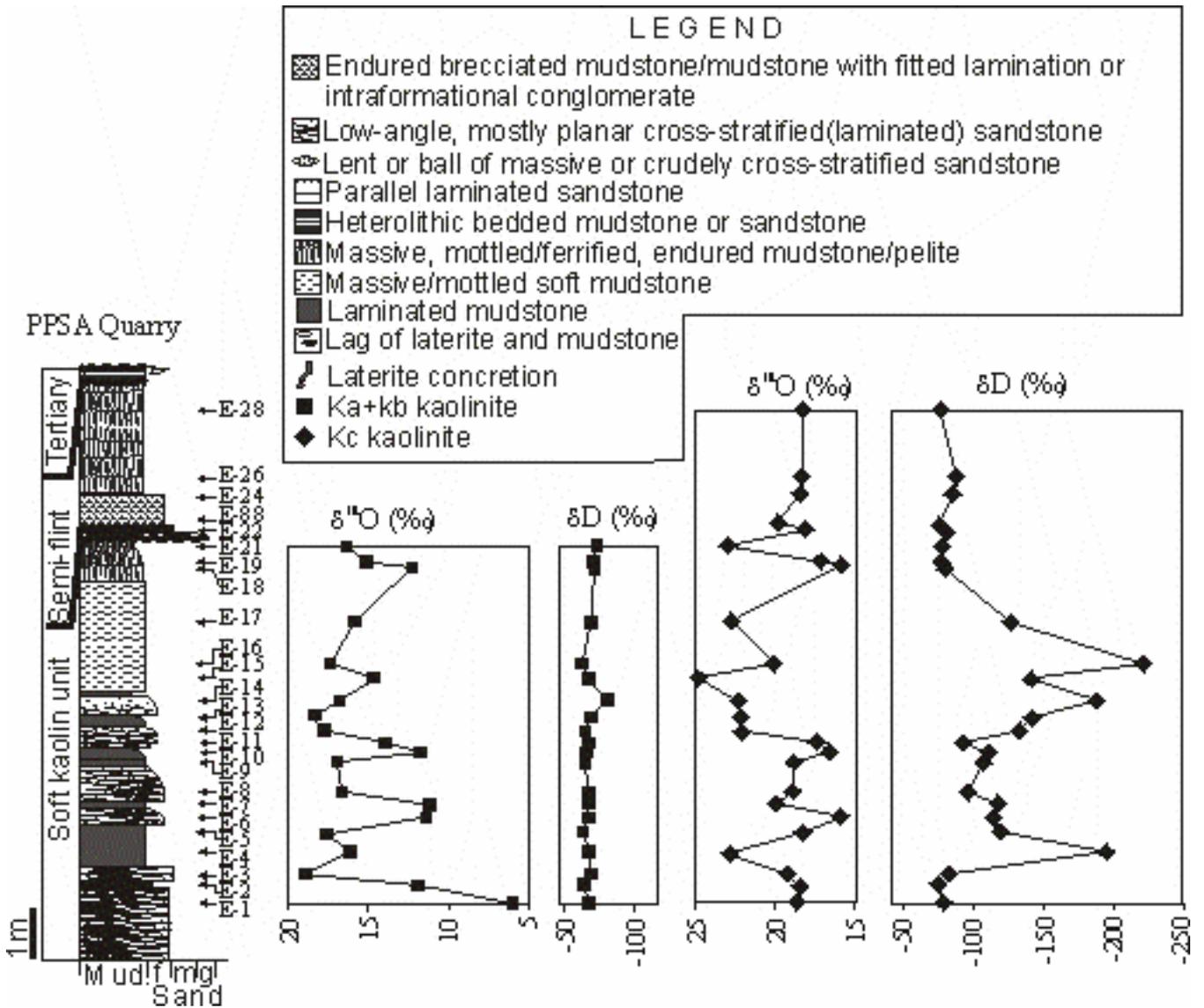
Figure 4.3 Lithostratigraphic profiles of the PPSA quarry, with the corresponding δD and δ^{18}O isotope values.
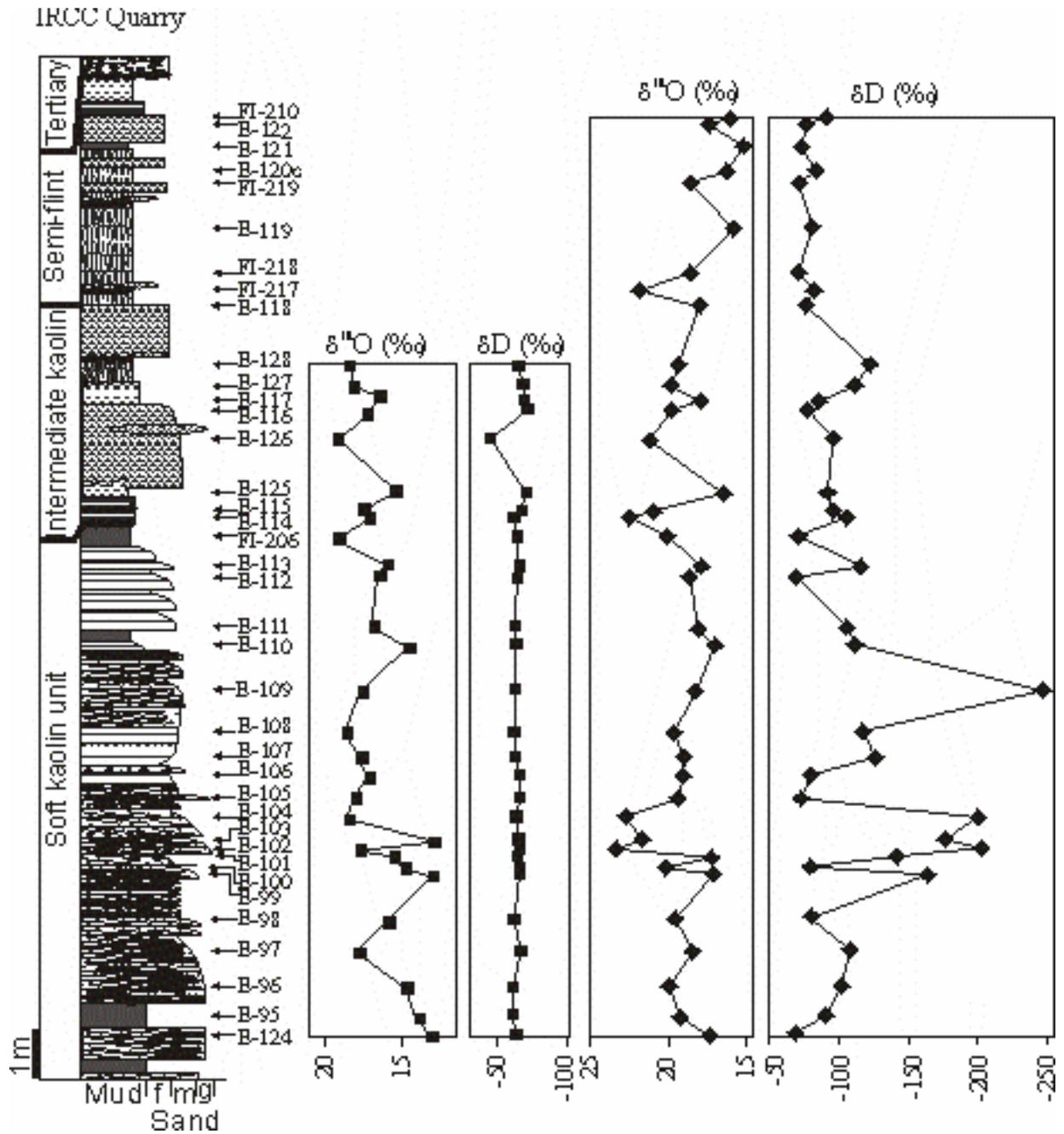
Figure 4.4 Lithostratigraphic profiles of the IRCC quarry, with the corresponding δD and δ^{18}O isotope values (See figure 3 for legend).
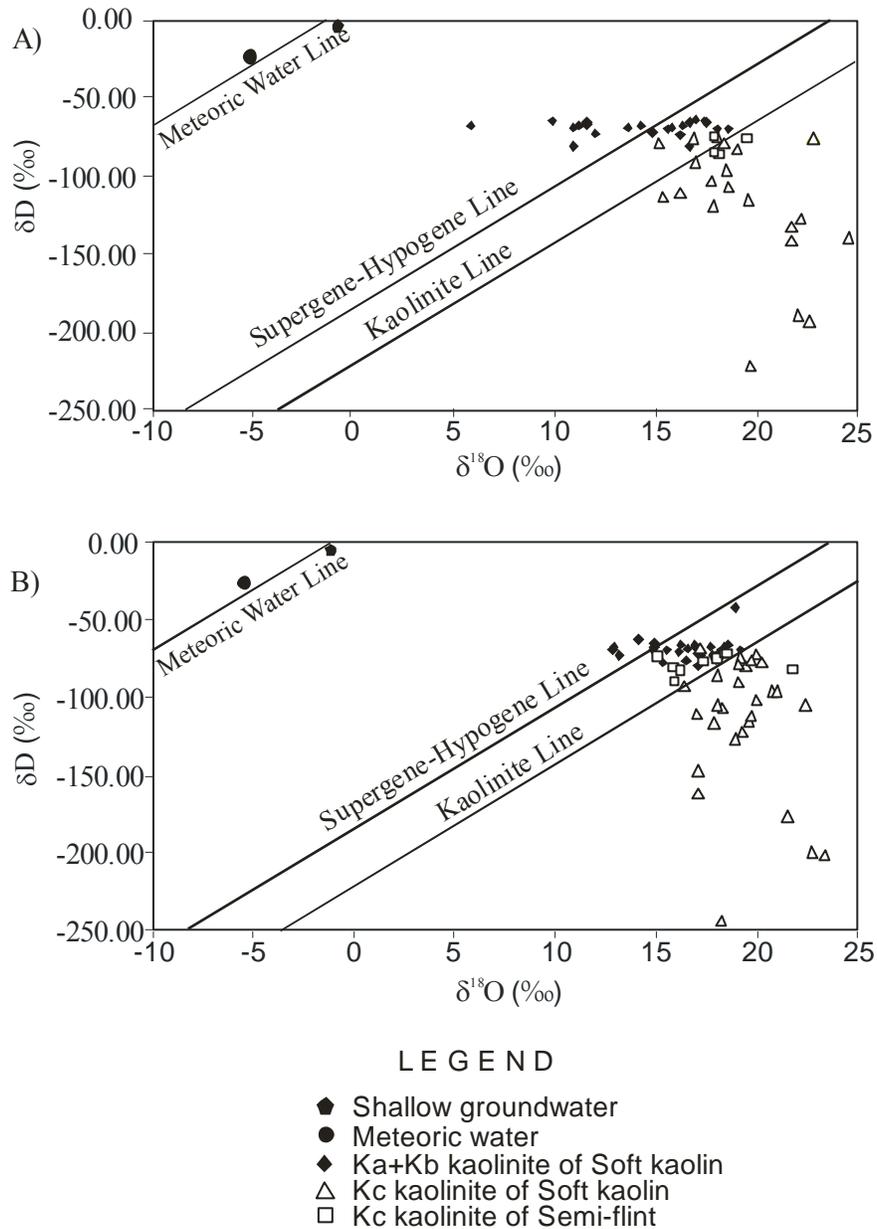
Figure 4.5 Binary diagram with plots of δD and δ^{18}O isotopic values of the kaolinites of the study area, as well as of the modern meteoric water and groundwater. Also plotted are the kaolinite line (Savin and Epstein, 1970a), the supergene/hypogene line (Sheppard *et al.*, 1969) and the meteoric water line (Craig, 1961). See text for discussions.

4.5 DISCUSSION

4.5.1 Evaluating the influence of the modern meteoric water

A first issue to be approached before using the isotope data for tracing the history of kaolinite formation in the Rio Capim area is to evaluate the influence of the modern meteoric waters that might have been in contact with these deposits. Although the studied strata are freshly exposed, modern kaolinitization is possible considering the geographic location in a humid equatorial area, where descending waters might have an influence at several meters of depth. To test this possibility, the $\delta^{18}O$ and δD values of a kaolinite in equilibrium with the modern meteoric water were estimated with basis on the measured $\delta^{18}O$ and δD values for this water. Despite the fact that only one water sample for each studied locality was collected, the resulting $\delta^{18}O$ and δD values revealed to be consistent with meteoric waters obtained from other Amazonian areas (see Salati et al., 1979).

Once the $\delta^{18}O$ and δD values from the meteoric waters are known, the isotope values of a kaolinite formed in equilibrium with these waters can be estimated with basis on the following equations of Savin and Epstein (1970a):

$$\alpha^{ox}_{(kao\text{-}water)}= \frac{1+\delta^{18}O_{kao}/1000}{1+\delta^{18}O_{water}/1000} \quad\quad (1)$$

$$\alpha^{Hy}_{(kao\text{-}water)}= \frac{1+\delta D_{kao}/1000}{1+\delta D_{water}/1000} \quad\quad (2)$$

Where $\alpha^{ox}_{(kao\text{-}water)}$ and $\alpha^{Hy}_{(kao\text{-}water)}$ are the kaolinite fractionation factors with respect to oxygen and hydrogen, respectively. According to measurements considering samples collected from a wide geographic distribution, these authors, as well as Lambert and Taylor (1971), proposed that the $\alpha^{ox}_{(kao\text{-}water)}$=1.027 and $\alpha^{ox}_{(kao\text{-}water)}$=0.97. If these values are applied to the study

area, then the $\delta^{18}O_{kao}$ and δD_{kao} values expected to be in equilibrium with the meteoric water in the modern environment would be 26.69‰ and 25.25‰, and –33.98‰ and –31.07‰ in the PPSA and IRCC quarries, respectively.

To test these values, calculations of the $\delta^{18}O_{kao}$ and δD_{kao} isotope values were also obtained directly applying the equations:

$$1000\ \ln\alpha_{(kao\text{-}water)}=2.5\ (10^6)\ (T^{-2})\text{-}2.87\ \text{for the oxygen} \qquad (3)$$
(Land and Dutton, 1978)

$$1000\ \ln\alpha_{(kao\text{-}water)}=\text{-}4.53\ (10^6)\ (T^{-2})\text{+}19.4\ \text{for the hydrogen} \qquad (4)$$
(Lambert and Epstein, 1980)

Where T is the modern annual mean temperature, which is 28°C (or 301°K) for the study area. Considering these equations, the obtained $\delta^{18}O_{kao}$ and δD_{kao} values revealed to be very close to the above, i.e., 24.72‰ and 23.70‰ for the $\delta^{18}O$, and –34.01 ‰ and -31.10‰ for the δD in the PPSA and IRCC quarries, respectively.

The data obtained from the two procedures presented above are comparable, and revealed $\delta^{18}O$ and δD values that are much heavier than those measured from any of the kaolinite samples collected from the study area. Therefore, the measured kaolinite isotope data are not in equilibrium with the modern weathering environment.

The Ipixuna Formation is often overlain by a Miocene and/or post-Miocene succession, known as the Barreiras and Post-Barreiras Formation (Santos Jr. and Rossetti, 2003; Rossetti, 2004). In the particular case of the studied profiles, these deposits average 25 m thick. Despite the porous nature imposed by the prevalence of well sorted and well rounded sandstones, it is presumed that this thickness, added to the presence of shales and, locally, iron cements along unconformities (see Rossetti, 2004), might have acted as barrier for descending waters in the modern environment.

Hence, the measured isotope values of the kaolinite samples might reflect the isotope composition of either past meteoric or groundwaters that have been in contact with the Ipixuna Formation since its deposition. Alternatively, the data might be related to contaminations caused

by primary or authigenic minerals that could be not eliminated from the samples, as discussed in the following.

4.5.2 Isotope behavior of the Ka+Kb kaolinites

The basic principle used for interpreting kaolinite isotope data is that, once formed, this mineral remains isotopically unaltered under surface and near-surface conditions (Lawrence and Taylor, 1971, 1972; O'Neil and Kharaka, 1976; Savin and Hsieh, 1998). Thus, the measured isotope values would reflect the isotopic composition of the water during the kaolinite formation, unless further mineralogical transformations take place.

As shown in the previous session, there is a wide variation of the $\delta^{18}O$ values plotted along the studied profiles (i.e., 12.79‰ and 6.39‰ for the PPSA and IRCC quarries, respectively), though the range of variation for the δD (i.e., 9.88‰ and 16.40‰ for the PPSA and IRCC quarries, respectively, disregarding samples E14 and E126) is considered negligible (e.g., Zhou and Dobos, 1994). Considering the plots of $\delta^{18}O$ versus δD values (Fig. 4.5) from both studied quarries, and comparing them with proposed meteoric (Craig, 1961), kaolinite (Savin and Epstein, 1970a) and supergene/hypogene (Shepard et al., 1969) lines, a great part of the Ka+Kb kaolinites would have formed supergenically, but not under influence of the paleoweathering. Considering this diagram, it could also be indicated that a significant amount of these kaolinites, particularly in the PPSA quarry, would have been related to a hypogene origin. However, under this condition, a more stable kaolinite polymorph would be dickite (Savin and Epstein, 1970a), which was not found in the studied deposits, even as traces. It seems that the hypogene origin suggested in this diagram is due to the large variation of the $\delta^{18}O$ values, at the same time that the corresponding δD values remained relatively constant. Therefore, the binary diagram of Figure 4.5, worldwide used for distinguishing kaolinites of various origins, seems to be not very useful to understand the mode of formation of the kaolinites from the Rio Capim area.

The relative stability of the δD values is taken as an indication that once formed the Ka+Kb kaolinites of the studied area remained isotopically stable. Under isotopic fractionation at low temperature, the hydrogen exchange between the mineral and the associated water occurs at much higher rates than with the oxygen, usually negligible (O'Neil and Kharaka, 1976; Bird and Chivas, 1988, Longstaffe and Ayalon, 1990). Thus, the cause for the wide oscillation of the $\delta^{18}O$

values is not related to equilibrium with interacting waters, but it reflects mineralogical contaminations. These issues are discussed in the following, but first one must compare the isotope values obtained for the kaolinite samples with ancient meteoric and ground waters. This is necessary in order to decipher whether the kaolinite formed during past weathering or burial conditions.

As widely considered by many authors (e.g., Savin and Epstein, 1970a,b; Lawrence and Taylor, 1971, 1972; Mizota and Longstaffe, 1996; Janssen, 1985; Giral-Kacmarcik et al., 1998; Gilg, 2000; Gilg et al., 2003; Girard et al., 2000), the groundwater collected today from a given stratigraphic unit would keep the isotopic composition of the groundwater during the time of kaolinite formation. Knowing the $\delta^{18}O$ and δD values for the groundwater, the temperature from this water can be calculated through the equation:

$$\delta^{18}O_{water} = -11.99 + 0.338\ T\ (^oC) \qquad \text{(Yurstever and Gat, 1981)} \qquad (5)$$

Application of this equation to the Rio Capim area indicates a groundwater temperature around 19.2^{o}C. To calculate the $\delta^{18}O$ value for the ancient meteoric water, an estimation of the paleotemperature at the surface must be provided. The Ipixuna Formation seems to have been deposited in an altitude similar to its present location. This is suggested by the altitude of the Ipixuna Formation in the Rio Capim, which is comparable to those areas where this unit is overlain by a well developed lateritic paleosol, recorded in adjacent tectonically stable terrains. Assuming that tectonics was negligible, a surface water temperature of nearly 17.2 ^{o}C can be estimated, considering a thermal gradient of circa 2°C, for a maximum burial of 60-70 m. This temperature is consistent with global temperature values, which estimates colder late Cretaceous to early Tertiary climates, characterized by temperatures ranging from 15-20°C (Savin, 1977).

Applying the estimated ancient surface temperature to equation (5), the $\delta^{18}O$ value for the surface water is –6.17‰, disregarding seasonal fluctuations. This value can be applied to the general equation (6) or the proposed local equation (7) in order to calculate the δD for the corresponding water, as follows:

$$\delta D = 8\ \delta^{18}O + 10 \text{ (Craig, 1961)} \qquad (6)$$

$$\delta D = 8.1 \, \delta^{18}O + 11 \quad \text{(Reis et al., 1977)} \quad (7)$$

Based on these calculations, the δD values for the ancient surface water in the Rio Capim area are –39.41‰ and –38.97‰, respectively. Applying these values to equations (3) and (4), and combining with equations (1) and (2), the $\delta^{18}O_{kao}$ and δD_{kao} formed in equilibrium with the ancient meteoric water would have been equivalent to 20.84‰ and –71.77‰ (-71.35‰ if δD_{water}=–38.97‰), respectively. On the other hand, applying these same procedures, but using the $\delta^{18}O$=-4.9‰ and δD=-22.5‰ obtained for the groundwater, the $\delta^{18}O_{kao}$ and δD_{kao} formed in equilibrium with this groundwater would have been equivalent to 21.73‰ and –55.43‰, respectively.

Therefore, it can be noticed from the above development that the $\delta^{18}O$ values for the Ka+Kb kaolinites calculated from both the ancient meteoric water and the temporally equivalent groundwater are heavier than the values measured from the kaolinite samples, while the δD values do not differ much. This is also shown by calculations of fractional factors using the isotope data measured from Ka+Kb kaolinites, considering the $\delta^{18}O$ and δD values calculated for the ancient surface water, and using equations (1) and (2), resulted in values for the oxygen of 1.009 and 1.010 and for the hydrogen of 0.97 and 0.97 for the PPSA and IRCC, respectively. These fractionation values are much lower than the $\alpha^{ox}_{(kao-water)=}1.027$ expected in weathering environments, while for the hydrogen are coincident (Savin and Epstein, 1970; Lawrence and Taylor, 1971, 1972).

Based only on the above comparisons, one cannot distinguish whether the Ka+Kb kaolinites formed in a diagenetic environment or associated to a paleoweathering. On the other hand, as previously mentioned, our ongoing studies point to formation of Ka+Kb kaolinites under influence of intrastratal fluids during sediment burial. This is suggested by the coarse-grained nature of the kaolinite crystals that are formed by replacement of framework grains. This characteristic, added to the good preservation of the sedimentary structures, is more consistent with mineralogical replacements taking place at a certain depth. Given the similarities of the isotopic values obtained for the Ka+Kb kaolinites with the estimated isotopic signal of kaolinites formed near the surface and under influence of groundwater, one can propose that the diagenetic environment was most likely located still under influence of the paleoenviroment, i.e., during early diagenesis. Under this condition, mineralogical replacements might take place at low

pressure and temperature, and the intrastral waters might receive a contribution from descending meteoric waters, which might result in isotopic exchanges.

Considering the isotopic equilibrium of the Ka+Kb kaolinites with shallow groundwaters, the wide variation of the $\delta^{18}O$ values could be attributed to mineralogical contaminations from framework grains. As shown by optical studies, the soft kaolin, dominated by Ka and Kb kaolinites, displays horizons with quartz, feldspar and muscovite grains, in great part derived from igneous (including volcanics) and metamorphic rocks. These minerals, though subordinate, show variable rates of replacement by kaolinites. During this process, the kaolinite must go completely into solution in order to adopt the isotopic composition of the interacting waters (Jassen, 1985). It seems that not all the framework grains were completely dissolved to form the kaolinite. In fact, there are many examples of entirely kaolinitized quartz and feldspar grains preserving their original shapes, meaning they did not go completely into solution before kaolinite was formed. Under this condition, it is more likely that the kaolinite will retain at least some of the isotope composition of the parent mineral, instead of going into equilibrium with interacting waters. Studies performed on a large number of igneous and metamorphic rocks indicate low $\delta^{18}O$ values that are usually lower relative to corresponding kaolinites (Silverman, 1951; Taylor and Epstein, 1962; Garlick and Epstein, 1967). Therefore, it is possible that the lower $\delta^{18}O$ values of the Ka+Kb kaolinites (i.e., average of 14.83‰ and 16.47‰ for the PPSA and IRCC quarries, respectively) relative to the calculated groundwater (i.e., 21.73‰) reflect a lower isotopic composition of the parent materials. As the large bulk of the minerals present in the framework, with exception of muscovite, do not show hydrogen in their composition, only the oxygen would respond to this mineralogical contamination, while the hydrogen would show equilibrium with the interacting water.

4.5.3 Isotope behavior of the Kc kaolinites

Considering only the soft kaolin unit, the isotope data for both oxygen and hydrogen of the Kc kaolinite are much more variable when compared to the Ka+Kb kaolinites. As occurs with those kaolinites, the measured isotope data of the Kc kaolinite display lower $\delta^{18}O$ and lighter δD values than those expected for kaolinites that would have been formed in contact with the modern meteoric water. The isotope $\delta^{18}O$ and δD values measured from the Kc kaolinite are lighter than

the expected values calculated above for both the ancient meteoric water and the temporally corresponding groundwater. In addition, the fractionation factors calculated using the same procedure as indicated for the Ka+Kb kaolinites, *i.e.*, considering the $\delta^{18}O$ and δD values calculated for the ancient surface water, resulted in values for the oxygen of 1.0134 and 1.013, and for the hydrogen of 0.937 and 0.922 for the PPSA and IRCC, respectively. Combination of these data led to the conclusion that the oxygen and the hydrogen are not in equilibrium, neither with the ancient meteoric water, nor with the corresponding groundwater.

The large variation of the Kc kaolinite from the soft kaolin on both isotope values (Figs. 4.3-5) might be attributed to significant isotopic exchange after kaolinite formation. The fact that the $\delta^{18}O$ curves from both of the studied quarries follow the same pattern of oscillation than the corresponding Ka+Kb kaolinites is taken as an indication that the Kc kaolinites originated, at least in part, from replacement of those kaolinites. Regardless the isotopic exchanges, the finer-grained kaolinite seems to still keep the isotopic signature of the coarser-grained kaolinites. It is noteworthy that these interpretations are in good agreement with optical studies, which indicate formation of Kc kaolinites from Ka+Kb kaolinites, as previously mentioned on the geological context session. In addition, it is important to remember that our ongoing studies also reveal that a large volume of the Kc kaolinite in the soft kaolin unit derives directly from replacement of detritic clay minerals associated to muddy layers interbedded with sandstones. The presence of quartz, feldspar and muscovite grains in the silty fraction of these mudstones might have also caused isotopic contamination, as discussed for the case of the Ka+Kb kaolinites.

However, part of the Kc kaolinite from the soft kaolin unit might have additionally formed during the development of a paleosol horizon related to the top unconformity. In part, this is demonstrated by the fact that there is a gradual upward increase in the frequency of Kc kaolinite near this unconformity. The paleosol is more expressive in the PPSA quarry (Fig. 4.3), where the more stable $\delta^{18}D$ values obtained for corresponding samples (i.e., E18, E19 and E21) indicate a fractional factor of 0.97 for the hydrogen, calculated with basis on the estimated ancient meteoric water. This value fits perfectly with the $\alpha^{Hy}_{(kao-water)} = 0.97$ expected in weathering environments (Savin and Epstein, 1970; Lawrence and Taylor, 1971, 1972). Thus, it is proposed that as the soft kaolin unit was exposed to the surface, its interaction with ancient meteoric waters might have initiated an isotopic re-equilibration, with a first response on the hydrogen, in general more suitable for isotopic exchange.

For the case of the Kc kaolinite from the semi flint unit, the isotope values are, in general, relatively lighter than the isotopic composition of the kaolinite calculated from the groundwater and ancient meteoric water (Tab. 1). Exception is the hydrogen values, which are comparable (i.e., <10‰) to those obtained for the ancient meteoric water (Figs. 4.3 and 4.4). In addition, the fractional factors with respect to the oxygen calculated for the ancient surface water is 1.012 and 1.011, and for the hydrogen is 0.957 and 0.96 for the PPSA and IRCC quarries, respectively. Thus, only the hydrogen is in equilibrium with this water.

Considering that the semi-flint unit is strongly affected by pedogenesis (e.g., Truckenbrodt et al., 1991; Kotschoubey et al., 1996; 1999; Costa and Moraes, 1998), it would be expected to have both isotopes in equilibrium with the calculated ancient meteoric water. However, the origin of the kaolinite in the semi-flint unit is complex. In part, there seems to have detrital kaolin derived from the underlying soft kaolin unit (Rossetti and Santos Jr., 2006). These are mixed with kaolinite derived from a paleoweathering, which did not take place necessarily only in one phase (Rossetti, 2004). In addition, our ongoing studies reveal that the top of the semi-flint unit display fractures filled by kaolinite booklets, which could not be extracted from the analyzed samples. It is also noteworthy to recall that the semi-flint unit is highly contaminated with iron oxides. All these factors might have acted together in order to result in a complex isotopic signature for the Kc kaolinite.

4.6 CONCLUSIONS

The main conclusions that arise from this study are:

1. The results obtained from $\delta^{18}O$ and δD analyses revealed values that are consistent when both of the studied profiles are compared.

2. None of the isotope curves are in equilibrium with calculated values of kaolinites that would be formed in equilibrium with the modern local meteoric water.

3. Tests made with different grain sizes indicated values that are similar for the Ka and Kb kaolinites, but these display values that are not comparable to the Kc kaolinites, even when samples from a same stratigraphic unit are compared. These differences in isotopic data are related to distinct genesis for the two analyzed kaolinite categories.

4. Binary diagrams contrasting $\delta^{18}O$ and δD values, worldwide applied for distinguishing supergenic from hypogenic kaolinites, as well as those formed under weathering conditions, can not be applied to the Rio Capim Kaolin. In the case of the Ka+Kb kaolinites of the soft kaolin unit, this is because the $\delta^{18}O$ values display a large range of variation, while the δD is relatively constant, which results in plots of several samples into the hypogenic field. In addition, the corresponding Kc kaolinite for both isotopes display highly oscillating curves, with δD that are anomalously light when compared with most of the kaolinites described in the literature. This characterizes samples recording isotopic exchanges after kaolinite formation.

5. Despite these problems, optical studies, combined with comparisons of δD isotope values from the Ka+Kb kaolinites, led to suggest that these reflect values expected for kaolinites formed in contact with the groundwater. The discrepant $\delta^{18}O$ values are attributed to mineralogical contaminations imposed by the different degrees of replacement of quartz, feldspar, muscovite and lithics grains. The large variation of the Kc kaolinite isotopic values in the soft kaolin unit shows significant exchange after kaolinite formation. However, a similar pattern of variation of the $\delta^{18}O$ curves on both of the studied area is attributed to an origin linked to coarser grained kaolinites formed in the sandstones, as well as detrital clays from mudstones, which also contain mineralogical contaminants similar to the sandstones in the silty grain size.

6. Although the semi-flint contains a large volume of paleosol, the $\delta^{18}O$ and δD isotope values indicated that the corresponding Kc kaolinite is not in equilibrium with the ancient meteoric water. This is attributed to the fact that the origin of these kaolinites might have been variable, including kaolinites derived from the underlying soft kaolin unit, kaolinites formed during different phases of paleoweathering, as well as later phases of coarse-grained kaolinites formed along fractures.

7. The present investigation undertaken in the Rio Capim area led to the conclusion that the application of $\delta^{18}O$ and δD might help to substantially increase the understanding of the processes involved in the kaolinite formation, particularly when combined with optical information.

REFERENCES

AZEVEDO R.P. 1991. *Tectonic Evolution of Brazilian Equatorial Continental Margin Basins*. London. Royal School of Mines Imperial College, 412 p. (PhD thesis)

BIRD M.I. & CHIVAS A.R. 1988. Stable isotope evidence for low temperature kaolinite wethering and post-formational hydrogen isotope exchange in Permian kaolinite. *Chemical geology* 72, 249-265.

BOULVAIS P.; VALET J.-M.; ESTEOULE-CHOUX J.; FOURCADE S.; MARTINEAU F. 2000. Origin of kaolinitization in Brittany (NW France) with emphasis on deposits over granite: stable isotopes (O,H) constraints. *Chemical Geology* 168, 211-223.

BOWEN G.J. & REVENAUGH J. 2003. Interpolation the isotopic composition of modern meteoric precipitation. *Water Resources Research* 39, 1-13.

BOWEN G.J. & WILKINSON B. 2002. Spatial distribution of $\delta^{18}O$ in meteoric precipitation. *Geological Society of America* 30, 315-318.

CLAYTON R.N. & MAYEDA T.K. 1963. The use of bromine pentafluoride in the extraction of oxygen from oxides and silicates for isotopic analysis. *Geochimita et Cosmochimica Acta* 27, 43-52.

COLEMAN M.L.; SHEPHERD T.J.; ROUSE J.E.; MOORE G.R. 1982. Reduction of water with zinc for hydrogen analysis 54, 993-995.

COSTA J.B.S.; BEMERGUY R.L.; HASUI Y.;BORGES M.S. 2001. Tectonics and paleogeography along the Amazon River. *Journal of South American Earth Sciences* 14, 335-347.

COSTA M.L. & MORAES E.L. 1998. Mineralogy, geochemistry and genesis of kaolins from the Amazon region. *Mineralium Deposita* 33, 3-297.

CRAIG H. 1961. Isotope variation in meteoric waters. *Science* 133, 1702-1703.

CRUZ M.D.R. & REYES E. 1998. Kaolinite and dickite formation during shale diagenesis: isotopic data. *Applied Geochemistry* 13, 95-104.

EPSTEIN S.; SHARP R.P.; GOW A.J. 1965. Six year record of oxygen and hydrogen isotope variations in South Pole Firn. *Journal Geophysics Research* 70, 1809-1814.

FREEDMAN I. 1953. Deuterium contends of natural water and others substances. *Geochimita et Cosmochimica Acta* 4, 89-103.

FRICKE H.C. & O'NEIL J.R. 1999. The correlation between $^{18}O/^{16}O$ ratios of meteoric water and surface temperature: its use in investigating terrestrial climate change over geological time. *Earth and Planetary Science Letters* 170, 181-196.

GALVÃO M.V.G. 1991. *Evolução Termodinâmica da Bacia do Marajó, Estado do Pará, Brasil.* Ouro Preto. Universidade Federal de Ouro Preto, 193 p. (Dissertação de Mestrado)

GARLICK G.D. & EPSTEIN S. 1967. oxygen isotope ratios in coexisting minerals of regionally metamorphosed rocks. *Geochimita et Cosmochemica Acta* 31, 181-214

GILG H.A. 2000. D-H evidence for the timing of kaolinization in Northeast Bavaria, Germany. *Chemical Geology* 170, 5-18.

GILG H.A. & SHEPPARD S.M.F. 1996. Hydrogen isotope fractionation between kaolinite and water revisited. *Geochimita et Cosmochimica Acta* 4, 89-103.

GILG H.A.; WEBER B.; KASBOHM J. ; FREI R. 2003. Isotope geochemistry and origin of illite-smectite and kaolinite from the Seilitz and Kemmlitz kaolin deposists, Sexony, Germany. *Clay Minerals* 38, 95-112.

GIRAL-KACMARCIK S.; SAVIN M.S.; NAHON, D.B.; GIRARD J.P.; LUCAS Y.; ABEL L.J. 1998. Oxygen isotope geochemistry of kaolinite in laterite-forming processes, Manaus, Amazonas, Brazil. *Geochimita et Cosmochimica Acta* 62, 1865-1879.

GIRARD J.-P.; FREYSSINET P.; AND CHAZOT G. 2000. Unraveling climatic change from intraprofile in oxygen and hydrogen isotopic composition of goethite and kaolinite in laterites: An integrated study from Yaou, Frech Guiana. *Geochimita et Cosmochimica Acta* 64, 409-426.

GÓES A.M. 1981. *Estudo Sedimentológico dos Sedimentos Barreiras, Ipixuna e Itapecuru, no Nordeste do Estado no Pará e Noroeste do Maranhão*. Belém, Universidade Federal do Pará, Centro de Geociencias, 55 p. (Dissertação de Mestrado).

JAMES, A.E. & BAKER, D.R. 1976. Oxygen isotope exchange between illite and water at 22°C. *Geochimita et Cosmochimica Acta* 40, 235-240.

JANSSEN J.L. 1985. *Origin of vermicular and platy kaolinite crystal in Geogia Kaolins as explained by $^{18}O/^{16}O$ isotopic ratios*. Bloomington, Indiana University, 63 p. (M.Sc. Dissertation)

KOTSCHOUBEY B.; DUARTE A.L.S.; TRUCKENBRODT W. 1999. Cobertura bauxítica e origem do caulim do Morro do Felipe, Baixo Rio Jari, Estado do Amapá. *Revista Brasileira de Geociências* 29, 331-338.

KOTSCHOUBEY B.; TRUCKENBRODT W.; HIERONYMUS B. 1996. Depósitos de caulim e argila semi-flint no nordeste do Pará. *Revista Brasileira de Geociências* 26, 71-80.

LAMBERT S.J. & EPSTEIN S. 1980. Stable isotope investigations of an active geothermal sytem in Valles Caldera, Jemez Moutains, New Mexico. Journal Volcan. *Geotherma. Research* 8, 111-129.

LAND L.S. & DUTTON S.P. 1978. Cementation of a Pennsylvanian deltaic sandstone: isotope data. *Journal Sedimentary Petrology* 48, 1167-1176.

LAWRENCE J.R. & TAYLOR H.P. 1971. Deuterium and O-18 correlation: Clay minerals and hydroxides in Quaternary soils compared to meteoric waters. *Geochimica et Cosmochimica Acta* 35, 993-1003.

LAWRENCE J.R. & TAYLOR H.P. 1972. Hydrogen and oxygen systematics in weathering profiles. *Geochimica et Cosmochimica Acta* 36, 1377-1393.

LIU K.-K. & EPSTEIN S. 1984. The hydrogen isotope fractionation between kaolinite and water. *Isotope Geoscience* 2, 355-350.

LONGSTAFFE F.J. & AYALON A. 1990. Hydrogen-isotope geochemistry of diagenetic clay minerals from Cretaceous sandstone. Alberta. Canada: evidence for exchange. *Applied Geochemistry* 5, 657-668.

MARUMO K.; NAGASAWA K.; KURODA Y. 1980. Mineralogy and hydrogen isotope geochemistry of clay minerals in the Ohnuma geothermal area, northeastern Japan. *Earth and Planetary Science Letters* 47, 255-262.

MIZOTA C. & LONGSTAFFE F.J. 1996. Origin of Cretaceous and Oligocene kaolinites from the Iwaizumi clay deposit, Iwate, Northeastern Japan. *Clay and Clay minerals* 44, 408-416.

NASCIMENTO, M.S. & GÓES, A.M. 2005. Distribuição estratigráfica e proveniência de minerais das formações Ipixuna e Barreiras, região do Rio Capim, Sub-Bacia de Cametá, Estado do Pará. *Revista Brasileira de Geociências* 35, 49-58.

O'NEIL J.R. & KHARAKA Y.K. 1976. Hydrogen and oxygen isotope exchenge reactions between clay minerals and water. *Geochimita et Cosmochemica Acta* 40, 241-246.

REIS C.M.; TANCREDI A.C.F.N.S.; MATSUI E.; SALATI E. 1977. Caracterização das águas da região do Marajó através da concentração de O-18 e D. *Acta Amazônia* 7, 209-222.

ROSSETTI D.F. 2004. Paleosurfaces from northeastern Amazonia as a key for reconstructing paleolandscapes and understanding weathering products**.** *Sedimentary Geology* 169, 151-174.

ROSSETTI D.F. & SANTOS JR. A.E.A. 2003. Events of soft sediment deformation and mass failure in Upper Cretaceous estuarine deposits (Cametá Basin, northern Brazil) as evidence for seismic activity. *Sedimentary Geology* 161, 107-130.

ROSSETTI D.F. & SANTOS JR. A.E.A. 2006. Analysing the origin of the Upper Cretaceous-?Lower Tertiary Rio Capim semi flint (Pará State, Brazil): under a sedimentologic perspective. *Sedimentary Geology* 186, 133-144.

SALATI, E.; DALL'ÓLIO, A.; MATSUI, E.; GAT, J. R. 1979. Recycling of water in Amazon, Brazil: an isotopic study. *Geophysical Research. Water Resources Research* 15, 1250-1258.

SANTOS Jr. A.E.A. 2002. Reconstrução Paleoambiental e Estratigráfica de Depósitos Cretáceos e Terciários Expostos na Borda Sudeste da Sub-Bacia de Cametá, Norte do Brasil. Belém, Universidade Federal do Pará, Centro de Geociências, 131 p. (Dissertação de Mestrado).

SANTOS JR. A.E.A. & ROSSETTI D.F. 2003. Paleoambiente e estratigrafia da Formação Ipixuna, Área do Rio Capim, Leste da bacia de Cametá. *Revista Brasileira de Geociências* 33, 313-324.

SANTOS JR. A.E.A. & ROSSETTI D.F. 2006. Depositional model of the Ipixuna Formation (Late Cretaceous-?Early Tertiary), Rio Capim Area, northern Brazil. *Latin American Journal of Sedimentology and Basin Analysis* (in press).

SAVIN S.M. 1977. The history of the earth's surface temperature during the past 100 millions years. *Annual Review Earth Planetary Science*. 5, 319-355.

SAVIN S.M. & EPSTEIN S. 1970a. The oxygen and hydrogen isotope geochemistry of clay minerals. *Geochimica et Cosmochimica Acta* 34, 25-42.

SAVIN S.M. & EPSTEIN S. 1970b. The oxygen and hydrogen isotope geochemistry of ocean sediments and shales. *Geochimica et Cosmochimica Acta* 34, 43-63.

SAVIN S.M. & LEE M. 1988. Isotopic Studies of Phillosilicates. In: Bailey S.W. editor. Hydrous Phyllosilicates (exclusive for micas). Mineralogical Society of America. *Reviews in Mineralogy* 19, 189-223.

SAVIN S.M. & HSIEH J.C.C. 1997. The hydrogen and oxygen isotope geochemistry of pedogenic clay minerals: principles and theoretical background. *Geoderma* 82, 227-253.

SHEPPARD S.M.F.; NIELSEN R.L.; TAYLOR H.P.Jr. 1969. Oxygen and hydrogen isotope ratios of clay minerals from porphyry copper deposits. *Economic Geology* 64, 755-777.

SILVERMAN S.R. 1951. The isotopic geology of oxygen. *Geochimica et Cosmochimica Acta* 2, 26-42.

SOUSA D.J.L. 2000. *Caracterização Geológica, Mineralógica, Química e Física do Caulim da RCC - Rio Capim Caulim (PA)*. Belém, Universidade Federal do Pará, Centro de Geociências, 116 p. (Dissertação de Mestrado)

STERN L.A.; CHAMBERLAIN C.P.; REYNOLDS R.C.; JOHNSON G.D. 1997. Oxygen isotope evidence of climate change from pedogenetic clay minerals in the Himalayan molasses. *Geochimica et Cosmochimica Acta* 61, 731-744.

SUN S.-S & EADINGTON P.J. 1987. Oxygen isotope evidence for the mixing of magmatic and meteoric waters during Tin mineralization in the Mole Granite, New South Wales, Australia. *Economic Geology* 82, 42-52.

TABOR N.J. & MONTANEZ I.P. 2005. Oxygen and Hydrogen isotope compositions of permian pedogenic phyllosilicates: Development of modern surface domain arrays and implications for paleotemperature reconstrations. *Paleogeography, Paleoclimatology, Paleoecology* 223, 127-146.

TAYLOR H.P., JR. & EPSTEIN S. 1962. Relationship between $^{18}O/^{16}O$ ratios in coexisting minerals of igneous and metamorphic rocks. Part 1 Principles and experimental results. *Bulletin of the Geological Society of America* 73, 461-480.

TRUCKENBRODT W.; KOTSCHOUBEY B.; SCHELLMANN, W. 1991. Composition and origin of the clay cover on North Brazilian laterites. *Geologische Rundschau* 80, 591-610.

VILLEGAS J.M.C. 1994. *Geologia Estrutural da Bacia do Marajó*. Belém, Universidade Federal do Pará, Centro de Geociências, 119 p. (Dissertação de Mestrado)

VITALI, F.; LONGSTAFFE F.J.; MCCARTHY P.J.; PLINT A.G.; CALDWELL W.G.E. 2002. Stable isotope investigation of clay minerals and pedogenesis in an interfluve paleosol from the Cenomanian Dunvegan Formation, N.E. British Columbia, Canada. *Chemical Geology* 192, 269-287.

YAPP C.J. 1986. Oxygen and Hydrogen isotope variations among goethites (α-FeOOH) and the determination of paleotemperatures. *Geochimica et Cosmochimica Acta* 51, 355-364.

YURSTEVER Y. & GAT J.R. 1981. Atmospheric waters. IAEA, *Technology Representative Service*. 201, 103-142.

ZHOU T. & DOBOS S.K. 1994. Stable isotope geochemistry of kaolinite from the "White Section", Black ridge, Clermont, central Queensland: implication for the age and origin of the "White Section". *Clay and Clay Minerals* 42, 269-275.

ACKNOWLEDGEMENTS